Cellular mechanisms and novel treatments of skeletal muscle weakness in heart failure with preserved ejection fraction

Ever Espino Gonzalez

Submitted in accordance with the requirements for the degree of

Doctor of Philosophy

The University of Leeds

Faculty of Biological Sciences

School of Biomedical Sciences

October 2022

The candidate confirms that the work submitted is his own, except where work which has formed part of jointly-authored publications has been included. The contribution of the candidate and the other authors to this work has been explicitly indicated below. The candidate confirms that appropriate credit has been given within the thesis where reference has been made to the work of others.

Manuscripts arising from this thesis:

Espino-Gonzalez E, Tickle PG, Benson AP, Kissane RWP, Askew GN, Egginton S & Bowen TS (2021). Abnormal skeletal muscle blood flow, contractile mechanics, and fibre morphology in a rat model of obese-HFpEF. *J Physiol*, **599**(3), 981-1001.

Abstracts arising from this thesis:

Espino-Gonzalez E, Tickle PG, Scalabrin M, Pereira M, Gallagher H, Roberts L, Egginton S & Scott Bowen TS (2022). Impaired overload-induced skeletal muscle hypertrophy in heart failure is rescued by caloric restriction. *EMBO Workshop - Muscle formation, maintenance, regeneration and pathology.*

Espino-Gonzalez E, Tickle PG, Benson AP, Egginton S & Bowen TS (2020). Skeletal muscle fibre-type and oxygen transport limitations in obese-HFpEF. *J Cachexia Sarcopenia Muscle*.

Espino-Gonzalez E, Tickle PG, Benson AP, Egginton S & Bowen TS (2020). Heart failure with preserved ejection fraction induces anabolic resistance coupled with contractile, vascular and mitochondrial impairments. *Multidisciplinary Cardiovascular Research Centre (MCRC) Retreat.*

Espino-Gonzalez E, Tickle PG, Egginton S & Bowen TS (2019). Skeletal muscle weakness, atrophy, and abnormal blood flow response in an animal model of heart failure with preserved ejection (HFpEF). *Future Physiology 2019*, *Proc Physiol Soc* 45, C13.

Espino-Gonzalez E, Tickle PG, Garnham JO, Egginton S & Bowen TS (2019). Overload-induced skeletal muscle hypertrophy is impaired in a rat model of heart failure with preserved ejection fraction. *27th Northern Cardiovascular Research Group Meeting.*

Acknowledgements

First and foremost, I would like to thank my primary supervisor Dr. Scott Bowen for his invaluable advice, continuous support, and patience during my PhD study. His knowledge and experience have encouraged me in all the time of my academic research and daily life. I would also like to thank my co-supervisor Prof. Stuart Egginton for his invaluable scientific insight throughout this project; his input has successfully developed my research acumen and critical thinking skills. My gratitude extends to the National Council of Science and Technology of Mexico (CONACYT) and the Faculty of Biological Sciences for the funding opportunity to undertake my studies at the School of Biomedical Sciences, University of Leeds. Additionally, I would like to thank my friends, lab mates, colleagues, and research team – Muscle Biology Research Group (Bowen Lab) for a cherished time spent together in the lab, and in social settings; it is their kind help and support that have made my study and life in England an amazing time. Finally, I would like to express my gratitude to my parents, siblings, and wife. Without their understanding and encouragement, it would be impossible for me to complete my study. Their unfaltering love has, and always will be, the impetus for my success.

Abstract

Heart failure (HF) is no longer considered a simple syndrome of cardiac dysfunction but includes several skeletal muscle alterations that limit functional capacity and quality of life. However, compared to HF with reduced ejection fraction (HFrEF), skeletal muscle alterations induced by HF with preserved ejection fraction (HFpEF) remain poorly explored with limited treatments. This thesis, therefore, aimed to reveal new insights into the cellular mechanisms underlying skeletal muscle pathology in HFpEF by examining the effects of pharmacological, physical-loading (exercise), and nutritional interventions. Using a well-established obese rat model, this thesis provides new evidence that: HFpEF induces multiple skeletal muscle alterations, including contractile dysfunction, fibre atrophy, capillary loss and an impaired exercise hyperaemia; pharmacological treatments (Entresto and Vastiras) improved cardiac function in HFpEF but did not impact skeletal muscle remodelling; overload-induced skeletal muscle hypertrophy is impaired in HFpEF and linked to mitochondrial but not vascular impairments; and acute caloric restriction treatment in HFpEF partially restored the hypertrophic response that was related to improved myonuclear accretion. Collectively, these findings extend current knowledge of muscle pathophysiology in HFpEF and may facilitate future therapeutic approaches.

Table of Contents

List of Tables

List of Figures

Abbreviations

^{31}P-MRS	^{31}Phosphorus magnetic resonance spectroscopy
4E-BP1	4E-binding protein 1
ACC	acetyl-CoA carboxylase
ACCF	American College of Cardiology Foundation
ACEI	angiotensin-converting enzyme inhibitors
ACL	ATP-citrate lyase
ACTRIIB	activin receptor type 2B
ADP	adenosine diphosphate
AHA	American Heart Association
AKT	serine/threonine kinase
AMPK	5' adenosine monophosphate-activated protein kinase
ANOVA	analysis of variance
ANP	atrial natriuretic peptide
ARB	angiotensin receptor blockers
ARNI	angiotensin receptor neprilysin inhibitors
AT2R	angiotensin II receptor type 2
ATP	adenosine triphosphate
ATPase	adenosine triphosphatase
AVO_2	arterial–venous O_2 content
BCA	bicinchoninic acid
BIOPS	relaxing and biopsy preservation solution
BSA	bovine serum albumin
C:F	capillary-to-fibre ratio
Ca^{2+}	calcium
CD	capillary density
CDA	capillary domain area
C_{IV}	complex IV
CO	cardiac output
CR	caloric restriction
DEXA	dual-energy X-ray absorptiometry
DNA	Deoxyribonucleic acid
DOCA	deoxycorticosterone acetate
Drp1	dynamin-related protein 1
DSS	dahl salt-sensitive

DT-MRI	diffusion tensor magnetic resonance imaging
ECG	electrocardiogram
EDL	*extensor digitorum longus*
EDTA	ethylenediaminetetraacetic acid
EF	ejection fraction
E_{I+II}	complex I+II substrates in the maximal ETS state
eIF4E	eukaryotic translation initiation factor 4E
E_{II}	complex II substrates in the maximal ETS state
ESC	European Society of Cardiology
FCCP	carbonyl cyanide 4-(trifluoromethoxy)-phenylhydrazone
FCSA	fibre cross sectional area
FOXO	forkhead box protein O
GDF-15	growth differentiation factor-15
GDF-8	growth/differentiation factor-8
GH	growth hormone
GSK3	glycogen synthase kinase 3
HF	heart failure
HFpEF	heart failure with preserved ejection fraction
HFrEF	heart failure with reduced ejection fraction
IGF1	insulin-like growth factor 1
IGF1R	IGF1 receptor
IL-12	interleukin-12
IL-6	interleukin-6
IL-1β	interleukin-1ß
IR	insulin receptor
IRS1	insulin receptor substrate 1
LA	left atrium
LC3	microtubule-associated protein 1 light chain 3
LCD	local capillary density
LCFR	local capillary-to-fibre ratio
LVEF	left ventricular ejection fraction
MAFbx	muscle atrophy F-box
MHC	myosin heavy chain
MiR05	mitochondrial respiration medium
MRA	mineralocorticoid-receptor antagonists
MRI	magnetic resonance imaging

mRNA	messenger ribonucleic acid
mTOR	mammalian target of rapamycin
MuRF1	muscle RING finger 1
NF-κB	nuclear factor kappa-light-chain-enhancer of activated B cells
NYHA	New York Heart Association
O_2	oxygen
P	statistical significance value
PBS	phosphate buffered saline
PCr	phosphocreatine
P_i	inorganic phosphate
P_I	complex I substrates in the OXPHOS state
P_{I+II}	complex I+II substrates in the OXPHOS state
PI3K	phosphoinositide 3 kinase
PO_2	partial pressure of oxygen
Pol I	RNA polymerase I
Pol III	RNA polymerase III
PUFA	polyunsaturated fatty acids
RCR	respiratory control ratio
RIPA	radioimmunoprecipitation assay
RNA	ribonucleic acid
ROS	reactive oxygen species
rRNA	ribosomal ribonucleic acid
RWT	relative wall thickness
S6K1	p70 S6 kinase 1
SC	satellite cells
SDS	sodium dodecyl sulphate
SERCA	sarco(endo)plasmic reticulum Ca^{2+} ATPase
SGLT2I	sodium-glucose cotransporter 2 inhibitors
SICA-HF	Studies Investigating Co-morbidities Aggravating HF
SMAD2	mothers against decapentaplegic homolog 2
SMAD3	mothers against decapentaplegic homolog 3
SUIT	substrate, uncoupler, and inhibitor titration
SUnSET	surface sensing of translation
TA	*tibialis anterior*
TAC	transverse aortic constriction
TMPD	*N,N,N',N'*-tetramethyl-*p*-phenylenediamine

TNF	tumor necrosis factor
TNF-α	tumour necrosis factor alpha
UPS	ubiquitin–proteasome system
$\dot{V}O_{2peak}$	peak pulmonary oxygen uptake
ZSF1	zucker fatty/spontaneously hypertensive HF F1 hybrid
ΔAVO_2	arterial-venous O_2 content

Chapter 1 Introduction

1.1 Prologue

Chronic heart failure (HF) represents one of the biggest challenges in cardiology. Several cardiovascular co-morbidities including coronary artery disease, valvular disease and hypertension frequently end in HF, which carries a considerable health cost, morbidity and mortality burden (Coats *et al.*, 2017; Metra & Teerlink, 2017). Nearly half of all patients with HF are classified as having HF with preserved ejection fraction (HFpEF) (Dunlay *et al.*, 2017), a heterogeneous syndrome often accompanied by obesity, hyperglycaemia and hypertension (Silverman & Shah, 2019). Individuals suffering from this syndrome have a poor quality of life and regularly experience exercise intolerance, which is widely recognised as the hallmark and most common symptom of HFpEF (Haykowsky & Kitzman, 2014). One key factor closely associated with exercise intolerance in HFpEF is skeletal muscle dysfunction, which is the result of several structural, metabolic and contractile abnormalities (Tucker *et al.*, 2018), and is associated with increased mortality (Ruiz *et al.*, 2008). However, compared to classic HF with reduced ejection fraction (HFrEF), skeletal muscle alterations induced by HFpEF still remain poorly explored. This can be explained by the recent emergence of the HFpEF population as well as the limited availability of both human muscle samples and experimental models.

To date, the most promising approach for HFpEF-associated muscle dysfunction seems to be a combination of exercise, nutritional, and optimized medical treatment. Nonetheless, evidence from most clinical pharmacological trials have

been negative in terms of beneficial clinical outcomes (Sharma & Kass, 2014; Fukuta *et al.*, 2016), which highlights the need for further research and consideration of alternative approaches. This thesis, therefore, aimed to identify what basic mechanisms contribute to the skeletal muscle pathophysiology in HFpEF and evaluate a range of therapeutic pharmacological, exercise and nutritional interventions.

1.2 Heart failure with preserve ejection fraction (HFpEF)

1.2.1 Definition and epidemiology

According to the latest American College of Cardiology Foundation (ACCF)/American Heart Association (AHA)/European Society of Cardiology (ESC) guidelines (McDonagh *et al.*, 2021; Heidenreich *et al.*, 2022). HF is defined as a multifaceted clinical condition caused by structural and/or functional cardiac changes that affect the ability of the heart to pump a sufficient supply of blood to meet the body's requirements. Common signs and symptoms of HF include fluid retention, pulmonary congestion, elevated jugular venous pressure, dyspnoea, ankle swelling, and exercise intolerance (Ponikowski *et al.*, 2016). The main terminology used to diagnose the type of HF is based on measurement of the left ventricular ejection fraction (LVEF): HF with preserved EF (HFpEF: EF ≥ 50%) and HF with reduced EF (HFrEF: EF ≤ 40%) (McDonagh *et al.*, 2021). HF severity is often classified according to symptomatic status, most commonly using the subjective New York Heart Association (NYHA) functional classification system which is a strong predictor of mortality (Scrutinio *et al.*, 1994). Other more objective approaches to define HF severity and prognosis include the exercise-dependent Weber and Ventilatory classifications (Guazzi *et al.*, 2021).

HF affects approximately 37.7 million people globally and the prevalence is rapidly increasing due to ageing and improved treatments that allow better managements of cardio-metabolic disorders (Vos *et al.*, 2012; Ziaeian & Fonarow, 2016). HF affects nearly 2% of the world's adult population, mainly people aged ≥70 years (Metra & Teerlink, 2017), with roughly 50% categorized as having HFpEF (Dunlay *et al.*, 2017). The epidemic of HFpEF is related to the increasing rate of co-morbidities that are frequently observed in this syndrome, including obesity, diabetes, hypertension and coronary artery disease (Owan *et al.*, 2006; Steinberg *et al.*, 2012; Dunlay *et al.*, 2017; McHugh *et al.*, 2019). Together, these cause failure in several organs including the heart, lungs, adipose tissue, liver, kidney, but also the skeletal muscle. In HFpEF, approximately 20% of HFpEF patients exhibit loss of skeletal muscle mass and reduced strength (Bekfani *et al.*, 2016). Muscle defects are strong predictors of quality of life and mortality, and directly contribute to exercise intolerance in HFpEF (von Haehling *et al.*, 2017; Suzuki *et al.*, 2018). Collectively, this identifies skeletal muscle as a key therapeutic target in HFpEF, yet we still poorly understand what mechanisms are involved and what treatments can rescue muscle health.

1.2.2 Treatment

Identifying effective pharmacological treatments for HFpEF remains a challenge. Whereas treatments that ameliorate the neurohormonal overactivation (e.g., mineralocorticoid-receptor antagonists (MRA) and angiotensin receptor blockers (ARB)) have shown beneficial outcomes in HFrEF (Pitt *et al.*, 1999; McMurray *et*

al., 2003; Zannad *et al.*, 2011; Vaduganathan *et al.*, 2020), they have not improved long-term morbidity and mortality in HFpEF (Yusuf *et al.*, 2003; Cleland *et al.*, 2006; Massie *et al.*, 2008; Pitt *et al.*, 2014). Several therapies for HFpEF with different underlying comorbidities (e.g., hypertension and hyperglycaemia) have been studied and show some but limited benefits. These include angiotensin-converting enzyme inhibitors (ACEI), ARB, MRA, angiotensin receptor neprilysin inhibitors (ARNI), β-blockers, drugs targeting the nitric oxide-soluble guanylyl cyclase—cyclic guanosine monophosphate-protein kinase G pathway, organic and inorganic nitrates, phosphodiesterase-5 inhibitors, soluble guanylyl cyclase stimulators, treatments targeting inflammation and myocardial fibrosis, cell therapy, drugs targeting mitochondria, pressure monitoring, pacemakers, left ventricular expanders, pericardiectomy, and lifestyle modifications such as exercise and caloric restriction (Lam *et al.*, 2018; Silverman & Shah, 2019; Kim & Park, 2021). However, most of these treatments have been cardio-centric and have probably not worked well as they do not provide a systemic, multi-organ approach to treat the marked heterogeneity amongst patients. Only recently did sodium-glucose cotransporter 2 inhibitors (SGLT2I) become the first pharmacological treatment that reduced the risk of cardiovascular deaths and hospitalizations in HFpEF patients (Anker *et al.*, 2021). SGLT2I have also shown to ameliorate patient-reported symptoms and physical limitations, and improve exercise performance in HFpEF patients (Nassif *et al.*, 2021).

1.3 Exercise intolerance in HFpEF

The hallmark of HF is exercise intolerance, which is the result of both age- and HF-related physiological changes (Coats *et al.*, 2017). Exercise intolerance can be objectively quantified by the reduction in peak oxygen consumed during maximal aerobic exercise ($\dot{V}O_{2peak}$) e.g., as used within the Weber's classification. Importantly, impaired $\dot{V}O_{2peak}$ is strongly predictive of a worse prognosis in all types of HF and associated with increased mortality (Nadruz *et al.*, 2017). There is considerable controversy regarding the mechanisms responsible for exercise intolerance in HF patients, especially in HFpEF. Some studies have demonstrated that cardiac function poorly correlates to exercise tolerance in HFpEF (Mohammed *et al.*, 2014), whereas others suggest that reduced exercise capacity is mainly attributable to cardiac output limitations (Abudiab *et al.*, 2013).

Importantly, impaired cardiovascular function seems to explain only some but not all of exercise intolerance seen in HFpEF with evidence strongly suggesting that skeletal muscle defects are also important contributors (Haykowsky & Kitzman, 2014; Miyagi *et al.*, 2018). Various studies have reported that HFpEF patients exhibit clear structural skeletal muscle alterations. Studies Investigating Co-morbidities Aggravating Heart Failure (SICA-HF) evaluated 117 patients with HFpEF and found reduced skeletal muscle mass (measured by DEXA) in approximately 20% of the patients, which was associated with impaired exercise capacity (Bekfani *et al.*, 2016). Other changes reported in HFpEF, compared to healthy age-matched humans, include reduced percent body/leg lean mass (Haykowsky *et al.*, 2013a) and greater thigh intermuscular fat (Haykowsky *et al.*, 2014). Importantly, HFpEF patients with reduced muscle mass have a two-fold

increased risk of cardiac death compared with patients with preserved muscle mass (*via* multivariate Cox proportional hazards model) (Matsumura *et al.*, 2020). As such, understanding the basics of skeletal muscle function, structure, and mass are important for better understanding how a muscle pathology contributes towards HFpEF.

1.4 Skeletal muscle physiology

The primary function of skeletal muscle is contraction, which allows locomotion and breathing. However, from a metabolic perspective, skeletal muscle plays a central role in maintaining body temperature. Skeletal muscle also acts as a storage source for amino acids and carbohydrate. Amino acids released from muscle can be use by other tissues including the heart and the brain for synthesizing organ-specific proteins (Wolfe, 2006). These amino acids also contribute to the maintenance of blood glucose levels during starvation (Frontera & Ochala, 2015).

1.4.1 Basic structure and function

Skeletal muscle consists of thousands of muscle fibres wrapped together by layers of connective tissue including the epimysium, which surrounds the entire muscle, the perimysium, which surrounds bundles of muscle fibres, and the endomysium, which surrounds each muscle fibre (Figure 1.1). Muscle fibres are composed of myofibrils that are arranged in a unique striated pattern forming sarcomeres, the basic contractile units of skeletal muscle composed of myofilaments proteins. The most abundant myofilaments proteins are actin and myosin (comprising ~70 % of the total protein content of a single fibre), although

many other proteins also contribute to the structure of the cytoskeleton (e.g., titin, nebulin) that allow muscle contraction (Frontera & Ochala, 2015). Other cellular elements of muscle fibres that support force production include the T tubule system, the sarcoplasmic reticulum, and mitochondria. Nerves serve as a pathway for electrochemical impulses called action potentials that cause membrane excitation, a fundamental step in muscle contraction. T-tubules are extensions of the cell membrane that allow the conduction of the nerve action potential to the interior of the cell. The sarcoplasmic reticulum is a network of tubules and cisternae specialized for regulating calcium homeostasis during muscle contraction. Muscle contraction begins with the generation of an action potential that depolarises the T tubules causing calcium release from lateral sacs of sarcoplasmic reticulum. Calcium binds to the troponin–tropomyosin complex, which removes the blocking action of tropomyosin from the actin binding sites. Actin then joins myosin ATPase to split ATP into ADP and P_i, which releases energy that produces myosin crossbridge movement. As new ATP binds to the myosin head, the actin-myosin bond weakens and the crossbridge detaches. When muscle stimulation terminates, calcium moves back into lateral sacs of sarcoplasmic reticulum *via* ATP-dependent SERCA pumps, which decreases intracellular calcium concentration and restores inhibitory action of troponin-tropomyosin complex. Mitochondria are the main organelles that allow sustained ATP resynthesis and thus termed energy generators, by converting oxygen and nutrients into ATP (Frontera & Ochala, 2015). Given this requirement, skeletal muscles also have an abundant supply of capillaries to deliver oxygen, nutrients, and hormones while removing waste products to and from the muscles (Egginton, 2011). Skeletal muscle cells are also post mitotic and therefore contain muscle stem (or satellite) cells (SC), located between the sarcolemma

and the basal lamina. SC can differentiate into mature muscle fibres which can either help form new muscle fibres or support hypertrophic growth (Frontera & Ochala, 2015).

1.4.2 Muscle fibre types

Depending on their contractile and metabolic properties, muscle fibres are broadly classified as slow-twitch oxidative Type I and fast-twitch glycolytic Type II. Based on differential myosin heavy chain gene expression, there is further classification of Type II fibres into three major subtypes: IIa, IIb and IIx, although humans do not appear to have type IIb (Schiaffino & Reggiani, 2011). Type I fibres have slow speed of contraction but are more resistance to fatigue, whereas Type II fibres provide greater force production but fatigue faster. Muscle fibres can generate ATP *via* oxidative (aerobic) and glycolytic (anaerobic) pathways. The relative contribution of these two pathways determines the metabolic fibre type. Oxidative fibres have reduced ATPase activity but are rich in myoglobin (the oxygen carrier and pigment responsible for the red colour), have more mitochondrial enzymes, and are surrounded by more capillaries. In contrast, glycolytic fibres have high ATPase and creatine kinase activity but have low myoglobin content, reduced mitochondrial enzymes and less capillaries per fibre (Schiaffino & Reggiani, 2011). Muscle fibre types can transform in response to mechanical stimuli (e.g., exercise) and metabolic perturbations. For example, high physical activity promotes fast-to-slow twitch transformation (Hultman, 1995), whereas obesity is associated with a shift towards fast-twitch phenotype (Denies *et al.*, 2014) (Figure 1.1).

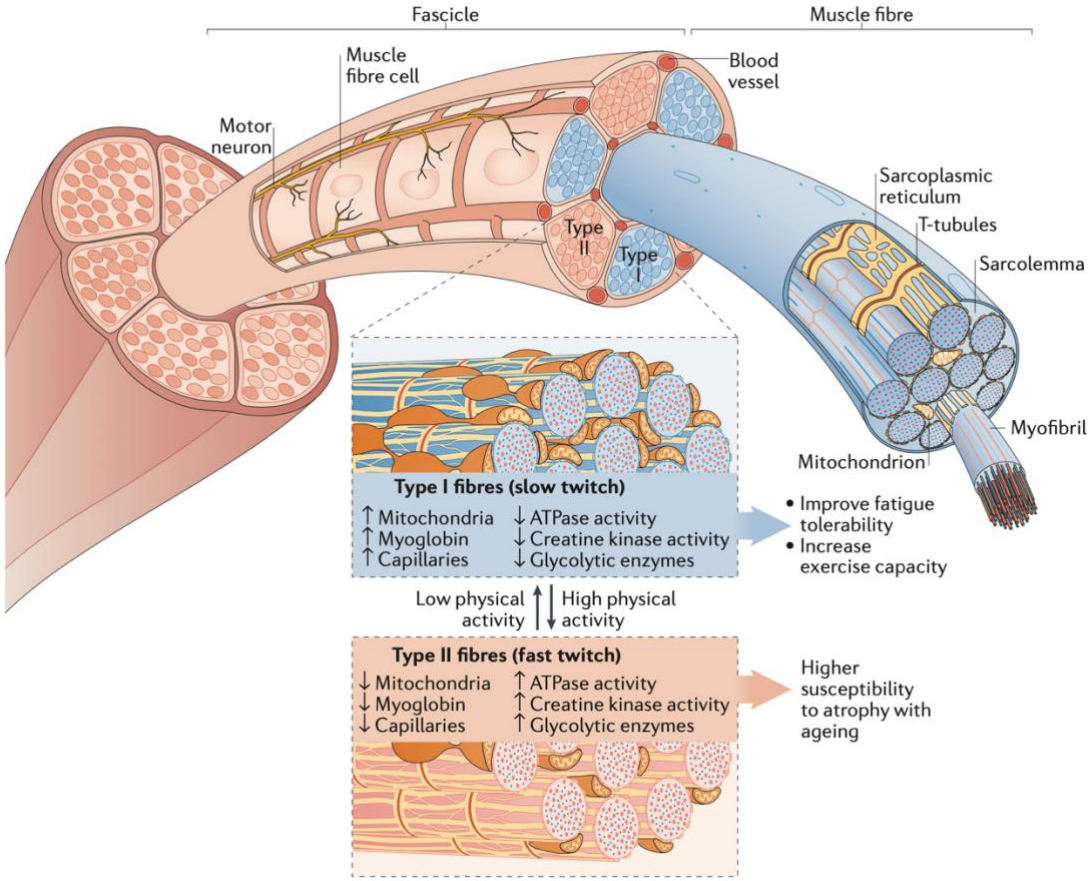

Figure 1.1. Skeletal muscle structure. Skeletal muscle is a complex heterogeneous tissue composed of fibres with diverse contractile and metabolic properties. Figure taken from von Haehling et al., *Nat Rev Cardiol*. 2017.

1.4.3 Muscle mass regulation

Skeletal muscle is the largest organ in the body comprising about ~40-50% of individual body mass (Frontera & Ochala, 2015). Skeletal muscle mass and morphology can be assessed by different techniques including whole-body measurements (e.g., dual x-ray absorptiometry and bioelectrical impedance), localised measurements (e.g., magnetic resonance imaging, peripheral computed tomography, and ultrasound), microscopic assessments (e.g., histological analyses of fibre size, type, and capillarity) and ultramicroscopic and molecular assessments (e.g., transmission electron microscopy and omics technologies) (Haun *et al.*, 2019). Loss of skeletal muscle mass is caused by a

complex interplay between numerous catabolic and anabolic pathways that culminate in a state where protein degradation exceeds protein synthesis.

Protein degradation: Four key protein degradation pathways cause skeletal muscle loss (Figure 1.2), including the ubiquitin–proteasome system (UPS) and the autophagy-lysosomal system, but also but to a lesser degree the calpain and apoptosis mediated caspase pathways. In the UPS, E3 ligases bind selective proteins for ubiquitination and subsequent degradation by the 26S proteasome. Although numerous E3 ligases are recognised, MuRF1 (also known as TRIM63) and MAFbx (also known as FBXO32) show the highest expression in models of muscle wasting (Bodine *et al.*, 2001a; Gielen *et al.*, 2012), and are considered major indicators of skeletal muscle loss. Muscle mass can also be affected by the autophagy-lysosomal pathway, a well-recognised intracellular degradation system by which cytoplasmic materials including proteins are degraded in the lysosomal machinery pathway (Sandri, 2013; Weber *et al.*, 2019). Key triggers of protein degradation include pro-inflammatory cytokines and members of the transforming growth factor-ß family, such as myostatin, also known as growth/differentiation factor-8 (GDF-8) (von Haehling *et al.*, 2017). Elevated levels of TNF and IL-6 promote protein degradation mediated by the UPS, autophagy and apoptosis initiated by caspases (von Haehling *et al.*, 2017). Myostatin, on the other hand, triggers catabolic processes and inhibits transcription of genes that cause proliferation of skeletal muscle cells (Carnac *et al.*, 2007). It binds to activin receptor type 2B (ACTRIIB), and then subsequent downstream mediators phosphorylate mothers against decapentaplegic homolog 2 (SMAD2) and SMAD3 to upregulate atrogene transcription (Han & Mitch, 2011; von Haehling *et al.*, 2017).

Protein synthesis: Testosterone and ghrelin are among the major hormonal regulators of protein synthesis (Figure 1.2), but also growth hormone (GH), which secretes insulin-like growth factor 1 (IGF1). IGF1 binds to the IGF1 receptor (IGF1R) and the insulin receptor (IR), which stimulates phosphorylation of insulin receptor substrate 1 (IRS1). IRS1 activates the phosphoinositide 3 kinase-serine/threonine-protein kinase-mammalian target of rapamycin (PI3K-AKT-mTOR) signalling pathway, which promotes protein synthesis and inhibits glycogen synthase kinase 3 (GSK3) and forkhead box protein O (FOXO). Hence a close cross-talk exists between anabolic and catabolic signalling pathways, where Akt acts as a major inhibitor of FOXO transcription (von Haehling *et al.*, 2017) .

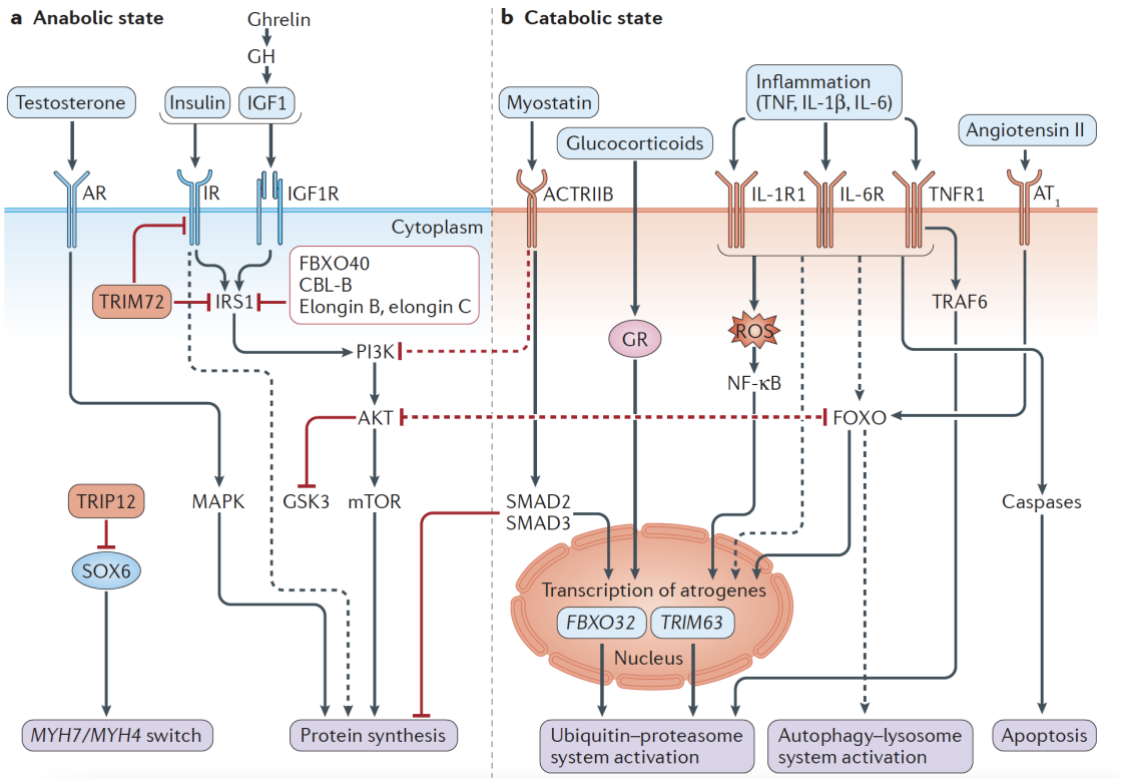

Figure 1.2. Signalling pathways controlling skeletal muscle mass. Skeletal muscle mass is regulated by a complex interplay between numerous catabolic (i.e., the ubiquitin-proteasome system, the calpain pathway, the autophagy-lysosomal system and apoptosis) and anabolic (e.g., the PI3K–AKT–mTOR signalling pathway) pathways. Figure taken from von Haehling et al., *Nat Rev Cardiol*. 2017.

mTOR is widely recognised as a major regulator of protein synthesis and skeletal muscle hypertrophy in response to various mechanical stimuli, such as resistance exercise and synergistic ablation (Goodman, 2014, 2019; Hodson *et al.*, 2019). mTOR is a serine/threonine kinase that integrates environmental and intracellular changes including nutrient availability and energy status, to direct cell growth, differentiation, autophagy, survival, and metabolism (Liu & Sabatini, 2020). Inhibition of mTOR with rapamycin (a selective blocker of mTOR) or by genetic blockade, results in impaired hypertrophy in several models, while its genetic activation is sufficient to cause hypertrophy *in vivo* (Bodine *et al.*, 2001b). mTOR promotes protein synthesis *via* phosphorylation of 4E-binding protein 1 (4E-BP1) and p70 S6 kinase 1 (S6K1) (Liu & Sabatini, 2020). Phosphorylation of 4E-BP1 inhibits its ability to sequester eukaryotic translation initiation factor 4E (eIF4E), a key component of the eIF4F cap-binding complex. Upon phosphorylation by mTORC1, 4E-BP1 releases eIF4E and enhances 5′ cap-dependent translation of mRNAs, which results in increased protein synthesis (Hara *et al.*, 1997; Gingras *et al.*, 1999). On the other hand, phosphorylation of S6K1 promotes ribosomal biogenesis by phosphorylating the ribosomal protein S6 (Chauvin *et al.*, 2014). S6K1 increases transcription of rRNA (the primary component of ribosomes) by improving the activity of RNA polymerase I (Pol I) and RNA polymerase III (Pol III) (Hannan *et al.*, 2003; Mayer *et al.*, 2004) (Michels *et al.*, 2010).

The increase in protein during muscle hypertrophy can be achieved by increasing RNA (as discussed above) but also by maintaining the same level of RNA from each nucleus and adding new nuclei to fibres *via* SC (Blaauw &

Reggiani, 2014). This has been confirmed using the surgical synergist ablation model, also known as compensatory overload (Rosenblatt & Parry, 1992; Adams *et al.*, 2002), which is considered a fundamental model to investigate the basic mechanisms of skeletal muscle hypertrophy (Terena *et al.*, 2017). This model consists of the surgical removal of all or part of synergistic muscles to generate chronic functional overload that causes hypertrophy in the region of ~20-65% (Lowe & Alway, 2002). This method provides a unique opportunity to study cellular changes that would be difficult to observe in models of modest muscle hypertrophy such as exercise (Lowe & Alway, 2002). Since adult myonuclei are postmitotic and cannot divide, it is suggested that during hypertrophy, SC undergo proliferation, differentiation and fusion with existing myofibers in order to provide new myonuclei for growing muscle cells and maintain an optimal myonuclear domain size (Petrella *et al.*, 2006; Petrella *et al.*, 2008; Phillips, 2014; Snijders *et al.*, 2015). This is supported by experiments where overload-induced muscle hypertrophy was prevented in SC-deficient rodents (Rosenblatt & Parry, 1992; Rosenblatt *et al.*, 1994; Adams *et al.*, 2002; Egner *et al.*, 2016). However, findings from other studies have yielded contradictory results (Rosenblatt & Parry, 1993; Lowe & Alway, 1999), and techniques for SC depletion where DNA replication is inhibited either pharmacologically or by γ-irradiation have been questioned (McCarthy & Esser, 2007). Overall recent advances in our understanding of what mechanisms control muscle mass and function have become important for better understanding the muscle pathology in HFpEF.

1.5 Skeletal muscle alterations observed in HFpEF

1.5.1 Muscle size

Few invasive muscle biopsies have been taken from patients with HFpEF, which have limited our understanding. Histological analyses of the *vastus lateralis* muscle demonstrated that compared to healthy adults, patients with HFpEF had a lower percentage of Type I oxidative muscle fibres and this was associated with reduced $\dot{V}O_{2peak}$ (Kitzman *et al.*, 2014). As such, more work has been done in skeletal muscle of HFpEF animal models, although identification of a gold-standard animal model mimicking human HFpEF has been challenging. Available rodent models of HFpEF include the Dahl salt-sensitive (DSS) rat, the Zucker fatty/spontaneously hypertensive heart failure F1 hybrid (ZSF1) rat, the postmenopausal ZSF1 rat, the iNOS KO mouse, and the transverse aortic constriction (TAC) surgery/deoxycorticosterone acetate (TAC/DOCA) mouse. Importantly, these animal models differ in terms of comorbidities (e.g., hypertension, hyperglycaemia, obesity and exercise intolerance) and skeletal muscle alterations (see Table 1.1.) However, a recent study demonstrated that compared to the DSS rat and the TAC/DOCA mouse, the ZSF1 rat shows the highest overlap to the human skeletal muscle phenotype (Goto *et al.*, 2020).

Table 1.1. *Skeletal muscle alterations in animal models of HFpEF*

	ZSF1 rats	Postmenopausal ZSF1 rats	DSS rats	iNOS KO mice	TAC/DOCA mice
Comorbidities	Hypertension Hyperglycaemia Obesity Exercise intolerance	Hypertension Hyperglycaemia Obesity Exercise intolerance	Hypertension Exercise intolerance	Hypertension Hyperglycaemia Obesity Exercise intolerance	Hypertension Exercise intolerance
Muscle mass	↓	↑	↔	?	?
FCSA	↓	↔	↓	?	?
Contractile function	↓	↓	↓	↔	?
Capillarisation	↓	↔	?	?	?
Mitochondrial function	↓	↓	↓	?	?

↑ Increase, ↓ Decrease, ↔ Unchanged, ? Unknown

Oxidative (*soleus*) and glycolytic (*extensor digitorum longus*, EDL) muscle biopsy samples from obese ZSF1 rats demonstrated a ~40% and 50% reduction in fibre cross sectional area (FCSA), respectively. Moreover, compared to controls, *soleus* and EDL wet-mass at 20 weeks were reduced in HFpEF rats. Interestingly, the atrophy was not reversed by 8 weeks of endurance exercise training (Bowen *et al.*, 2018). Other animal models of HFpEF including the DSS rat (Bowen *et al.*, 2015), the TAC/DOCA mouse (Goto *et al.*, 2020)., and the iNOS KO mouse (Schiattarella *et al.*, 2019) have been characterised but found contradictory findings, with the ZSF1 rat remaining as the one that best replicate the skeletal muscle phenotype of HFpEF patients (Goto *et al.*, 2020).

1.5.2 Vascular changes

Initial studies showed reduced capillary supply in HFpEF patients, represented as capillary-to-fibre ratio (C:F) *vs* age-matched controls, and this was an independent predictor of $\dot{V}O_{2peak}$ (Kitzman *et al.*, 2014). Reduced C:F was also observed in the soleus and EDL muscles of obese-HFpEF ZSF1 rats (Bowen *et*

al., 2018). In terms of direct measures, peripheral blood flow remains unexplored in HFpEF although some non-invasive studies suggest that HFpEF patients have blunted functional hyperaemia (Lee *et al.*, 2016b; Marechaux *et al.*, 2016; Kishimoto *et al.*, 2017; Weavil *et al.*, 2021), but this is not consistent (Hundley *et al.*, 2007; Haykowsky *et al.*, 2013b; Lee *et al.*, 2016a; Zamani *et al.*, 2020). Discrepancies may be attributed in part to differences in the muscle studied, different measurement techniques, and patient heterogeneity (Loai *et al.*, 2021; Ratchford *et al.*, 2022). Vascular dysfunction related to reduced capillary supply could also impact arterial–venous O_2 content (ΔAVO_2), which is a metric of O_2 extraction. Some (Bhella *et al.*, 2011a; Haykowsky *et al.*, 2011; Dhakal *et al.*, 2015) but not others (Abudiab *et al.*, 2013; Santos *et al.*, 2015) have reported that HFpEF affects peripheral O_2 extraction. Importantly, these studies used the Fick equation to estimate exercise capacity ($\dot{V}O_2 = Q \cdot \Delta AVO_2$) which assumes that cardiac output (Q) and ΔAVO_2 are independent of each other. However, while ΔAVO_2 integrates several non-cardiac O_2 factors (e.g., muscle diffusion and mitochondrial O_2 consumption), its value also depends on Q. For example, faster transit times of red blood cells through local capillaries means less time for O_2 diffusion into muscle mitochondria, which in turn can compromise ΔAVO_2. Indeed, HF reduces the proportion of capillaries that support red blood cell flux at rest and during exercise (Poole *et al.*, 2012). Unperfused capillaries at rest remain stagnant during contractions, which limits muscle O_2 diffusing capacity and thus ΔAVO_2 (Poole *et al.*, 2012). Endothelial dysfunction may also contribute to the impaired ability of HFpEF patients to widen ΔAVO_2 and augment peripheral O_2 extraction during exercise (Bhella *et al.*, 2011a; Haykowsky *et al.*, 2011; Dhakal *et al.*, 2015; Houstis *et al.*, 2018; Zamani *et al.*, 2020). Endothelial dysfunction, as a result of reduced nitric oxide production, can inhibit peripheral

vasodilation and regional blood distribution thus affecting ΔAVO_2 (Vella *et al.*, 2011). More studies examining leg/muscle ΔAVO_2, fibre size and capillarisation are warranted to clarify the role of the macro- and microcirculation in HFpEF. While data suggest that anatomical and functional alterations at the microvascular level contribute to the pathophysiology of HFpEF, direct invasive measurements to reinforce these suggestions are still missing.

1.5.3 Mitochondrial function

Most studies on skeletal muscle mitochondria have been performed in HFrEF, with less known about HFpEF. ^{31}Phosphorus magnetic resonance spectroscopy (^{31}P-MRS) is recognised as the gold standard for measuring mitochondrial function *in vivo*. Using this technique, HFpEF patients demonstrated more rapid phosphocreatine (PCr) depletion, lower oxidative phosphorylation ATP production, greater anaerobic glycolysis ATP production, and delayed PCr recovery during exercise. (Bhella *et al.*, 2011a; Weiss *et al.*, 2017). This indicates a clear shift from reliance of oxidative to glycolytic metabolism that predisposes towards exercise intolerance. Direct measures of muscle samples have extended these findings. Animal experiments demonstrated that *soleus* biopsies from HFpEF (DSS) rats had reduced enzyme activity of citrate synthase (Bowen *et al.*, 2015), a well validated biomarker for mitochondrial content and oxidative capacity (Larsen *et al.*, 2012). A recent study also showed that mitochondrial density is lower in HFpEF patients comparing to healthy controls and HFrEF patients, with expression of mitochondrial genes reduced (Bekfani *et al.*, 2020). This is reinforced by HFpEF patients having lower expression of porin, mitofusin 2, and citrate synthase in the *vastus lateralis* – markers of content and

morphology. Importantly, the expression of porin and mitofusin 2 was positively related to both $\dot{V}O_{2peak}$ and 6 minute walk distance (Molina *et al.*, 2016). However, contradictory evidence found porin expression was increased in muscle tissue of HFpEF patients and obese-HFpEF (ZSF1) rats (Goto *et al.*, 2020). More studies are clearly warranted to define the mitochondrial signature in HFpEF.

1.5.4 Contractile function

So far, only a few studies have investigated the effect of HFpEF on skeletal muscle contractile function. A recent *in vivo* study confirmed that compared to age-matched healthy individuals and HFrEF patients, HFpEF patients have reduced muscle strength during knee extension (Bekfani *et al.*, 2020), while diaphragm weakness was linked to reduced exercise capacity and poor quality life (Meyer *et al.*, 2001; Yamada *et al.*, 2016; Miyagi *et al.*, 2018). However, most studies have been performed in HFrEF and little remains known about the effect of HFpEF on diaphragm function and structure. In isolated whole-limb muscles, *in vitro* contractile function of two different animal models of HFpEF has been tested. The first study used DSS rats and found the *soleus* muscle was more fatigable in HFpEF rats and maximal tetanic specific force was lower (Bowen *et al.*, 2015). Subsequent experiments in ZSF1 rats demonstrated that absolute and specific limb skeletal muscle forces were reduced in obese-HFpEF rats compared to lean controls (Bowen *et al.*, 2018; Schauer *et al.*, 2021; Kelley *et al.*, 2022) but not fatigue (Bowen *et al.*, 2018). Moving from whole muscle to single muscle fibres, no study has directly addressed this *per se*. However, compared to non-diseased controls, a combined HF population (6 HFrEF and 4

HFpEF patients) exhibited lower myosin heavy chain protein content, coupled with impaired single muscle fibre maximal Ca^{2+}-activated tension in Type I fibres from *vastus lateralis* muscle. Importantly, physical activity levels were similar between groups, indicating fibre contractile dysfunction were induced by HF rather than inactivity alone (Miller *et al.*, 2009). Collectively, these data suggest that HFpEF negatively affects skeletal muscle contractile performance, but more research is still needed.

1.6 Mechanisms of skeletal muscle weakness in HFpEF

1.6.1 Inflammation

A pro-inflammatory phenotype of HFpEF is increasingly recognised. Several studies have shown that HFpEF patients have an increased serum concentration of IL-6 and tumour necrosis factor alpha (TNF-α) (Kalogeropoulos *et al.*, 2010; Fulster *et al.*, 2013; Adams *et al.*, 2021). Another study compared circulating inflammatory cytokines between HFrEF, HFpEF and control rats and confirmed concentrations of TNF-α were elevated in HFrEF, whereas interleukin-1ß (IL-1β) and interleukin-12 (IL-12) were higher in HFpEF (Seiler *et al.*, 2016). However recent research showed that serum concentrations of IL-1β are not different between patients with HFpEF, HFrEF and sedentary controls (Adams *et al.*, 2021). HFpEF patients have also shown elevated concentrations of growth differentiation factor-15 (GDF-15), a hormone produced in response to mitochondrial, metabolic and inflammatory stress, and this was associated with higher levels of Kynurenine, a biogenic amine and metabolite of tryptophan (Bekfani *et al.*, 2022).

Elevated IL-6 and TNF-α concentrations are known to activate the NF-κB signalling pathway, which modulates immune, inflammatory and cell proliferative responses, thereby exacerbating the physiological state of skeletal muscle (Mourkioti & Rosenthal, 2008). In HFrEF patients, pro-inflammatory cytokines can promote the generation of reactive oxygen species (ROS) and activate FOXO proteins, which trigger the expression of atrogenes MuRF1 and MAFbx (von Haehling *et al.*, 2017). However, this interaction between pro-inflammatory cytokines, ROS and protein degradation remains unexplored in HFpEF, with some data causing further complication by showing HFpEF reduced muscle ROS and proteolysis in hypertensive rats (Bowen *et al.*, 2015; Seiler *et al.*, 2016). To date, only systemic inflammation has been studied in HFpEF, whereas local inflammation in the skeletal muscle remains unexplored.

1.6.2 Protein degradation

Increased expression levels of MuRF1 and MAFbx and increased ubiquitinated proteins and proteasome activity have been observed in HFpEF patients when comparing to healthy controls (Goto *et al.*, 2020; Adams *et al.*, 2021). Impairments in the UPS or related proteins have also been observed in animal models of HFpEF including obsese-ZSF1 rats and DSS rats (Bowen *et al.*, 2017b; Goto *et al.*, 2020), while pharmacological inhibition of MuRF1 (*via* small molecules) attenuated HFpEF-induced impairments in muscle atrophy and dysfunction in obese-ZSF1 rats (Adams *et al.*, 2022). In terms of autophagy, the ratio of LC3 I/II was down regulated in human muscle biopsies and obese-ZSF1 rats (Goto *et al.*, 2020), which is in accordance to previous research (Bowen *et al.*, 2018). Taken together, these observations demonstrate that changes to both

UPS and autophagy are present in HFpEF, with obese ZSF1 rats closely reflecting changes in patients. Compared with HFrEF and healthy controls, HFpEF patients showed increased skeletal muscle myostatin expression and this was associated with impaired muscle strength (Bekfani *et al.*, 2020). Furthermore, various studies have reported that myostatin is increased in the serum (Gruson *et al.*, 2011), skeletal muscle (Lenk *et al.*, 2012) and heart (Fernández-Solà *et al.*, 2011) of HFrEF patients, while myostatin deletion from heart prevented skeletal muscle atrophy in HFrEF mice (Heineke *et al.*, 2010). Taken together, these findings suggest that skeletal muscle protein degradation in HFpEF is likely mediated by myostatin, although direct evidence still is missing.

1.6.3 Protein synthesis

To date, limited studies in HFpEF have focused on muscle growth and anabolic resistance (impaired protein synthesis). How HFpEF affects mTOR signalling and protein synthesis in skeletal muscle remains to be elucidated. Data from a mixed HF patient (HFrEF n = 6; HFpEF n = 5) study showed that phospho- or total protein contents of mTOR, 4E-BP1 and S6K1 in skeletal muscle were not different between HF patients and healthy controls, although phospho-mTOR/mTOR was associated to knee extensor strength (Toth *et al.*, 2011). In relation to the IGF1 axis, some (Barroso *et al.*, 2016; Bruno *et al.*, 2020) but not all (Faxén *et al.*, 2017) human studies showed that HFpEF patients have reduced IGF1 serum levels. Further, HFpEF (DSS) rats exhibited lower IGF1 gene expression in the soleus muscle compared to controls (Seiler *et al.*, 2016); yet, this remains to be confirmed in skeletal muscle of HFpEF patients. Maintenance

of muscle mass is also regulated by the anabolic effects of testosterone and a recent study demonstrated that 37% of HFpEF patients had testosterone deficiency (Bruno *et al.*, 2018), but the interaction on skeletal muscle in HFpEF remains to be established. In addition to increases in net protein synthesis *via* Akt-mTOR signalling axis, muscle hypertrophy can occur by addition of new myonuclei *via* SC. The role of SC on skeletal muscle mass at baseline or in response to mechanical stimuli in HFpEF remains unexplored, although HFrEF studies have provided promising data. For example, muscle regeneration was reduced in HFrEF mice and was accompanied by a blunted increase expression of AT2R, an important regulator of SC differentiation (Yoshida & Delafontaine, 2016). Further, skeletal muscle myoblasts from HFrEF patients showed reduced proliferative activity with similar morphological and myogenic differentiation responses (Sente *et al.*, 2016). In contrast, another study found that functional properties of muscle stem cells from HF patients are not dramatically affected (Dmitrieva *et al.*, 2019). More research is clearly needed to determine whether SC contribute to the skeletal muscle deficits associated with HF and especially HFpEF.

1.7 Treatments of skeletal muscle weakness in HFpEF

1.7.1 Exercise training

Exercise training remains the only proven treatment to improve skeletal muscle health in HF. In the first single-blinded randomized exercise trial (4 months endurance exercise training x 3 day/week) in older HFpEF patients, $\dot{V}O_{2peak}$, exercise time, 6-minute walk distance, and physical quality of life were all improved without altering cardiac function and structure (Kitzman *et al.*, 2010).

This highlights non-central organs as key determinants of exercise tolerance in HFpEF rather than cardiac factors alone, which is supported by other studies (Edelmann *et al.*, 2011). Importantly, however, these trials were mainly focused on the cardiorespiratory function and little is known about how exercise directly affects skeletal muscle structure and function in this syndrome with most data coming from experimental models. The ZSF1 HFpEF rat model was evaluated after 8 weeks of high-intensity interval training (3 x week; 4 intervals at 90% $\dot{V}O_{2peak}$ for 4 minutes, with 3 minutes of recovery at 60% $\dot{V}O_{2peak}$) or moderate-continuous training (5 x week at 60% $\dot{V}O_{2peak}$) and muscle impairments could not be reversed by exercise training (Bowen *et al.*, 2017b; Bowen *et al.*, 2018). Collectively, these studies suggest that, although exercise can clearly improve the quality of life of this population, further research is still needed on how it affects skeletal muscle.

1.7.2 Nutritional treatment

Nutrition can influence skeletal muscle structure and function, but little is known about its therapeutic potential in HF patients. To date, one study investigated the effects of caloric restriction (CR) in obese-HFpEF patients for 20 weeks and confirmed diet significantly increased $\dot{V}O_{2peak}$, thigh muscle area, muscle function, and quality of life scores (Kitzman *et al.*, 2016). Importantly, the combination of diet and exercise produced a synergistic effect (Kitzman *et al.*, 2016). This identifies CR as a potential effective therapy to counteract the HFpEF pathology, potentially by benefiting skeletal muscle defects. Other nutritional treatments implemented in HFrEF patients that may have benefits to skeletal muscle and be relevant for HFpEF include amino acid supplementation (Aquilani

et al., 2008) dietary (inorganic) nitrates (McDonagh *et al.*, 2019), vitamin D supplementation (Jiang *et al.*, 2016) and omega 3 polyunsaturated fatty acids (PUFA) (Mehra *et al.*, 2006).

1.7.3 Pharmacological treatment

Whether clinical medications used in HFpEF (e.g., SGL2I, ARNI) benefit skeletal muscle to provide functional and clinical benefits remains poorly explored, but encouraging data exists in HFrEF. A small study in HFrEF patients showed that a 6-month treatment with the ACEI Enalapril (n = 8) or Losartan (n = 8) improved exercise capacity and reversed fibre type shifts (Vescovo *et al.*, 1998). In addition, the magnitude of myosin heavy chain (MHC) changes was associated with improvements in exercise capacity (Vescovo *et al.*, 1998), while Enalapril may prevent cardiac cachexia (Anker *et al.*, 2003). Importantly, the ARNI Entresto, which combines Valsartan and Sacubitril, has been proven to be superior to Enalapril in HFrEF patients regarding cardiovascular deaths and HF hospitalizations (McMurray *et al.*, 2014). However, compared to Valsartan, Entresto failed to reduce the same endpoints in HFpEF patients (n = 4822) (Solomon *et al.*, 2019). Further, a recent study demonstrated that Entresto improved cardiac measures in HFpEF rats but did not impact gross measures of muscle wet-mass and function (Schauer *et al.*, 2021). MRA have also shown beneficial effects on muscle quality in hypertensive rats (Hernández *et al.*, 1996) and on exercise capacity in HFpEF patients (Edelmann *et al.*, 2013). Taken together, these findings suggest that cardiovascular medications including SGLT2I, ACEI and MRA may improve exercise capacity in HFpEF patients, but their impact on skeletal muscle structure and function remains unclear. Other

specific medications used in HFrEF that may benefit muscle atrophy include ghrelin (Nagaya *et al.*, 2004), testosterone (Toma *et al.*, 2012) and myostatin inhibitors (Jasuja & LeBrasseur, 2014) although neutral findings or side effects such as diarrhoea, confusion and involuntary muscle contractions are common (Jasuja & LeBrasseur, 2014). Overall, more research is needed to identify effective pharmacological treatments for HFpEF-associated muscle deficits.

1.8 Overall aims and objectives of thesis

HFpEF is characterised by a skeletal muscle pathology that remains poorly understood with limited treatments. This is partly due to the muscle phenotype in HFpEF remaining poorly defined, which has prevented clear therapeutic targets being identified and developed. Indeed, it remains poorly tested if pharmacological drugs used to treat the HFpEF condition directly benefit skeletal muscle health, as is the case for other non-pharmacological treatments such as exercise training or CR. As such, the overall aim of this thesis is to reveal new insights into the fundamental mechanisms underlying the skeletal muscle pathology in HFpEF by examining the effects of pharmacological, exercise/mechanical-load, and nutritional interventions. Using a well-established obese-experimental rat model, this thesis aimed to:

i. Comprehensively characterise skeletal muscle function, morphology, and vascularity in HFpEF.

ii. Determine whether clinically relevant cardiovascular medications improved the skeletal muscle phenotype in HFpEF.

iii. Determine if skeletal muscle hypertrophy is reduced following increased mechanical-load in HFpEF.

iv. Determine if caloric restriction could restore skeletal muscle health in HFpEF.

We hypothesized that HFpEF is characterised by a skeletal muscle pathology, but this can be partially reversed following treatment with pharmacological, exercise, and/or dietary interventions.

Chapter 2 General methods

2.1 Ethical approval

This thesis includes four studies. All procedures and experiments included in Results I, III, and IV were performed in accordance with the UK Scientific Procedures (Animals) Act 1986 and local approval was given by the University of Leeds Animal Welfare and Ethical Review Committee. Experiments in Results II were performed with collaborators at University of Oslo, Norway, and approved by the Norwegian Food Safety Authority committee (Mattilsynet) for animal research (FOTS protocol number 15886) in accordance with the national regulations, the European Convention for the Protection of Vertebrate Animals used for Experimental and Other Scientific Purposes (ETS No.123), and the European Directive 2010/63/EU on the protection of animals used for scientific purposes.

2.2 Animals

Male obese (HFpEF) and lean (controls) diabetic Zucker fatty/spontaneously hypertensive heart failure F1 hybrid (ZSF1) rats were purchased from Charles River at 13-18 weeks of age. This hybrid rat is a cross between a ZDF female and an SHHF male rat. While both lean and obese ZSF1 rats inherit the hypertension gene, only the obese ZSF1 rats inherit a mutation in the leptin receptor gene (*Lepr*^{fa}*Lepr*^{cp}*/Crl*) that drives weight gain and metabolic impairments associated with typical signs of HFpEF developing as early as 10 weeks of age (Schauer *et al.*, 2020) and well established after 20 weeks (Leite *et al.*, 2015; Franssen *et al.*, 2016; van Dijk *et al.*, 2016; Bowen *et al.*, 2017b). All

rats were kept at a 12 h light/dark cycle. Unless stated, rats were fed ad libitum with standard chow and access to water.

2.3 Cardiometabolic function

Hearts were perfused and immersion fixed *ex vivo* using low osmolality Karnovsky's fixative, then imaged using a diffusion-weighted fast spin echo sequence at a resolution of 120 μm isotropic (Teh *et al.*, 2016). These data were used to calculate mean thicknesses of the left and right ventricular free walls and the septum, for tissue located in the middle third of the distance between the base and apex of the appropriate ventricular cavity. Myocyte helix angles (quantifying myocyte inclination with respect to the short axis of the heart) were extracted from regions in the left and right ventricular free walls and the septum as previously described (Benson *et al.*, 2011); myocyte disarray in these regions was quantified using the R^2 of a 5^{th} order polynomial fit to the helix angles plotted as a function of transmural distance (Benson *et al.*, 2008). All DT-MRI analyses were carried out using in-house software. Cardiometabolic impairments were confirmed by measures of body weight, mean arterial pressure (*via* an implanted carotid catheter (PP10)) with a blood pressure transducer (BP transducer, AD Instruments, UK) and blood glucose levels (*via* a commercial blood glucose meter (FreeStyle Mini Meter).

Cardiac function was assessed by transthoracic echocardiography using a VEVO 3100 high-resolution *in vivo* imaging system from VisualSonics. Briefly, animals were maintained under anesthesia (1.5-2% isoflurane mixed with oxygen) on a pre-warmed ECG transducer pad with body temperature and ECG

monitored. Measurements were made with an MS250 transducer, frequency set at 20 MHz. B-mode measurements in the parasternal long axis view were obtained to assess the function and dimension of the left ventricle (LV). M-mode tracings through the aortic root and the left atrium (LA) were used to assess LA diameter. LVEF was calculated as 100 * ((LV Vol;d - LV Vol;s) / LV Vol;d). LV mass was estimated by the formula: 1.053 * ((LVID;d + LVPW;d + IVS;d)3 - LVID;d3). Relative wall thickness (RWT) was calculated as 2 * LVPW;d / LVID;d.7 E and A waves in LV filling velocities were assessed *via* pulsed-wave Doppler in the parasternal long axis view. Early (E wave) and late (A wave) ventricular filling velocities were assessed *via* pulsed-wave Doppler in an apical 4-chamber view. Myocardial velocities (e' and A') were measured using tissue Doppler imaging at the level of the basal septal segment of the LV in an apical 4-chamber view. Cardiac output (CO) was estimated from the dimension of the LV on the M-mode view.

2.4 Synergist muscle ablation

To induce EDL hypertrophy, unilateral synergistic surgical ablation of the *tibialis anterior* (TA) muscle was performed as previously described (Frischknecht & Vrbova, 1991). Briefly, rats were weighed and anaesthetised with an intraperitoneal injection of chloralhydrate (45 mg.100 g^{-1} body mass). Under aseptic conditions, the TA muscle was then separated from the underlying structures by blunt dissection and cut as close as possible to its proximal insertion, ensuring that no damage to surrounding tissue occurred, while keeping the EDL muscle insertion intact. The contralateral limb was used for sham surgery, in which TA and EDL muscles were identified but not separated. During

recovery from surgery, all rats received a subcutaneous injection of the analgesic buprenorphine (0.03 mg/kg body weigh). All rats were ambulatory throughout the 14-day experimental period, and no postoperative complications were detected. The compensatory overload model allows a paired comparison between contralateral and overloaded muscles, which avoids biases resulting from the use of different animals (Thomson & Gordon, 2006).

2.5 *In situ* muscle performance and femoral artery blood flow

In situ measurements of muscle function and blood flow were made under surgical anaesthesia, which was induced with isoflurane (4 % in 100 % oxygen) and maintained throughout experiments by constant syringe pump infusion (30-35 mg kg^{-1} h^{-1}) of Alfaxalone (Jurox, Crawley, UK) delivered *via* an implanted jugular vein catheter. *In situ* functional assessment of muscle performance was determined as previously described (Egginton & Hudlicka, 1999; Tickle *et al.*, 2020). In brief, EDL isometric twitch force was recorded *via* a lever arm force transducer (305B-LR: Aurora Scienctific, Aurora, ON, Canada) following surgical extirpation of the overlying synergist TA muscles. Electrical stimulation of the EDL (0.3 ms pulse width) was accomplished *via* electrodes placed adjacent to the popliteal nerve (Hudlická *et al.*, 1977), with initial electrical pulses (1 Hz) delivered to determine optimal muscle length and supramaximal current delivery. Simultaneous measurement of bilateral blood flow was facilitated by placement of perivascular flow probes (0.7PSB; Transonic, Ithaca, NY, USA) on the proximal portion of the femoral artery, adjacent to the *profunda femoris* bifurcation (Tickle *et al.*, 2020). Quantification of resting and end stimulation flows enabled determination of the functional hyperaemia recruited during stimulation (see Figure 2.1). Blood flow data is provided (ml min^{-1}) and after

normalisation for blood pressure variation, vascular conductance (ml min^{-1} mm Hg^{-1}). All data were recorded *via* PowerLab and LabChart software (AD Instruments, UK).

EDL twitch and maximal tetanic force, as well as fatigue resistance, were also assessed. Fatigue resistance was quantified by monitoring isometric force throughout a period of continuous 10 Hz stimulation for 3 min. A fatigue index (FI) was then calculated as: (end-stimulation twitch tension/peak twitch tension) x 100. An average of five consecutive twitches was used to quantify end stimulation and peak EDL tension. Differences in the magnitude of the absolute tetanic force generated between groups were taken into account by employing a second bout of fatigue stimulation, such that absolute forces in HFpEF were initially similar to those attained in controls (i.e., matched initial force) (Ferreira *et al.*, 2010). This protocol is relevant for clinical translation of muscle fatigue, where daily tasks in patients are often dependent upon absolute rather than relative force. Thus, by adjusting the stimulation frequency in HFpEF rats to around 25 Hz, tetanic force was increased and matched to the level recorded in the lean group, with fatigue allowed to proceed over 3 min. In addition, tetanic force production was quantified by 200 Hz stimulation (200 ms duration) after a minimum of 10 min recovery from fatigue, as determined by restoration of pre-fatigue resting blood flow. All protocols were performed in exactly the same order for each rat, thus minimising any effects of methodological variation. Force is presented in absolute units (g) and normalised to wet mass (g mg^{-1}).

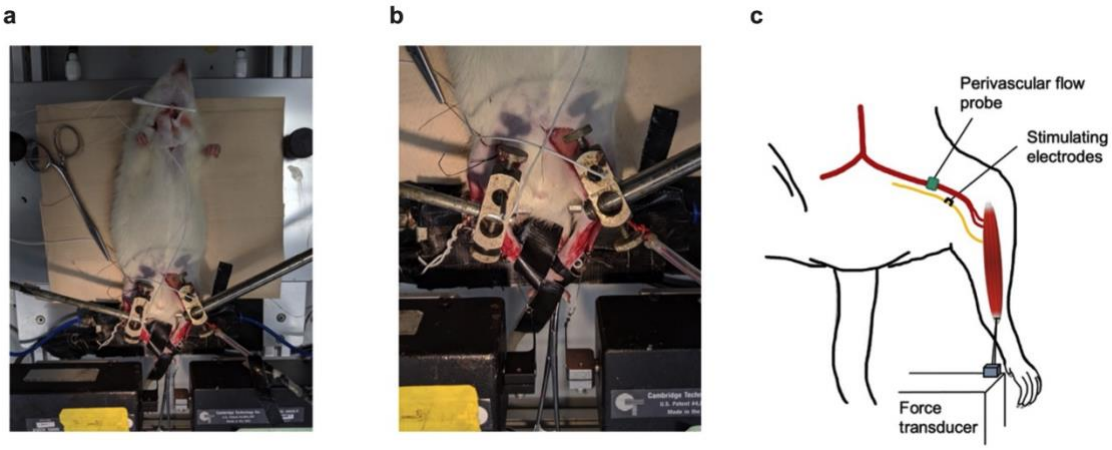

Figure 2.1. *In situ* assessment of muscle performance and femoral artery blood flow. *Extensor digitorum longus* (EDL) muscle was electrically stimulated (0.3 ms pulse width) *via* electrodes placed adjacent to the popliteal nerve, while isometric force was recorded via a lever arm force transducer. Simultaneous measurement of bilateral blood flow was facilitated by placement of perivascular flow probes **(a-c)**.

2.6 *In vitro* functional assessment

Immediately following euthanasia, the soleus and diaphragm were excised and prepared in a Krebs-Henseleit solution (117 NaCl, 4.7 KCl, 1.2 $MgSO_4$, 1.2 KH_2PO_4, 24.8 $NaHCO_3$, 2.5 $CaCl_2$, 11.1 glucose; in mmol l^{-1}) at 4°C equilibrated with 95% O_2 /5% CO_2. For the soleus, silk sutures (4.0) attached to tendons at either end were used to suspend the muscle vertically in a buffer-filled organ bath between a hook and a length-controlled lever system (305C, Aurora Scientific, Aurora, Canada). *In vitro* field stimulation using platinum electrodes was provided *via* a high-power bipolar stimulator (701C, Aurora Scientific) outputting supramaximal current (700 mA; 1 s train duration; 0.25 ms pulse width). After optimal contractile length (L_0) was determined, the muscle was thermoequilibrated in a Krebs-Henseleit solution for 15 min at ~21°C (Bowen *et al.*, 2017a). For the diaphragm, a bundle of muscle fascicles (~2-3 mm wide) was removed from the medial section of the left costal diaphragm leaving two ribs and a section of the central tendon intact. The muscle bundle was transferred to

a flow-through muscle chamber and anchored between a base and ergometer (series 300B-LR, Aurora Scientific Inc.) and stimulated through parallel platinum electrodes using a stimulus isolation unit (0.2 ms pulse width; UISO model 236, Hugo Sachs Elektronik). After L_0 was determined, the diaphragm bundle was thermoequilibrated in a Krebs-Henseleit solution for at least 15 min at 37°C. Each muscle was circulated with oxygenated (95% O_2/5% CO_2) Krebs-Henseleit solution throughout each experiment.

The soleus underwent two protocols: isometric force-frequency and isotonic force-velocity. The force-frequency relationship was determined in response to pulses at 1, 15, 30, 50, 80, 120 and 150 Hz, with 1 min of recovery between contractions. After a 5 min period in which muscle length was measured using digital callipers, the soleus was subjected to a series of after loaded-isotonic contractions to determine the force-velocity relationship, where the muscle was allowed to shorten against external loads (80 - ~5% of the maximal tetanic force; each separated by 1 min for the soleus or 5 min for the diaphragm) after being stimulated at 150 Hz for 300 ms. Shortening velocity was determined 10 ms after the first change in length and on the linear section of the transient (605A DMA software, Aurora Scientific). For the diaphragm, maximal isometric twitch and tetanic (250 ms train at 150 Hz), isotonic force-velocity (as above), and work-loop protocols were performed. Muscle performance assessed using the work loop technique included simulating performance *in vivo*, by subjecting the muscle to cyclical length changes and phasic stimulation (Josephson, 1985). A sinusoidal length change at a range of cycle frequencies (1-15 Hz) and strain amplitude of 0.065 L_0 was imposed on the muscle and, for each cycle frequency, the timing and duration of stimulation were optimised to maximise net work.

Isometric tetanic contractions and cyclical contractions at 5 Hz were performed periodically to monitor any decline in the preparation, assessed by expressing isometric stress (isotonic contractions) and net work relative to maximal values. A linear decline in performance was assumed in correcting data for preparation decline. A period of 5 min was allowed following isotonic and work loop contractions for recovery. To assess the muscle's ability to sustain work, a fatigue test was done by subjecting the muscle to a series of cyclical contractions (cycle frequency 2 Hz, strain amplitude 0.065 L_0, phase - 20 ms relative to peak length, 210 ms stimulation duration). Custom software was used to control muscle length and stimulation and to acquire length and force data (CEC Testpoint version 7) *via* a D/A data acquisition card (DAS1802AO, Keithley Instruments). Data were acquired at a sample frequency of 10 kHz (isometric and isotonic) or 1000 x cycle frequency (work loops).

At the end of each experiment, the muscle was blotted on paper tissue and wet mass recorded. Force (N) was normalised to muscle cross-sectional area (CSA; cm^2) after dividing muscle mass (g) by the product of L_0 (cm) and estimated muscle density (1.06 g/cm^3) to allow specific-force (i.e., stress) in N/cm^2 to be calculated (Close, 1972). Shortening velocity was normalised to optimal muscle length (in L_0/s), while power was calculated as the product of shortening velocity and force normalised to muscle mass (in W/kg). Twitch properties (i.e., peak force, time-to-peak tension and half relaxation time) as well as maximal isometric tetanic force (i.e., P_0) were calculated. A hyperbolic-linear relationship was fit to the force-velocity data to determine the maximum shortening velocity (V_{max}), peak isotonic power ($\dot{W}_{max}$) and the power ratio ($\dot{W}_{max}/(P_0 \times V_{max})$), a measure of the curvature of the force-velocity relationship (Marsh & Bennett, 1986).

2.7 Mitochondrial respiration

In situ mitochondrial respiration (JO2) was assessed in permeabilised EDL muscle fibres using high resolution respirometry (Oxygraph-2k: Oroboros Instruments, Innsbruck, Austria), as described elsewhere (Bowen *et al.*, 2015). Samples were dissected in BIOPS solution (Table 2.1), permeabilized in saponin (50 µg/ml) for 30 min, washed (twice) in MIR06 for 10 min, weighed and immediately transferred to the chambers of the high-resolution respirometer, where each chamber contained 2 mL of MiR05 at 37°C. Chambers were oxygenated (~450 nmol·mL^{-1}) before starting the experiments. A standard described substrate, uncoupler, and inhibitor titration (SUIT) protocol (Grassi *et al.*, 2017) was then used for measuring leak respiration with complex I substrates (L_I) and oxidative phosphorylation with complex I (P_I) and complex I+II substrates (P_{I+II}) as well as uncoupled respiration in the presence of complex I+II (E_{I+II}) and complex II substrates (E_{II}). Substrates were injected in the following order: blebbistain (2 µL), glutamate (10 µL), malate (2.5 µL), pyruvate (5 µL), ADP (10 µL), cytochrome c (5 µL), succinate (20 µL), FCCP (1 µL), rotenone (5 µL), antimycin A (5 µL), ascorbate (5 µL), TMPD (5 µL) and sodium azide (10 µL). Cytochrome c was added to evaluate the integrity of the mitochondrial outer membrane (samples with a >15% increase in respiration rate were excluded) and intrinsic function was assessed following normalization to mitochondrial content (complex IV activity; C_{IV}) in addition to the coupling efficiency (i.e., respiratory control ratio, RCR: complex I phosphorylated state/complex I leak respiration).

Table 2.1. *Solutions and compounds used to make BIOPS*

Solution/Compound	Final con.	Molecular weight	Stock solution	Addition to 1 litre	Source and product code
CaK_2EGTA	2.77 mM		100	27.7 ml	
K_2EGTA	7.23 mM		100	72.3 ml	
Na_2ATP	5.77 mM	551.01.00		3.141 g	Sigma A2383
$MgCl_2 \cdot 6\ H_2O$	6.56 mM	203.03.00		1.334 g	Sigma M9272
Taurine	20 mM	125.01.00		2.502 g	Sigma T0625
Na_2Phosphocreatin	15 mM	255.01.00		4.097 g	Sigma P7936
Imidazole	20 mM	68.01.00		1.362 g	Sigma S6750
Dithiothreitol	0.5 mM	154.02.00		0.077 g	Sigma D0632
MES hydrate	50 mM	195.02.00		9.76 g	Sigma M0895

2.8 Histological analyses

Mid-portions of the right costal diaphragm and limb muscles (EDL and soleus) were mounted in optimal cutting temperature embedding medium (Thermo Scientific, Loughborough, UK), frozen in liquid nitrogen-cooled isopentane and stored at -80°C. To identify muscle fibre types, sections (10 µm thick) were fixed for 2 minutes in 2 % paraformaldehyde, washed in phosphate-buffered saline (PBS; P4417, Sigma-Aldrich, St Louis, MO) and blocked for 10 minutes in 1% BSA (A6003, Sigma-Aldrich, St Louis, MO). Sections were then incubated for 60 min with monoclonal-myosin heavy chain (MHC) antibodies BA-D5 (IgG2B, 1:1000) and SC-71 (IgG1, 1:500) for Type I and Type IIa fibres, respectively (Developmental Studies Hybridoma Bank, Iowa City, IA, USA). The remaining unstained fibres were considered to be Type IIb/IIx, as previously validated (Al-Shammari *et al.*, 2019). After washing in PBS, sections were incubated for 60 min with secondary antibodies Alexa Fluor 555 (conjugated goat anti-mouse IgG, 1:1000, A-21422, Thermo Fisher Scientific, Waltham, MA) and Alexa Fluor 488

(conjugated rabbit anti-mouse IgG, 1:1000, A11059, Thermo Fisher Scientific, Waltham, MA). Muscle fibre boundaries were labelled with a rabbit anti-laminin antibody (1:200; L9393, Sigma-Aldrich, St Louis, MO), an extracellular matrix glycoprotein within the basement membrane. Finally, capillaries were stained with a carbohydrate-binding protein (lectin) specific to rodent endothelial cells, *Griffonia simplicifolia* lectin I (GSL I; Vector Labs, Peterborough, UK; FL-1101). Slides were then imaged at magnifications of x10 (soleus and EDL) and x20 (diaphragm) using the Nikon Eclipse E600 (Nikon, Tokyo, Japan) optical microscope attached to a digital camera (QIMAGING, MicroPublisher™ 5.0 RTV, Surrey, BC, Canada). Subsequent image analysis with the stand-alone graphic user interface, DTect, and a MATLAB-based oxygen transport modeller (The MathWorks, Cambridge, United Kingdom; (Al-Shammari *et al.*, 2019)) enabled calculation of fibre-type-specific cross-sectional area (FCSA), capillary-to-fibre ratio (C:F), capillary density (CD), capillary domain area (CDA), local capillary-to-fibre ratio (LCFR), local capillary density (LCD) and estimated tissue oxygen tension (PO_2). Multiple regions of interest of each muscle (3 for the diaphragm and 2 for the EDL and soleus) were randomly assigned to establish an unbiased counting frame, taking into account the regional heterogeneity across muscles (Kissane *et al.*, 2018). In general, each region of interest of the soleus and EDL muscle contained ~ 150 fibres and the diaphragm ~ 70 fibres.

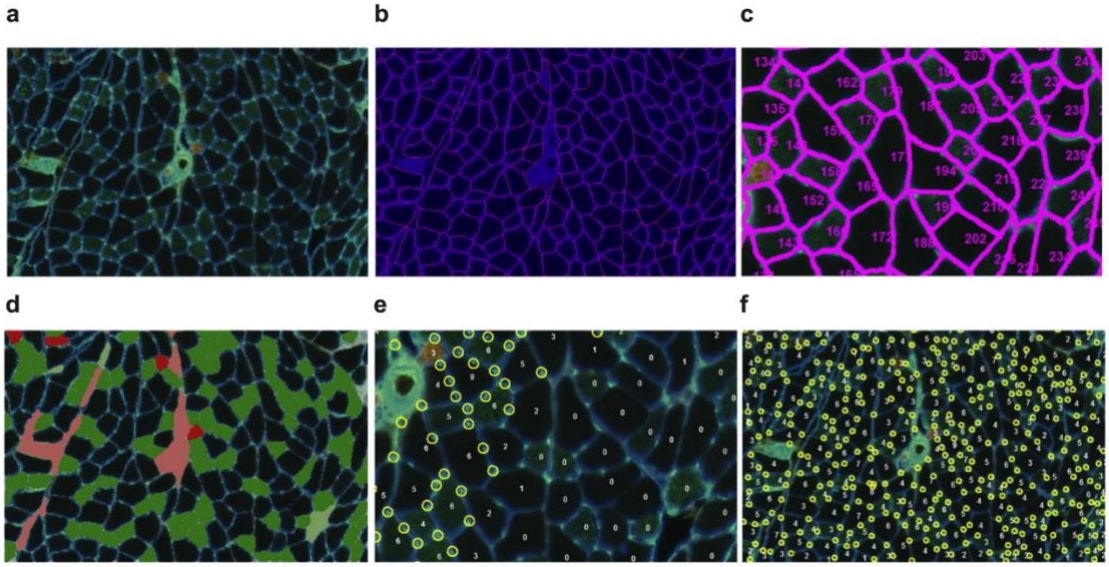

Figure 2.2. Histological analysis of fibre type and capillarity. Fibre segmentation and isoform identification was performed using Dtect, which is coded in MATLAB. This software identifies the blue stained lamina **(a, b)** to delineate fibre boundaries with a magenta outline **(c)**. Dtect then uses the different MHC isoform stains to classify all fibres into the three primary phenotypes: types I, IIa, and IIb/IIx **(d)**. Capillaries are manually identified on the fibre boundaries **(e, f)**, which are then used to generate fibre type-specific morphometric indices of capillarisation.

To characterise muscle fibrosis, soleus cryosections were stained with Sirius red (Sigma-Aldrich, St Louis, MO, USA). Briefly, sections (10 µm thickness) were hydrated with distilled water, incubated with Picro-Sirius Red (1 h), rinsed in acetic acid solution (0.5%), and dehydrated in absolute alcohol. The relative area of the sections occupied by Sirius red staining was then calculated using ImageJ software.

EDL cryosections (10 µm thickness) were stained with DAPI to quantify the number of nuclei per fibre. Sections were fixed for 2 minutes in 2% paraformaldehyde, washed in PBS (P4417, Sigma-Aldrich, St Louis, MO) and blocked for 10 minutes in 1% BSA (A6003, Sigma-Aldrich, St Louis, MO). Muscle fibre boundaries were labelled with a rabbit anti-laminin antibody (1:200; L9393,

Sigma-Aldrich, St Louis, MO). Sections were then incubated for 60 min with Alexa Fluor 488 (conjugated rabbit anti-mouse IgG, 1:1000, A11059, Thermo Fisher Scientific, Waltham, MA) and mounted in slides using mounting medium with DAPI. Three washes with PBS were performed between each step. Myonuclei and fibres were manually counted in images using ImageJ software. A nucleus was identified as a myonucleus if it met one of the following criteria: 1) it was clearly located within the fibre boundary; 2) it was on the boundary facing inside the fibre; or 3) >50% of the area fell inside the fibre boundary (Liu *et al.*, 2013).

2.9 *In silico* muscle PO_2 modelling

Our model applied mathematical and computational frameworks to generate theoretical predictions of the cross-sectional distribution of PO_2 in the EDL, soleus and diaphragm using a custom MATLAB 'oxygen transport modeller', as previously described (Al-Shammari *et al.*, 2019). Briefly, using digitised images of muscle cryosections, individual fibre boundaries were identified, a phenotype assigned, and capillary locations defined. A computational framework was then established allowing a mathematical mesh of equations to be superimposed on realistic geometry. Tissue PO_2 measurements were then derived by incorporating estimates (applied similarly in each group) of capillary radius (1.8–2.5 × 10^{-4} cm), muscle oxygen consumption (15.7 × 10^{-5} ml O_2 ml^{-1} s^{-1}), myoglobin concentration (10.2 × 10^{-3} ml O_2 ml^{-1}), O_2 solubility (3.89 × 10^{-5} ml O_2 ml^{-1} $mmHg^{-1}$) and diffusivity (1.73 × 10^{-7} cm^2 s^{-1}) as detailed elsewhere (Al-Shammari *et al.*, 2019), with direct measurement of these specific parameters beyond the scope of the present study described (Tickle *et al.*, 2020). As such,

any differences between groups in terms of mitochondrial function (or other assumed variables) were not accounted for in our model. Relevant biophysical parameters affecting O_2 diffusion from reputable sources were used in the mathematical model to generate predictions of the cross-sectional distribution of PO_2 in a muscle biopsy under simulated resting and maximal oxygen consumption conditions. As with all biological models, inherent limitations prevent full characterisation of the wide myriad of interacting variables; however, relative changes within a given tissue were the key output and are likely robust. In line with former studies (Al-Shammari *et al.*, 2019), compensation for differences in many parameters, e.g., myoglobin saturation, have relatively small effects on the documented outcomes due to the dominant effect of capillary supply and fibre size on peripheral O_2 transport.

2.10 Protein extraction and western blot analysis

Frozen muscle samples were homogenized in RIPA buffer (50 mM Tris, 150 mM sodium chloride, 1 mM EDTA, 1% NP-40, 0.25% sodium-deoxycholate, 0.1% SDS, 1% Triton X-100; pH 7.4) containing a protease and phosphatase inhibitor cocktail (Thermo Scientific A32961), sonicated, and centrifuged at 13,000 rpm for 10 min. The supernatant was collected, and protein content was quantified *via* BCA assay (Thermo Scientific 23225). Muscle homogenates with equal amounts of protein (20 µg) were mixed with loading buffer (126 mmol/L Tris-HCl, 20% glycerol, 4% SDS, 1.0% 2-mercaptoethanol, 0.005% bromophenol blue; pH 6.8), and separated by electrophoresis (1.5 hours at 90 V) on 8%-12% sodium dodecyl sulfate polyacrylamide gels and transferred to a nitrocellulose membrane (Amersham™ Protran® GE10600003). Membranes were stained

with Ponceau S to determine total protein content and rinsed with Tris-buffered saline/Tween solution (0.5 M NaCl; 50 mM Tris–HCl, pH 7.4; and 0.1% Tween 20). Membranes were then blocked with 5% milk or 5% BSA, and incubated overnight at 4°C with primary antibodies (see Table 2.1). After a 5-min wash (3x) in Tris-buffered saline/Tween solution, membranes were incubated with secondary antibodies (Table 2.2) for 1 h at room temperature. Membranes were again washed for 5 min (3x) in Tris-buffered saline/Tween solution, and labelled proteins were detected using an enhanced chemiluminescence system (iBright750, Invitrogen by Thermo Fisher Scientific CL750) and densitometry quantified using ImageJ software (Scion Corp., National Institutes of Health, Bethesda, MD, USA).

Table 2.2. *Antibodies used for western blot analysis*

Primary antibodies	Dilution	Company
4EBP1	1:1000	Cell Signaling Technology
p-4EBP1	1:1000	Cell Signaling Technology
S6	1:1000	Cell Signaling Technology
p-S6	1:1000	Cell Signaling Technology
AMPK	1:1000	Cell Signaling Technology
p-AMPK	1:1000	Cell Signaling Technology
Drp1	1:1000	Cell Signaling Technology
p-Drp1	1:1000	Cell Signaling Technology
ACC	1:1000	Cell Signaling Technology
p-ACC	1:1000	Cell Signaling Technology
ACL	1:1000	Cell Signaling Technology
p-ACL	1:1000	Cell Signaling Technology
p62	1:1000	Cell Signaling Technology
MuRF1	1:1000	Santa Cruz Biotechnology
PGC-1α	1:1000	GeneTex
OPA1	1:1000	Sigma-Aldrich
Puromycin	1:500	Sigma-Aldrich
Secondary antibodies	**Dilution**	**Company**
Anti-mouse IgG	1:2500	Cell Signaling Technology
Goat anti-mouse IgG2a	1:2500	Cell Signaling Technology
Anti-rabbit IgG	1:2500	Cell Signaling Technology

Chapter 3 Results I. Abnormal skeletal muscle blood flow, contractile mechanics, and fibre morphology in a rat model of obese-HFpEF

3.1 Introduction

Increasing prevalence of heart failure with preserved fraction (HFpEF) in the absence of recognised pharmaceutical treatment represents one of the biggest challenges to modern cardiology (Butler *et al.*, 2014; Sharma & Kass, 2014; Fukuta *et al.*, 2016). While the primary pathology of HFpEF is of cardiac origin, there is a poor correlation between heart dysfunction and the main symptom of exercise intolerance (Haykowsky & Kitzman, 2014). Many clinical trials have shown cardiac-orientated drugs are not associated with beneficial outcomes (Shah *et al.*, 2016). Recent investigations, therefore, have suggested non-cardiac 'peripheral' factors as major mechanisms limiting functional capacity and quality of life in patients with HFpEF, with skeletal muscle abnormalities receiving much attention (Adams *et al.*, 2017; Poole *et al.*, 2018; Zamani *et al.*, 2020). For example, animal and human studies have shown that HFpEF is associated with various skeletal muscle impairments that are closely associated with exercise intolerance and lower quality of life, including lower skeletal muscle mass and strength (Bekfani *et al.*, 2016), generalized fibre atrophy (Bowen *et al.*, 2018), fat infiltration (Haykowsky *et al.*, 2014; Zamani *et al.*, 2020), reduced capillary-to-fibre ratio (Kitzman *et al.*, 2014; Bowen *et al.*, 2018), reduced mitochondrial function and content (Bowen *et al.*, 2015; Molina *et al.*, 2016; Bowen *et al.*, 2017b), disrupted high-energy phosphate metabolism (Bhella *et al.*, 2011a; Weiss *et al.*, 2017), and impaired O_2 extraction (Dhakal *et al.*, 2015; Houstis *et al.*, 2018; Zamani *et al.*, 2020).

Despite recent progress, our current understanding of the skeletal muscle pathophysiology in HFpEF at both the structural and functional level is at its infancy, with only limited experimental data available (Poole *et al.*, 2018). For example, it remains controversial whether leg muscle arterial blood flow (i.e., perfusive O_2 transport) is impaired during exercise in HFpEF due to lack of direct measurements (Hundley *et al.*, 2007; Haykowsky *et al.*, 2013b; Lee *et al.*, 2016a), while fibre-type specific measures quantifying the degree of atrophy, capillary rarefaction, and muscle PO_2 remain poorly explored with only global indices of capillarisation being reported (Kitzman *et al.*, 2014; Bowen *et al.*, 2015; Bowen *et al.*, 2017b; Bowen *et al.*, 2018; Schauer *et al.*, 2020), despite major studies reporting conflicting findings regarding whether a perfusive or diffusive O_2 transport limitation impairs muscle O_2 extraction and thus exercise intolerance in HFpEF (Dhakal *et al.*, 2015; Houstis *et al.*, 2018; Zamani *et al.*, 2020). In addition, a knowledge gap exists in relation to potential sites of skeletal muscle dysfunction in HFpEF (Bowen *et al.*, 2015; Bowen *et al.*, 2017b; Bowen *et al.*, 2018; Schauer *et al.*, 2020), due to a lack of physiologically-relevant mechanical measures (i.e., shortening velocity and power) alongside insights into neuromuscular transmission *vs*. excitation-contraction failure. Beyond this, the majority of experimental work has been directed towards characterising the locomotor muscles despite key evidence showing respiratory muscle dysfunction is linked to exercise intolerance in HFpEF, as shown by non-invasive patient measures (Lavietes *et al.*, 2004; Yamada *et al.*, 2016) and direct diaphragm contractility measures in experimental models (Bowen *et al.*, 2015; Bowen *et al.*, 2017b). Similar to limb muscle, however, detailed quantification of diaphragm fibre-type morphology, capillarity, PO_2, and clinically-relevant functional

shortening or lengthening mechanical measurements (i.e., as occurs during breathing) remain largely undefined in HFpEF and are unlikely to follow a similar response to the locomotor muscles.

The present study, therefore, aimed to provide a more comprehensive assessment of the skeletal muscle phenotype in HFpEF, by applying *in vitro, in situ*, and *in silico* approaches to a validated obese cardiometabolic rat model, where *ex vivo* magnetic resonance imaging was used to characterise the degree of cardiac remodelling. Specifically, using hindlimb (soleus/EDL) and respiratory (diaphragm) muscle, we performed global and local fibre type-specific phenotyping of cross-sectional area, isoform, and capillarity alongside estimated muscle PO_2. In parallel, we also directly assessed key functional measures during rest and contractions, including hindlimb blood flow as well as neural- and direct-muscle stimulated contractile mechanics. We reasoned a better understanding of the skeletal muscle phenotype in HFpEF across multiple-system levels would provide important insights for better understanding the pathophysiology of exercise intolerance in this disease and help direct future patient experiments and therapeutic development in this field.

3.2 Methods

3.2.1 Ethical approval

All procedures and experiments were performed in accordance with the UK Scientific Procedures (Animals) Act 1986 and local approval was given by the University of Leeds Animal Welfare and Ethical Review Committee. All work conforms to the ethical requirements outlined by *The Journal of Physiology* (Grundy, 2015).

3.2.2 Animals

Obese (n=8) and lean (n=8) ZSF1 rats were compared at 20 weeks of age when HFpEF develops in the obese strain. All rats were maintained in a 12-hour light/ dark cycle, with standard chow diets (RM1 chow, SDS) and water provided *ad libitum*. Full details of animals are provided in Chapter 2 General methods: 2.2.

3.2.3 Cardiometabolic function

Cardiometabolic impairments associated with HFpEF were confirmed by measures of obesity, arterial pressure (*via* an implanted catheter with an ADI blood pressure transducer), blood glucose levels (*via* a commercial blood glucose meter) and cardiac remodelling (ex vivo; diffusion tensor imaging). Full details are provided in Chapter 2 General methods: 2.3.

3.2.4 *In situ* muscle performance and femoral artery blood flow

In situ EDL contractility (isometric twitch and maximal forces and fatigability) was assessed under surgical anaesthesia. Simultaneous measurement of bilateral blood flow was facilitated by placement of perivascular flow probes on the femoral artery. Full details are provided in Chapter 2 General methods: 2.5.

3.2.5 *In vitro* functional assessment

A diaphragm fibre bundle and the soleus were mounted vertically in a buffer-filled organ bath between a hook and force transducer for measurement of *in vitro* contractility (isometric and isotonic properties). Full details are provided in Chapter 2 General methods: 2.6.

3.2.6 Histological analysis

Analyses of fibre type-specific CSA, C:F, CD, LCFR, LCD and *In silico* muscle PO_2 were performed on soleus and diaphragm cryosections using DTect and a MATLAB-based oxygen transport modeller, as previously described (Al-Shammari *et al.*, 2019). Full details are provided in Chapter 2 General methods: 2.8.

3.2.7 Statistical analyses

Following appropriate checks of normality, between-group differences were assessed by unpaired two-tailed Student t-tests. Contractile relationships were analysed as 2-way repeated measures ANOVA followed by Bonferroni *post hoc* test, where appropriate. Analyses were performed in GraphPad Prism v.8. Data are presented as mean±SD, and the level of significance was set at $P < 0.05$ for all analyses.

3.3 Results

3.3.1 Cardio-metabolic phenotype

As previously noted (Leite *et al.*, 2015; Franssen *et al.*, 2016; van Dijk *et al.*, 2016; Bowen *et al.*, 2017b; Schauer *et al.*, 2020), by 20 weeks of age obese-ZSF1 rats have developed typical metabolic signs associated with HFpEF including obesity (Figure 3.1a), hyperglycaemia (Figure 3.1b) and hypertension (Figure 3.1c). In addition, obese rats developed cardiac remodelling typically associated with HFpEF that included RV hypertrophy (Figure 3.1d), although LV and septal wall enlargement was not observed at this time point (Figure 3.1e, f) and this was also similar for myocyte organisation/disarray in the RV, LV or septum (Figure 3.1g, h).

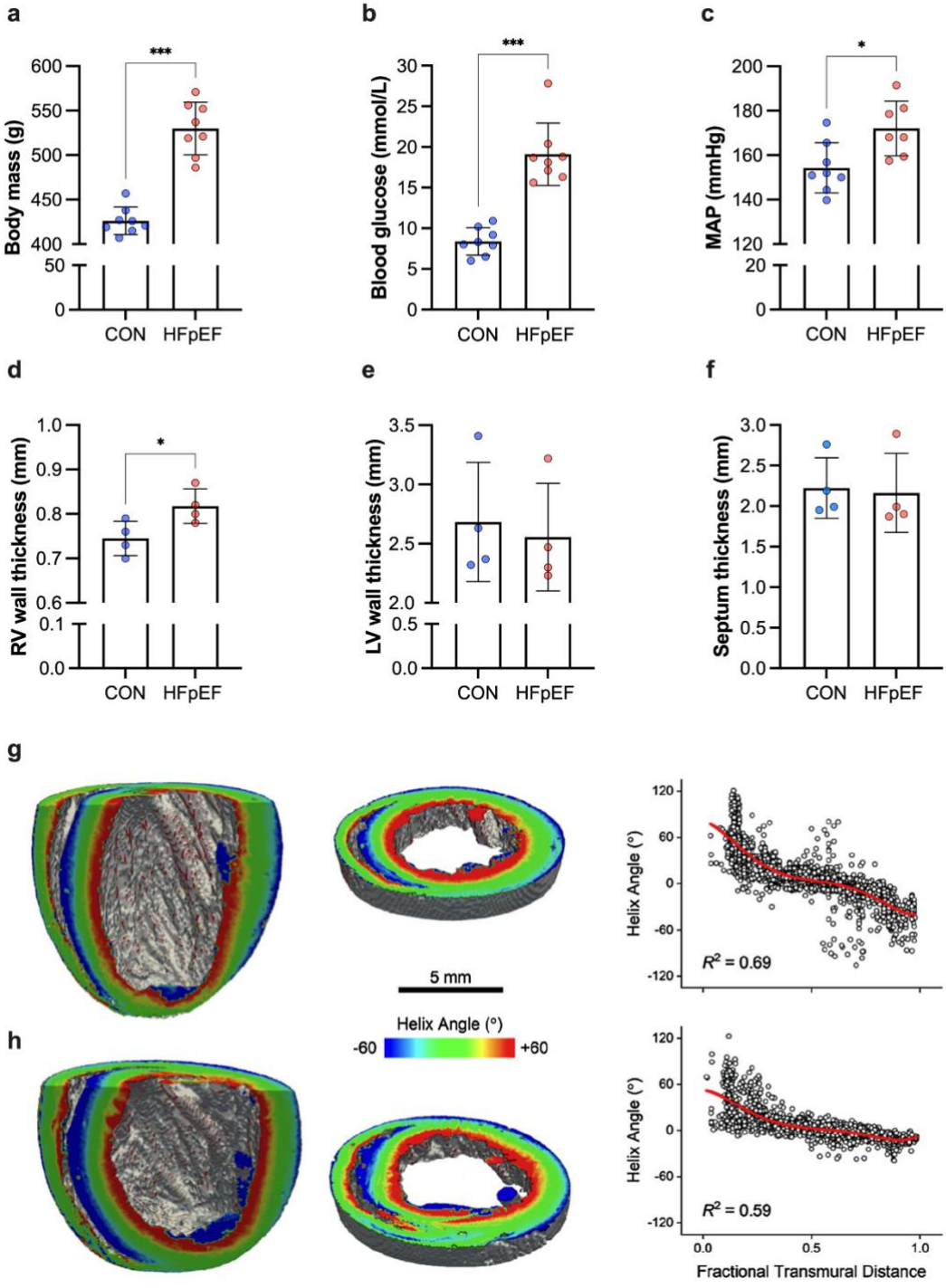

Figure 3.1. Cardio-metabolic characteristics. At 20 weeks of age, HFpEF rats developed obesity ($P < 0.001$) **(a)**, hyperglycaemia ($P < 0.001$) **(b)** and hypertension ($P = 0.012$) **(c)**. Compared to lean controls, obese HFpEF rats also showed increased right ventricular (RV) wall thickness ($P = 0.034$) **(d)**, however right ventricular (LV) wall and the septum thickness were not different between groups ($P = 0.719$ and $P = 0.849$, respectively) **(e, f)**. Left and middle panel: Long axis cuts (left) and short axis slices (middle) of representative lean **(g)** and obese **(h)** hearts, with myocyte helix (inclination) angle colour coded on the cut surfaces. Right panel: The helix angle in the RV free wall plotted as a function of

fractional transmural distance (0.0, endocardium; 1.0, epicardium) for representative lean **(g)** and obese **(h)** hearts. The red solid line is a 5th order polynomial fit to the data. Myocyte disarray is quantified by the R^2 of this fit.

3.3.2 Histological and *in vitro* functional characteristics of the soleus muscle

As shown in representative muscle sections (Figure 3.2a, b), soleus from obese-HFpEF rats demonstrated clear atrophy with a 26% lower wet-mass (Figure 3.2c) and a 23% lower CSA of both Type I and Type IIa fibres (Figure 3.2d) when compared to lean controls. No Type IIx/b fibres were detected in either group. HFpEF rats also had a lower numerical and areal composition of Type I fibres (Figure 3.2e, f), whereas these were higher in Type IIa fibres. In addition, HFpEF rats had a lower C:F (Figure 3.2g) but a higher CD (Figure 3.2h), indicating atrophy proceeded at a greater rate than capillary loss, while CDA remained unchanged (Figure 3.2i). Local analyses of capillary distribution revealed that HFpEF rats had lower LCFR in Type I fibres, although this was unchanged in Type IIa fibres (Figure 3.2j). In contrast, however, LCD in Type I fibres was higher in HFpEF rats, with no changes in Type IIa fibres (Figure 3.2k). To understand whether HFpEF influenced muscle PO_2, we simulated muscle oxygen tension under resting (Figure 3.3a-c) and maximal demand (Figure 3.3d-f). No differences between groups were found after calculation of muscle oxygenation at either rest (Figure 3.3c) or maximal rate of oxygen consumption (Figure 3.3f).

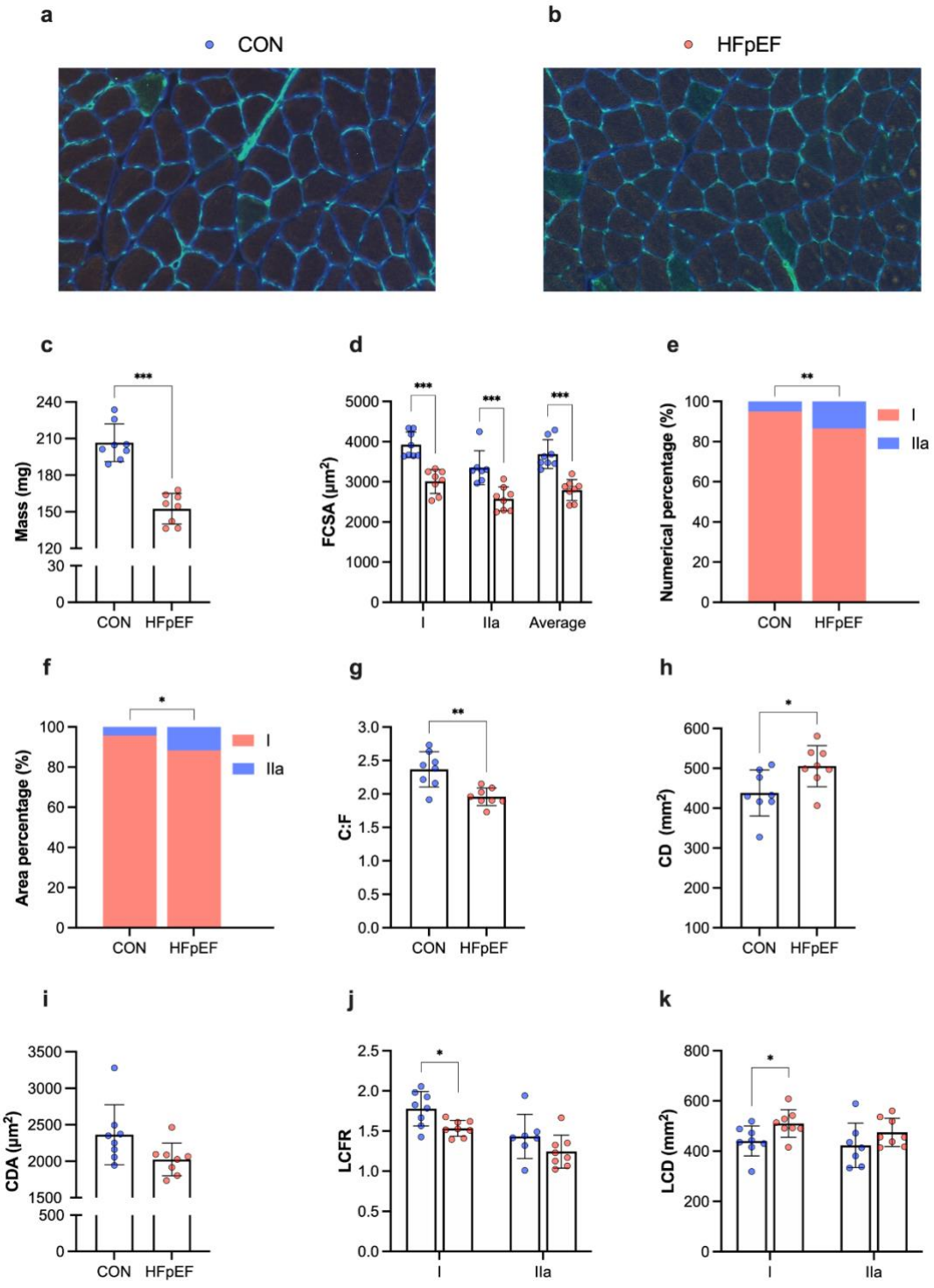

Figure 3.2. Histological features of the soleus muscle. Representative soleus sections from control **(a)** and obese-HFpEF **(b)**. Obese-HFpEF rats showed atrophy in the soleus muscle, with reduced wet muscle mass ($P < 0.001$) **(c)** and reduced CSA in both Type I ($P < 0.001$) and Type IIa fibres ($P = 0.001$) **(d)**. HFpEF rats also had a lower numerical and areal composition of Type I fibres ($P = 0.002$ and $P = 0.043$, respectively), whereas these were higher in Type IIa fibres ($P = 0.002$ and $P = 0.005$, respectively) **(e, f)**. Moreover, compared to lean controls, obese rats had reduced C:F ($P = 0.002$) **(g)**, whereas CD was increased ($P = 0.027$) **(h)** with no change in CDA ($P = 0.059$) **(i)**. Finally, local analyses of capillary distribution showed that HFpEF rats had lower LCFR in Type I fibres (P

= 0.011), although this was unchanged in Type IIa fibres (P = 0.154) **(j)**. In contrast, LCD in Type I fibres was increased in HFpEF rats (P = 0.029), with no changes in Type IIa fibres (P = 0.196) **(k)**.

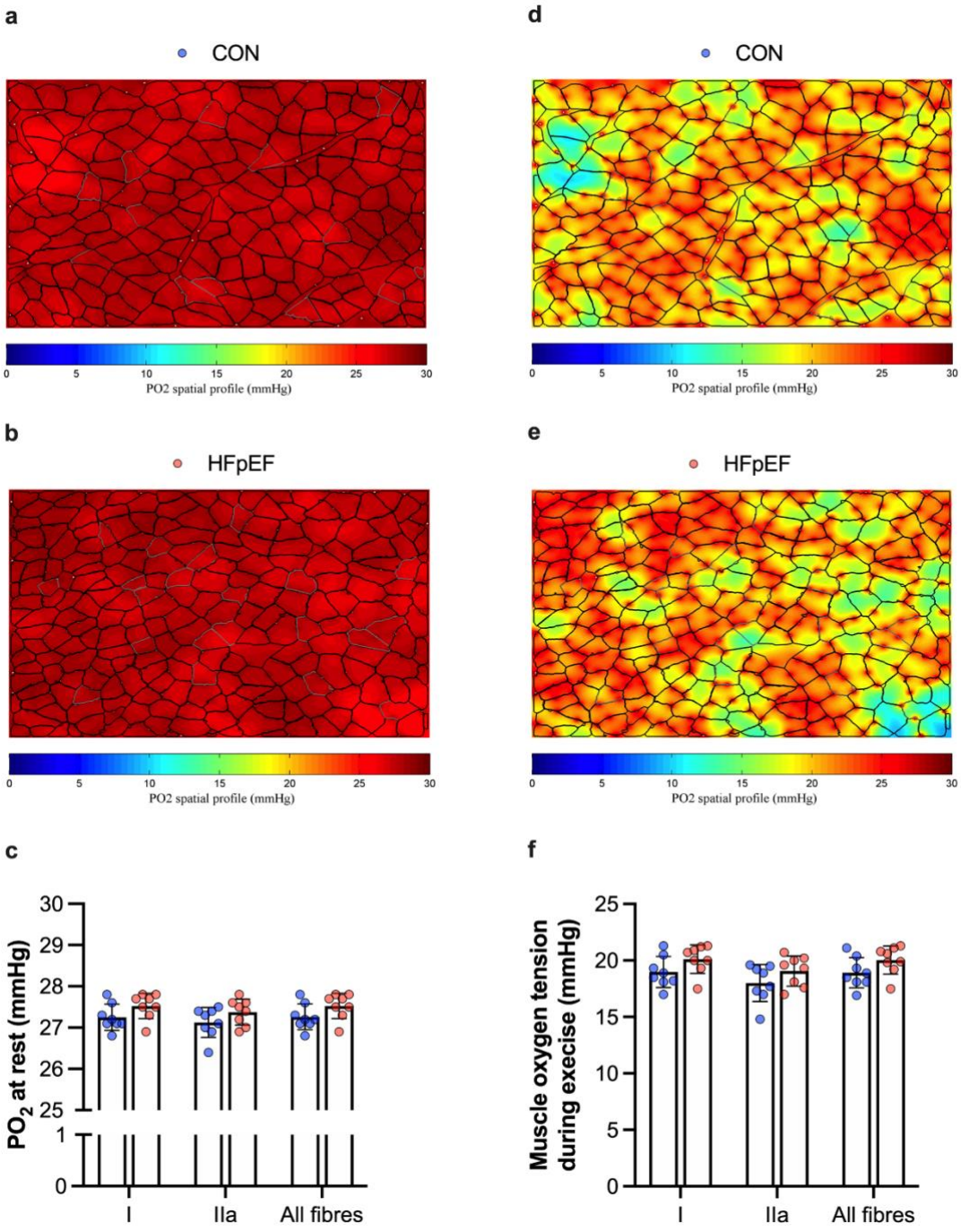

Figure 3.3. Modelling of soleus muscle oxygen tension. Simulation of muscle PO_2 at rest **(a, b)** and maximal rate of oxygen consumption **(d, e)** in representative images. There were no significant differences in simulations of muscle PO_2 at rest (Type I: P = 0.099, Type IIa: P = 0.167, all fibres: P = 0.102) **(c)** or at maximal rate of oxygen consumption (Type I: P = 0.109, Type IIa: P = 0.177, all fibres: P = 0.115) **(f)**. Areas of muscle hypoxia (PO_2 < 0.5 mmHg) are highlighted in blue.

The soleus generated lower absolute twitch and maximal forces in HFpEF compared to control rats (Figure 3.4a and Figure 3.4b, respectively), consistent with muscle atrophy, although after adjustment for muscle cross-sectional area there were no differences between groups in specific forces (Figure 3.4c and Figure 3.4d, respectively). Similarly, twitch characteristics of time to peak tension (Figure 3.4e) and half relaxation time (Figure 3.4f) remained unchanged. However, HFpEF rats had impairments to both shortening velocity (range 10-17 %) and mechanical power (range 14-22 %) when measured across different percentages of their maximal force (Figure 3.4g, h), suggesting HFpEF reduces intrinsic soleus contractile function related to muscle shortening rather than force generation.

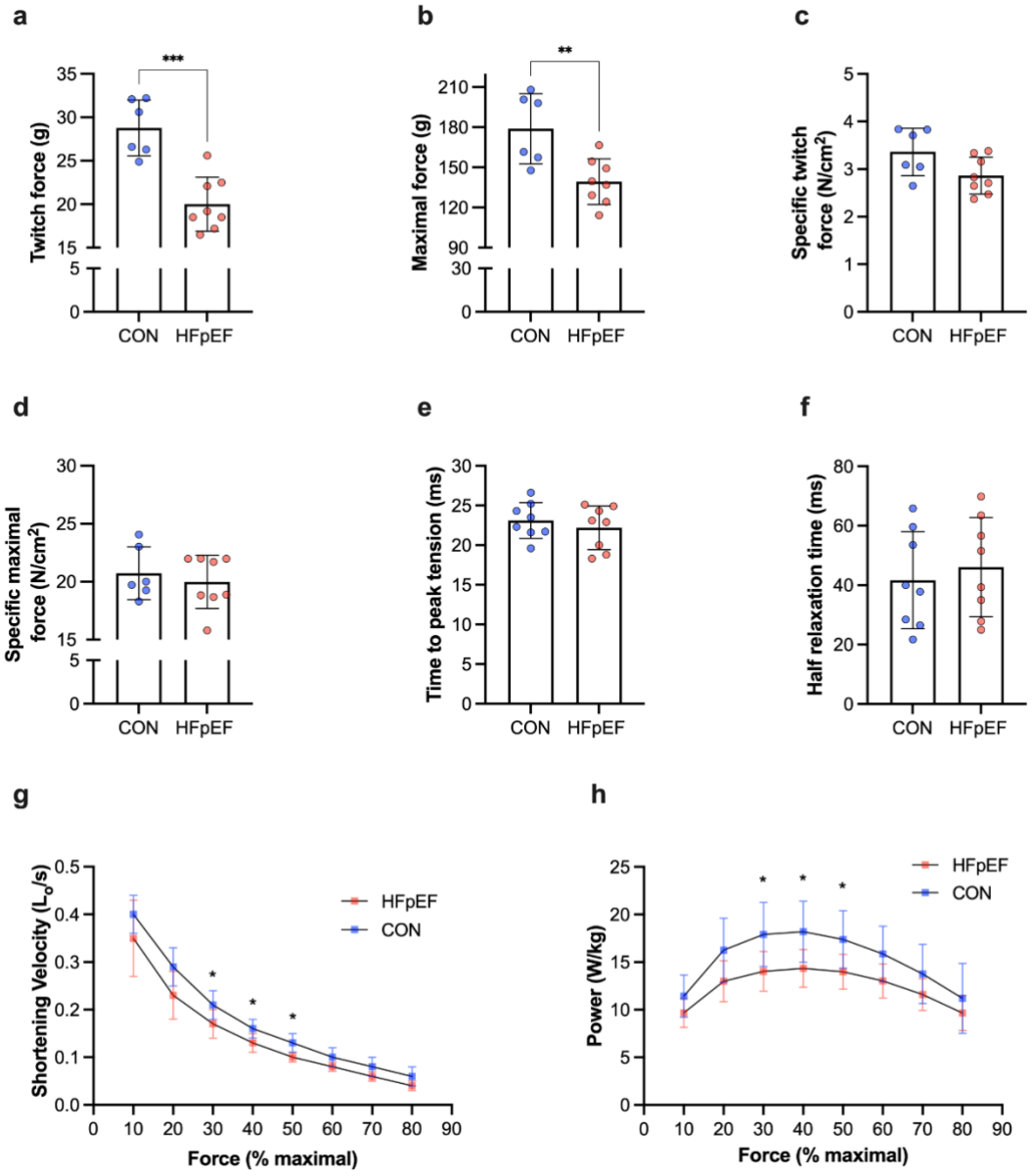

Figure 3.4. *In vitro* skeletal muscle function. The soleus of HFpEF rats showed lower absolute twitch force ($P < 0.001$) **(a)** and absolute maximal tetanic force ($P = 0.005$) **(b)**, although mass-specific twitch and maximal forces were similar between groups ($P = 0.056$ and $P = 0.557$, respectively) **(c, d)**. Similarly, time to peak tension and half relaxation time remained unchanged ($P = 0.474$ and $P = 0.603$, respectively) **(e, f)**. However, HFpEF rats showed impairments in shortening velocity and muscle power when measured across different percentages of their maximal force (30, 40 and 50%) ($P < 0.05$) **(g, h)**.

3.3.3 *In situ* muscle function and femoral artery blood flow

EDL muscle wet-mass was 26% lower in HFpEF rats (Figure 3.5a). This corresponded to lower absolute twitch and maximal forces of 27% and 33%, respectively (Figure 3.5b and Figure 3.5c, respectively). When normalised to

muscle mass, twitch and maximal specific forces were not different between groups (Figure 3.5d and Figure 3.5e, respectively), while relative fatigability was unaffected (Figure 3.5f). However, HFpEF rats tended to be around 26% more fatigable during the force-matched protocol (Figure 3.5g). While HFpEF rats had higher levels of resting femoral artery blood flow (Figure 3.5h), end-stimulation blood flow was not significantly different between groups (Figure 3.5i). However, HFpEF rats showed a severely blunted hyperaemic response of 73% increase in blood flow during repeated contractions (Figure 3.5j). Similarly, impairments in the hyperaemia calculated using vascular conductance was found in HFpEF (Figure 3.5k). Overall, this suggests that while obese-HFpEF does not induce muscle dysfunction related to neuromuscular transmission failure, a severe decrement to increased leg blood flow in response to exercise is apparent.

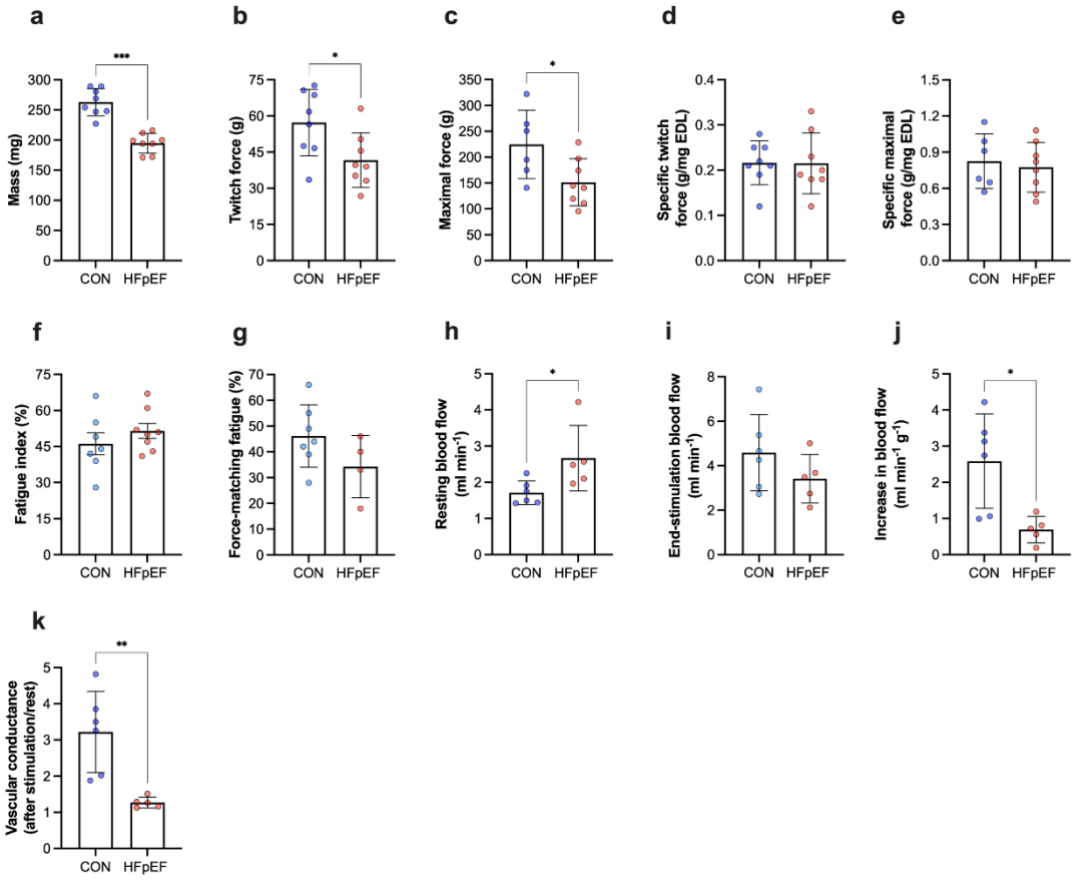

Figure 3.5. *In situ* EDL contractile function and femoral artery blood flow. Absolute twitch and maximal tetanic forces of the EDL muscle were lower in HFpEF rats than in controls (P = 0.016 and P = 0.030, respectively) **(b, c)**. However, when normalised to muscle mass, which was reduced in HFpEF rats (P < 0.001) **(a)**, these were not significantly affected (P < 0.968 and P = 0.675, respectively) **(d, e)**. The fatigue index was similar between groups (P = 0.325) **(f)**. However, HFpEF rats tended to be more fatigable during the force-matched protocol (P = 0.079) **(g)**. Resting femoral artery blood flow was augmented in HFpEF rats (P = 0.039) **(h), while end-stimulation blood flow was not significantly different between groups (P = 0.22) (i)**. In contrast, HFpEF rats showed an impaired increase in muscle-specific EDL blood flow during stimulation (P = 0.012) **(j)**. Moreover, a reduction in the functional hyperaemic scope was also found in HFpEF (P = 0.004) **(k)**.

3.3.4 Histological and functional characteristics of the diaphragm

Representative diaphragm sections from control and HFpEF rats are presented in Figure 3.6a, b. Average FCSA was similar between groups (Figure 3.6c), however compared to lean controls HFpEF increased FCSA in both type I and type IIa fibres by 46 % and 26 %, respectively (Figure 3.6c), but reduced type IIb/IIx FCSA by 22 %. Additionally, HFpEF rats had a higher numerical percentage of type I fibres (Figure 3.6d) and a higher area percentage of type I fibres (Figure 3.6e).

Global and local alterations were also observed in capillary distribution, with C:F and CD increased in HFpEF rats (Figure 3.6f and Figure 3.6g, respectively) but CDA remained unchanged (Figure 3.6h). HFpEF rats had increased LCFR in Type I and Type IIa fibres, whereas this was reduced in type IIb/IIx fibres (Figure 3.6i). In contrast, LCD was higher in HFpEF for Type IIb/IIx fibres, with no changes in Type I and Type IIa fibres (Figure 3.6j). We next estimated diaphragm PO_2 levels (Figure 3.7a-f) and found HFpEF elevated resting muscle oxygen tension (Figure 3.7c) and at maximal metabolic rates (Figure 3.7f), indicating improved muscle oxygenation in obese-HFpEF.

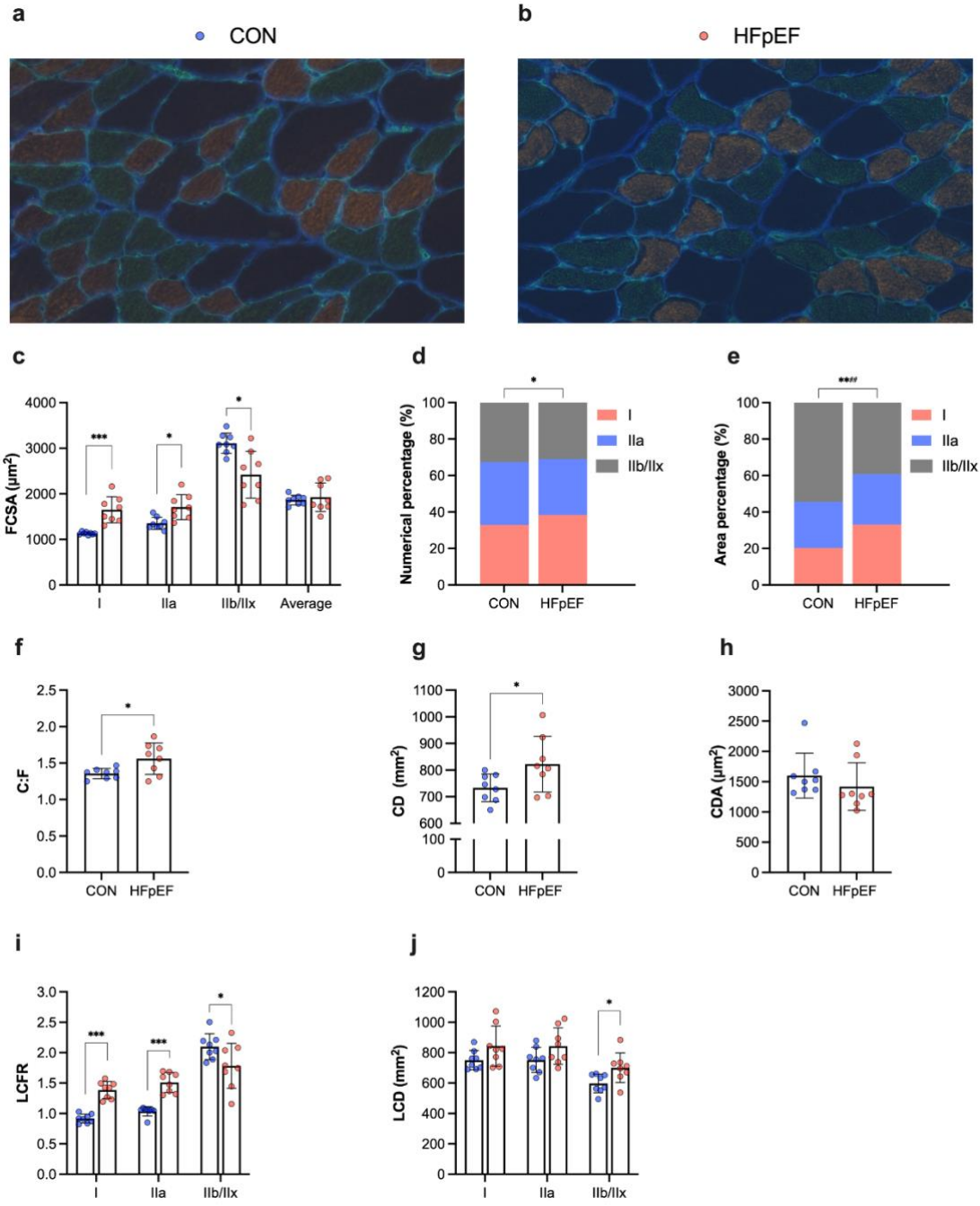

Figure 3.6. Histological features of the diaphragm. Representative diaphragm sections from control **(a)** and obese-HFpEF **(b)**. Compared to lean controls, HFpEF rats had increased CSA in Type I ($P < 0.001$) and Type IIa fibres ($P = 0.005$), whereas CSA of Type IIb/IIx fibres was reduced ($P = 0.004$) **(c)**. HFpEF rats also had a higher numerical percentage of Type I fibres ($P = 0.003$), although this remained unchanged in Type IIa ($P = 0.203$) and IIb/IIx fibres ($P = 0.545$) **(d)**. Additionally, HFpEF rats showed a higher area percentage of Type I fibres ($P < 0.001$), whereas this was unchanged in Type IIa fibres ($P = 0.449$) and reduced in Type IIb/IIx fibres ($P = 0.002$) **(e).** HFpEF rats also showed general and local alterations in capillary distribution. General changes included increased C:F ($P = 0.015$) **(f)** and CD ($P = 0.049$) **(g)**, although CDA remained unchanged ($P = 0.362$) **(h)**. Local changes included increased LCFR in Type I ($P < 0.001$) and Type IIa fibres ($P < 0.001$) and reduced LCFR in glycolytic/Type IIb/IIx fibres ($P = 0.040$) **(i)**. In contrast, however, HFpEF rats had increased LCD

in Type IIb/IIx fibres (P = 0.042), with no changes in Type I (P = 0.152) and Type IIa fibres (P = 0.128) **(j)**.

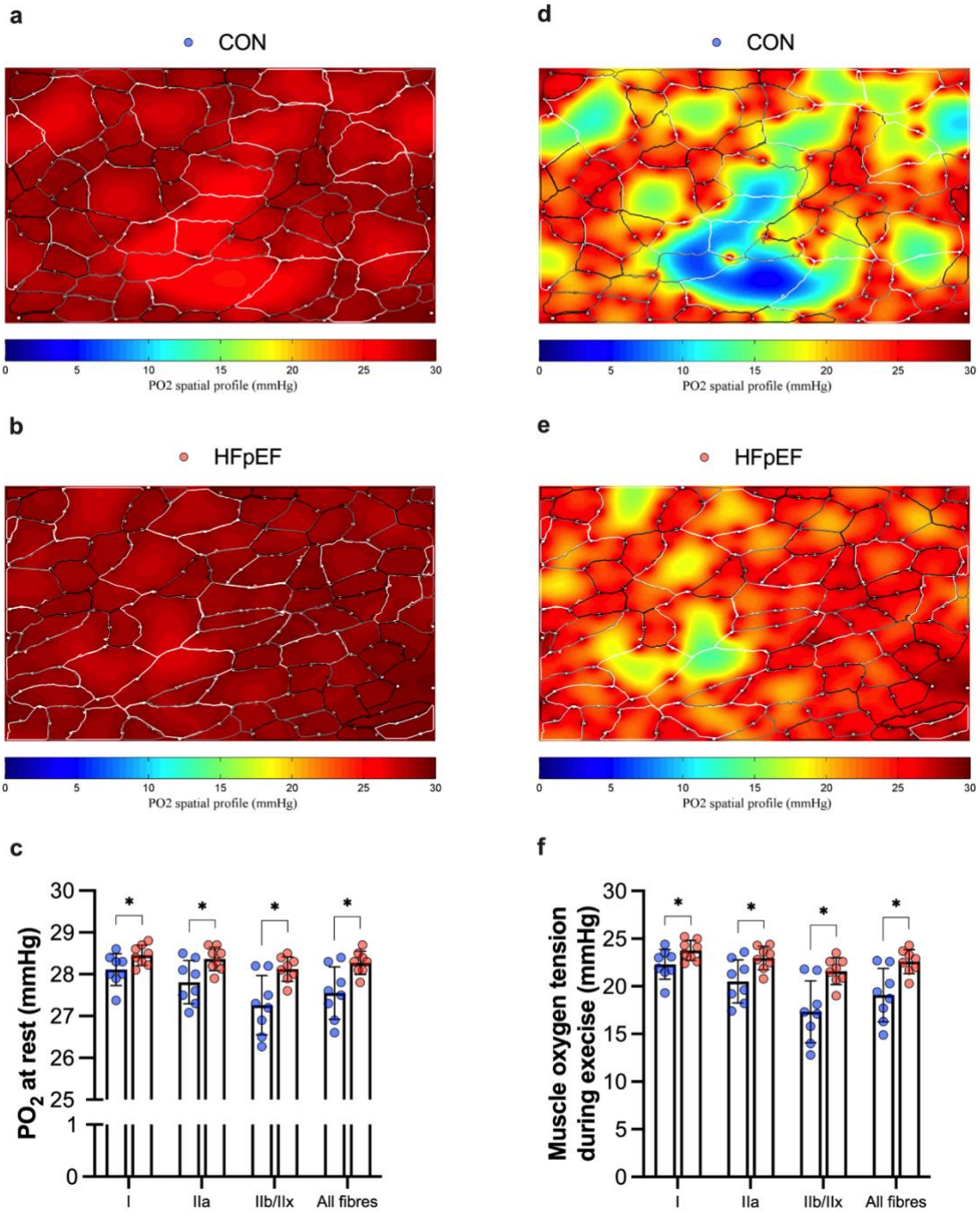

Figure 3.7. Modelling of diaphragm oxygen tension. Simulation of muscle PO_2 at rest **(a, b)** and maximal rate of oxygen consumption **(d, e)** in representative images. Compared to lean controls, HFpEF rats showed higher muscle oxygen tension at rest (Type I fibres: P = 0.043, Type IIa: P = 0.019, Type IIb/IIx: P = 0.006, all fibres: P = 0.009) **(c)** or at maximal rate of oxygen consumption (Type I: P = 0.045, Type IIa: P = 0.018, Type IIb/IIx: P = 0.004, all fibres: P = 0.006) **(f)**.

Isometric twitch and maximal tetanic stress of the diaphragm were similar between groups (Figure 3.8a and Figure 3.8b, respectively), however, analysis of twitch kinetics demonstrated that HFpEF rats had a slower time to peak tension (Figure 3.8c) while half relaxation time remained unchanged (Figure 3.8d). Similarly, there were no differences in isotonic properties as assessed by maximal shortening velocity or maximal isotonic power between groups (Figure 3.8e, f). During the cyclical contractions, there were no differences in the net power recorded at any given frequency and no difference in the cycle frequency that yielded maximum net power (i.e., 5 Hz for both groups) (Figure 3.8g). However, during repeated cyclical contractions the ability of the diaphragm to sustain work and power relative to the unfatigued state was reduced in HFpEF compared to controls and this occurred after relatively few cycles of work (Figure 3.8h).

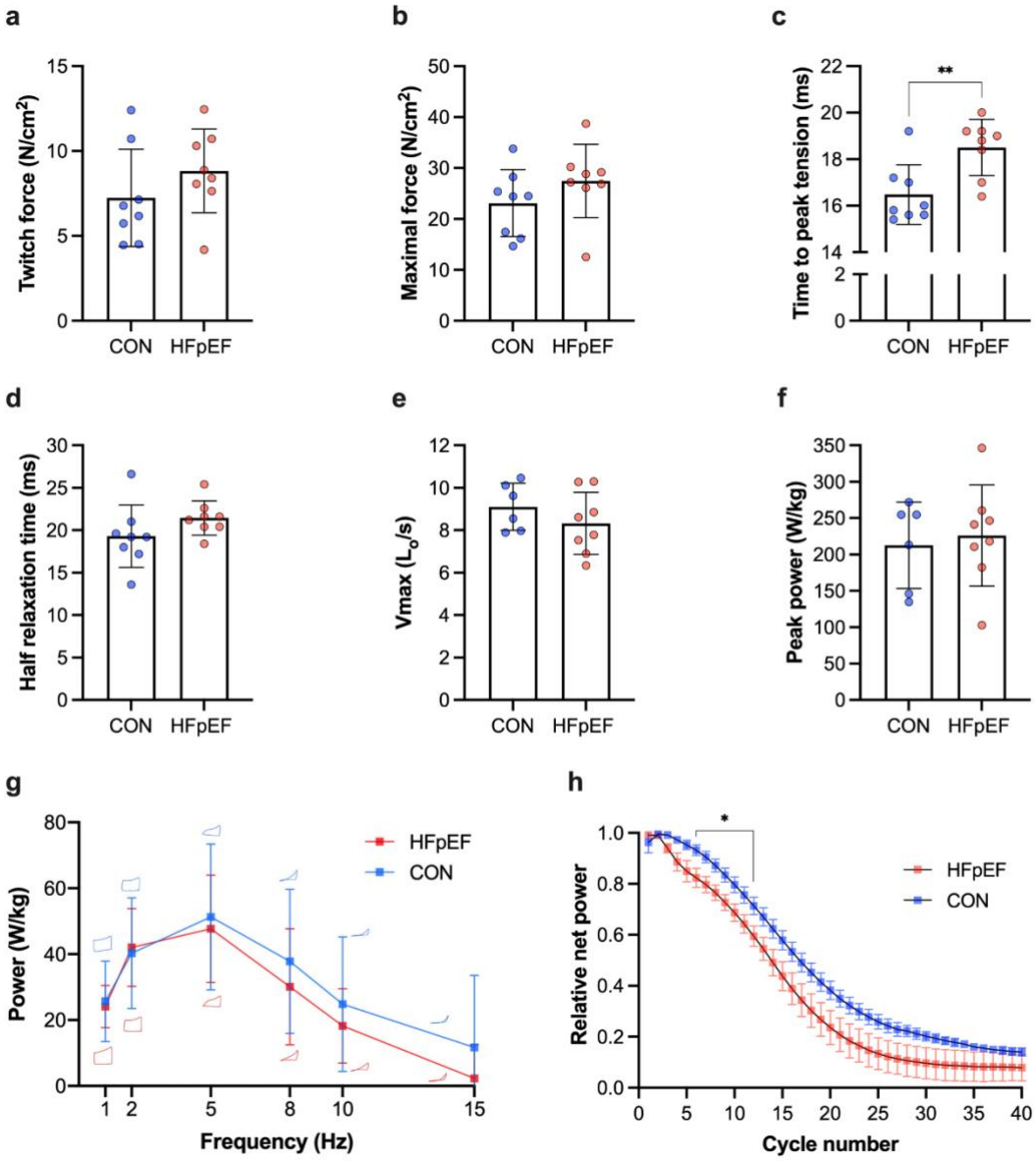

Figure 3.8. Functional properties of the diaphragm. Isometric twitch and tetanic stress of the diaphragm were not different between groups (P = 0.254 and P = 0.225, respectively) **(a, b)**. In contrast, HFpEF rats showed slowed time to peak tension (P = 0.006) **(c)**, although half relaxation time was not significantly affected (P = 0.170) **(d)**. There were no differences in maximal shortening velocity (V_{max}) (P = 0.278) (**e**) or peak isotonic power (P = 0.701) (**f**) between groups. During cyclical contractions, while the net power-cycle frequency relationship remained unaltered between groups (P > 0.05); typical work loops are shown at each cycle frequency for each group (**g**), relative fatigue was greater in HFpEF (P < 0.001) under cycles 6-12 **(h)**.

3.4 Discussion

This study has identified novel skeletal muscle impairments in obese-HFpEF that likely predispose towards the pathophysiology of exercise intolerance. The main findings from this study are:

i) Limb muscle weakness was closely associated with fibre atrophy in HFpEF, but isometric contractile properties were not impaired under neural- or direct-muscle assessments, indicating preserved isometric neuromuscular function.

ii) In contrast, limb isotonic muscle properties including shortening velocity and mechanical power were impaired in HFpEF.

iii) An abnormal leg blood flow response to exercise alongside fibre-type specific structural capillary loss were found in HFpEF.

iv) Significant remodelling of the diaphragm occurred in HFpEF including divergent fibre-type hypertrophy/atrophy, higher capillarity/PO_2, and a Type I fibre-type shift, with preserved muscle mechanics.

3.4.1 Impact of HFpEF on limb muscle function

A reduction in skeletal muscle mass in patients with HFpEF is strongly associated with reduced muscle strength and poor quality of life (Bekfani *et al.*, 2016). Muscle weakness is generally underpinned by either a reduction in muscle mass (i.e., atrophy) and/or intrinsic contractile dysfunction. In this study, we used *in vitro* (i.e., direct-muscle) and *in situ* (i.e., peripheral nerve) stimulation

approaches to assess isometric contractile properties in limb muscle. This allowed various sites in the muscle contractile process to be evaluated for dysfunction in HFpEF, including neuromuscular transmission and excitation-contraction coupling. Consistent with previous data where absolute maximal soleus force was reduced by ~20 % in HFpEF rats *vs.* controls (Bowen *et al.*, 2018; Schauer *et al.*, 2020), we observed that absolute twitch and maximal forces in both the soleus and EDL were lower in HFpEF rats. However, limb muscle weakness was closely associated with fibre atrophy as, after normalising for muscle mass, specific forces were not different between groups independent of whether neural and blood supply remained intact. This is important, as it indicates that neuromuscular transmission and excitation-contraction coupling is likely preserved under isometric contractions in obese-HFpEF.

However, most daily activities require the muscle to shorten against different loads to generate mechanical power and thus perform work. Therefore, assessment of muscle isotonic properties such as shortening velocity and power, which remained undefined in HFpEF, provide a more relevant assessment in relation to daily patient activities. Here, we observed that HFpEF rats had impairments to both shortening velocity and mechanical power in the soleus, which occurred in the absence of any Type I fibre-type shift. This rules out a fibre-type shift, therefore, as a potential underlying mechanism given myosin heavy chain isoform (i.e., rate of myosin ATP hydrolysis) is a key determinant of shortening velocity (Bottinelli *et al.*, 1991). In particular, in slow myosin isoforms shortening velocity is thought to be limited by the rate of ADP dissociation from actomyosin (Nyitrai *et al.*, 2006). Thus, our data suggest obese-HFpEF rats develop slowed rates of cross-bridge detachment through impaired ADP release,

potentially due to post-translational modifications of myosin related to oxidative stress or glycation, as previously reported in HFrEF (Coirault *et al.*, 2007) and ageing (Ramamurthy *et al.*, 1999). In further support, slowed cross-bridge kinetics have previously been reported in Type I and IIa fibres of vastus lateralis biopsies from patients with HFrEF (Miller *et al.*, 2010), although other mechanisms such as impaired sarcoplasmic reticulum calcium pumping cannot be ruled out. Overall, therefore, the significant loss of absolute limb force associated with muscle atrophy in HFpEF alongside intrinsic impairments related to shortening velocity would be predicted to severely reduce mechanical power and thus predispose towards exercise intolerance.

3.4.2 Impact of HFpEF on limb skeletal muscle morphology

Despite skeletal muscle morphological alterations being well investigated in HFrEF (Kennel *et al.*, 2015), little information is available on HFpEF from either animal or patient studies. Previous data from patients with HFpEF indicated the vastus lateralis Type I to Type II fibre-type shift and a lower global C:F ratio, which is associated with reduced $\dot{V}O_{2peak}$ (Kitzman *et al.*, 2014). Animal models (hypertensive or cardiometabolic) have shown in the soleus/EDL a significant fibre atrophy and a lower global C:F ratio (Bowen *et al.*, 2015; Bowen *et al.*, 2017b; Bowen *et al.*, 2018; Schauer *et al.*, 2020). Consistent with this, in the present study we found soleus muscle in HFpEF rats exhibited a fibre atrophy of 24% and fibre-type shift from Type I to Type IIa alongside a lower global C:F ratio of 17%. In contrast, however, we also provide new evidence that capillary density (CD) in the soleus was improved in HFpEF rats by 15% vs controls, and by using novel local measures of capillarity (i.e., LCRF, LCD), we identified this occured in a Type I-specific manner. These additional local indices allowed us to conclude

that a lower C:F ratio in HFpEF is specific to Type I fibres only (i.e., LCRF), suggesting slow- rather than fast-twitch fibres are more susceptible to microvascular impairments in this disease. However, the capillary supply per cross sectional area of Type I fibres (LCD) was in fact higher in HFpEF muscle. These global and local measures of capillarity where C:F was lower but CD higher in HFpEF are likely explained by the observed fibre atrophy, as CD is highly dependent upon fibre size (Egginton, 2011). This indicates that the degree of fibre atrophy exceeded the rate of capillary loss in HFpEF, thus increasing the CD, which has been suggested as an adaptive process to reduce diffusion distances across muscle fibres (Al-Shammari *et al.*, 2019), helping to discriminate structural from functional consequences of microvascular remodelling. In HFpEF, this may be a compensatory mechanism to preserve O_2 flux from capillary to myocyte and thus maintain a better PO_2 status across the muscle, not only in the face of capillary loss but also in response to the reported deficits in mitochondrial O_2 utilisation (Bowen *et al.*, 2015; Molina *et al.*, 2016; Bowen *et al.*, 2017b).

In this regard, data collected from patients with HFpEF have identified clear impairments in the ability to widen arterial-venous O_2 content (ΔAVO_2) and augment peripheral oxygen extraction during exercise compared to HFrEF or controls (Bhella *et al.*, 2011b; Haykowsky *et al.*, 2011; Dhakal *et al.*, 2015; Houstis *et al.*, 2018; Zamani *et al.*, 2020). It remains unclear whether the capillary loss we observed contributes to abnormal skeletal muscle O_2 extraction at peak exercise in HFpEF, with a peripheral O_2 diffusive limitation postulated as a major mechanism underpinning exercise intolerance in HFpEF (Dhakal *et al.*, 2015; Houstis *et al.*, 2018). To expand current knowledge (Dhakal *et al.*, 2015; Houstis

et al., 2018; Zamani *et al.*, 2020), we therefore used *in silico* modelling to provide the first fibre-type specific estimates of microvascular contribution to muscle oxygenation in HFpEF. We found muscle PO_2 was similar between HFpEF and control during simulated rest and at maximal exercise, which indicates adequate oxygenation is maintained in HFpEF with no evidence for enhanced tissue hypoxia. A recent patient study using forearm exercise found estimated peripheral O_2 diffusion was not different between HFpEF and controls (Zamani *et al.*, 2020), which contrasts with previous cycling studies where O_2 diffusion was significantly lower based on systemic hemodynamic, blood gas and pulmonary gas exchange measurements (Dhakal *et al.*, 2015; Houstis *et al.*, 2018). It should be noted that these patient studies did not measure leg/muscle ΔAVO_2, fibre size, capillarity, or microvascular distribution, which can all influence peripheral O_2 diffusion. While the current data do not allow us to confirm whether O_2 diffusion was impaired, our data suggest that fibre morphology and capillary distribution are unlikely to contribute to O_2 diffusive limitations in HFpEF. Interestingly, however, in contrast to HFrEF or controls, patients with HFpEF are unable to lower venous PO_2 during exercise and therefore have a blunted peripheral O_2 extraction response (Dhakal *et al.*, 2015; Houstis *et al.*, 2018; Poole *et al.*, 2018; Zamani *et al.*, 2020). Considering that the requirements for diffusive O_2 flux are largely set by mitochondrial ATP turnover rates (Gutierrez & Vincent, 1991), the degree of mitochondrial dysfunction would likely play a key role in determining the extent of muscle O_2 extraction in HFpEF (Bhella *et al.*, 2011a; Weiss *et al.*, 2017). In our study, estimated muscle PO_2 in HFpEF was not lower than controls at simulated maximal exercise, supporting the potential for a muscle O_2 diffusion limitation (Poole *et al.*, 2018). This is consistent with maintenance of a high muscle

oxygenation across the muscle in HFpEF (see below), supporting the more optimal functioning mitochondrial populations (Al-Shammari *et al.*, 2019). Clearly, more studies are warranted to clarify the role of limitations to muscle O_2 diffusion in HFpEF, however our present data of a reduced leg blood flow (see below) implicate a perfusive O_2 delivery limitation as one key mechanism blunting O_2 extraction in obese-HFpEF.

3.4.3 Impaired muscle blood flow response in HFpEF

Up until now, direct measures of leg (muscle) arterial blood flow had not been assessed in HFpEF, limiting mechanistic understanding. In the present study, using perivascular flow probes (the gold-standard for measuring volumetric blood flow in animal studies), we directly demonstrated that the functional hyperaemic response to exercise was blunted in HFpEF rats. These data support the concept that the peripheral response to exercise is impaired in HFpEF (Houstis *et al.*, 2018), and are consistent with non-invasive measurements in patients with HFpEF during knee-extensor exercise where impaired leg blood flow and vascular conductance occurred independently of limitations to heart rate, stroke volume and cardiac output (Lee *et al.*, 2016b) but contrast with recent isometric forearm data which did not find any change (Zamani *et al.*, 2020). However, some (Maréchaux *et al.*, 2016; Kishimoto *et al.*, 2017) but not others (Hundley *et al.*, 2007; Haykowsky *et al.*, 2013b; Lee *et al.*, 2016a; Zamani *et al.*, 2020) report an abnormal blood flood response to exercise in HFpEF patients when compared to controls, which is probably related to differences in the muscle studied, non-invasive and different measurements techniques, and patient heterogeneity. Overall, our data supports the potential for perfusive, feed-artery O_2 transport

limitations in HFpEF, which likely contributes to exercise intolerance in this disease (Poole *et al.*, 2018).

While the mechanisms underlying abnormal limb blood flow response to exercise in HFpEF remain unclear, endothelial function is impaired (Schmederer *et al.*, 2018) and postulated as a central mechanism underlying disease progression (Paulus & Tschöpe, 2013; Gevaert *et al.*, 2017; Schmederer *et al.*, 2018). Beyond this, upstream central impairments related to cardiac output likely play a major role (Wolsk *et al.*, 2019). It is also possible that the impaired functional hyperaemia induces a compensatory response in the microvasculature, thus improving or preserving CD and muscle PO_2 levels as we observed. The functional significance of abnormal limb blood flow during exercise in HFpEF remains unclear, and cannot explain the greater fatigability (26%) observed in HFpEF rats during the force-matched protocol, as they worked at a higher proportion of their maximal force generating capacity. Our data therefore indicates that skeletal muscle arterial blood delivery is potentially constrained during exercise in HFpEF, despite preserved muscle PO_2 levels as based on our current estimates. As such, at least in the context of this animal model, perfusive rather than O_2 diffusive limitations could play a more prominent role in modulating O_2 extraction in obese-HFpEF (Poole *et al.*, 2018; Zamani *et al.*, 2020), although its functional significance remains unclear.

3.4.4 Impact of HFpEF on diaphragm remodelling and muscle mechanics

Inspiratory (i.e., diaphragm) muscle weakness is evident and closely associated with symptoms of dyspnoea and poor prognosis in patients with HFpEF (Lavietes

et al., 2004; Hamazaki *et al.*, 2020). Multiple alterations to the diaphragm have been reported in HFpEF, including *in vitro* muscle weakness and fatigue alongside a Type II-to-I fibre type shift, fibre atrophy, and impaired *in situ* mitochondrial respiration in a hypertensive rat model (Bowen *et al.*, 2015). In contrast, we show remodelling of the HFpEF diaphragm that is reminiscent of exercise-training including fibre hypertrophy, increased mitochondrial content, and preserved fatigue-resistance, although evidence for mitochondrial uncoupling and a mild isometric contractile dysfunction have been noted (Bowen *et al.*, 2017b). The disparity in findings between models is likely explained by the co-morbidity of obesity and its associated chronic respiratory loading, which can act as a training stimulus to increase fibre size, mitochondrial function/content, and fatigue-resistance (Farkas *et al.*, 1994; Powers *et al.*, 1996). Whether similar findings are observed between obese *vs*. lean patients with HFpEF remains unknown.

Given that approximately 80% of HFpEF patients are obese (Shah *et al.*, 2016) and a recent distinct obese-HFpEF phenotype has been established (Obokata *et al.*, 2017), the present study contributes novel and highly-relevant data in relation to diaphragm plasticity. Until now, only limited data have been available with respect to fibre-type structure, isoform, and microvasculature of the diaphragm in HFpEF (Bowen *et al.*, 2015; Bowen *et al.*, 2017b). In the present study, we identified three major fibre types (Type I, IIa and IIb/IIx) to provide new evidence of a divergent hypertrophy/atrophy fibre remodelling in obese-HFpEF alongside increased indices of global and local capillarity (i.e., C:F and CD), and estimated levels of fibre oxygenation at rest and maximal exercise. Specifically, compared to controls, obese-HFpEF rats had increased Type I/IIa FCSA, and

reduced Type IIb/IIx FCSA, indicating compensatory adaptations in slow-twitch fibres. This observation corresponds to the morphometric alterations following unilateral denervation of rat diaphragm muscle, where hypertrophy in Type I fibres but atrophy in Type IIb/IIx fibres occurred (Aravamudan *et al.*, 2006) alongside increased CD (Paudyal *et al.*, 2018). Nevertheless, it remains unclear whether obese-HFpEF induces partial diaphragm muscle denervation in fast-twitch Type IIb/x as reported in other conditions such as aging (Elliott *et al.*, 2016).

Overall the obese-HFpEF diaphragm demonstrates improved indices of oxygen transport (increased capillarity and PO_2 distribution) that likely supports the observed shift towards an oxidative phenotype (i.e., higher proportion of Type I fibres, mitochondrial content, and antioxidative enzyme capacity (Bowen *et al.*, 2015; Bowen *et al.*, 2017b). This suggests that any functional diaphragm impairments developed in obese-HFpEF were likely offset by morphological adaptations. To decipher this potential trade-off, we performed *in vitro* isometric, isotonic and cyclical contractions on the diaphragm in one of the most detailed functional assessments in HFpEF to date. Our data indicate that impaired muscle mechanics and intrinsic diaphragm dysfunction generally do not develop early in the time course of obese-HFpEF (~20 weeks), with only a mild differences found compared to controls in terms of fatigability. Again, these data conflict with previous experimental data where a significant reduction in diaphragm stress during repeated isometric contractions was measured in rats during more advanced hypertensive-induced HFpEF (Bowen *et al.*, 2015). In the present study we also simulated *in vivo* respiratory muscle mechanics, by applying cyclical length changes and phasic stimulation to the muscle to generate cycles

of work, using the *in vitro* work-loop technique (Josephson, 1985). Similar to our isolated isometric and isotonic measures, net power output during unfatigued cyclical contractions in obese-HFpEF was unaffected, but we did observe mild fatigue effects during repeated cyclical contractions. Collectively, these data suggest respiratory muscle dysfunction is unlikely a key player in the pathogenesis of exercise intolerance in obese-HFpEF, at least during early disease progression.

3.4.5 Limitations

We did not use echocardiography or invasive haemodynamics to quantify the extent of left ventricular diastolic function and ejection fraction. However, this rat model has been validated and consistently develops key features of HFpEF as early as 10-15 weeks of age (Schauer *et al.*, 2020), including impaired diastolic function, preserved ejection fraction, myocardial remodelling, and exercise intolerance (Hamdani *et al.*, 2013; Leite *et al.*, 2015; Franssen *et al.*, 2016; van Dijk *et al.*, 2016; Bowen *et al.*, 2017b). Instead, we used MRI to confirm the presence of cardiac remodelling which occurred in the RV and this is known to be closely associated with HFpEF development in obese patients (Obokata *et al.*, 2017) and one of the strongest predictors of poor prognosis (Burke *et al.*, 2014). We also compared groups at a relatively early time point in the progression of HFpEF, which may limit translation of our findings to more advanced stages of the disease. In addition, while differences in physical activity levels between groups were not measured and cannot be ruled out as having an influence on our experimental measures, it is well established that disuse alone fails to account for the skeletal muscle impairments developed during heart failure (Simonini *et al.*, 1996; Miller *et al.*, 2009).

3.5 Conclusions

Rats with obese-HFpEF have a blunted hindlimb blood flow response to exercise alongside microvascular structural impairments, fibre atrophy, and isotonic contractile dysfunction, which may be important factors underlying exercise intolerance in this disease. In contrast, diaphragm phenotype was largely preserved, indicating a more prominent role for limb rather than respiratory muscle abnormalities in obese-HFpEF.

Chapter 4 Results II. Pharmacological treatments enhancing cardiac function in HFpEF do not impact skeletal muscle remodelling

4.1 Introduction

HFpEF remains a major challenge in cardiovascular medicine due to its high morbidity and mortality with increasing prevalence and lack of effective treatments (Butler *et al.*, 2014; Sharma & Kass, 2014; Fukuta *et al.*, 2016; Mishra & Kass, 2021a). Whereas treatments that ameliorate the neurohormonal overactivation (e.g., MRA and ARB) have shown beneficial outcomes in HFrEF (Pitt *et al.*, 1999; McMurray *et al.*, 2003; Zannad *et al.*, 2011; Vaduganathan *et al.*, 2020), these treatments have failed to improve long-term morbidity and mortality in HFpEF patients (Yusuf *et al.*, 2003; Cleland *et al.*, 2006; Massie *et al.*, 2008; Pitt *et al.*, 2014). Within the last 12 months, SGLT2I became the first pharmacological treatment that reduced the risk of cardiovascular deaths and hospitalizations in HFpEF patients (Anker *et al.*, 2021). As such, the potential for other drug therapies to improve clinical outcomes in HFpEF remains high. Several novel therapies for different HFpEF phenotypes have been studied and show promising results. For example, Entresto (Sacubitril/Valsartan), an ARNI, improved diastolic function, cardiac remodelling, and endothelial function in HFpEF patients and animal models (Gori *et al.*, 2019; Schauer *et al.*, 2021). Similarly, Vastiras (proANP$_{31-67}$), a novel compound derived from the linear fragment of atrial natriuretic peptide (ANP), improved cardiac structure (attenuated LV hypertrophy and reduced fibrosis) and function (normalised E/A i.e. a measure of diastolic dysfunction) in an experimental hypertensive rat (Altara *et al.*, 2020).

Whether drug therapies to improve cardiac function in HFpEF could have secondary (or even direct) effects to benefit skeletal muscle homeostasis remains poorly explored. For example, treatments improving cardiac function in HFpEF could benefit skeletal muscles *via* improved nutrient or O_2 delivery or reducing inflammation (Mishra & Kass, 2021b; Anderson *et al.*, 2022). However, exercise intolerance in HFrEF is still present even after normalisation of central cardiovascular function by pharmacological treatments (Maskin *et al.*, 1983) or heart transplantation (Stevenson *et al.*, 1990). This suggests that directly targeting the heart *per se* may not overcome symptoms of exercise intolerance and skeletal muscle abnormalities in HFpEF. In support, a preliminary study documented that Entresto failed to improve skeletal muscle weight and function in obese-HFpEF rats, despite improved cardiac function (Schauer *et al.*, 2021). However, this study lacked assessments of important morphological features, such as FCSA, fibre type distribution and capillarisation, which are known to be affected by HFpEF (Kitzman *et al.*, 2014; Bowen *et al.*, 2018). This chapter, therefore, aimed to determine whether Entresto alone or in combination with Vastiras (in order to increase cardiac function) caused beneficial skeletal muscle remodelling in experimental rats with HFpEF. Specifically, using both oxidative (soleus) and glycolytic (EDL) muscles, we performed global and local fibre-type specific phenotyping of CSA, isoform, and capillarity, alongside estimated fibrosis.

4.2 Methods

4.2.1 Ethical approval

This study was performed with collaborators at the University of Oslo, Norway. All procedures and experiments were approved by the Norwegian Food Safety Authority committee (Mattilsynet) for animal research (FOTS protocol number 15886) in accordance with the national regulations, the European Convention for the Protection of Vertebrate Animals used for Experimental and Other Scientific Purposes (ETS No.123), and the European Directive 2010/63/EU on the protection of animals used for scientific purposes.

4.2.2 Animals

Obese ZSF1 rats were compared to lean controls (CON) and were randomly assigned to the following groups: HFpEF+Vehicle (HFpEF+Ve), HFpEF+Entresto (68 mg/kg/day) (HFpEF+En) or HFpEF+Entresto (68 mg/kg/day)+Vastiras (50 ng/kg/day) (HFpEF+En+Va). Drug or vehicle was delivered *via* Alzet osmotic mini-pumps (Model 2004; mean pumping rate 2.28±0.07 µL/h, mean fill volume 1997.6±18.3 µL) implanted subcutaneously (as described by the manufacturer) for 10 weeks. Animals were treated with subcutaneous buprenorphine (0.05 mg/kg) as an analgesic 30 minutes before and up to 1-day postpump implantation. Vastiras was obtained from Madeline Pharmaceuticals Pty Ltd (Mount Barker, SA, Australia). The drug manufacturer recommends using 200 mmol/L NaCl with 10 mmol/L sodium acetate buffer (pH 5.5) as vehicle for the drug.

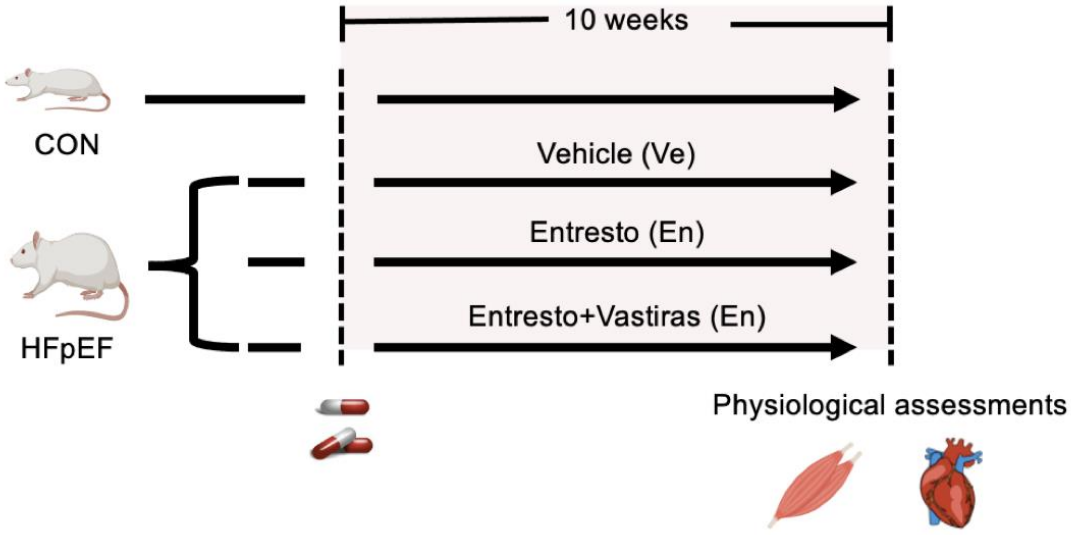

Figure 4.1. Protocol for Entresto and Vastiras treatment. Obese ZSF1 rats were randomly assigned to the following groups: HFpEF+Vehicle (HFpEF+Ve; n = 8), HFpEF+Entresto (HFpEF+En; n = 6) and HFpEF+Entresto+Vastiras (HFpEF+En+Va; n = 6), and compared to their respective lean controls (CON; n = 11). Cardiometabolic and skeletal muscle phenotypes were evaluated after 10 weeks of treatment.

4.2.3 Cardiometabolic function

Full details of metabolic features (body weight, systolic blood pressure and blood glucose levels), echocardiography and invasive haemodynamic measurements are provided in Chapter 2 General methods: 2.3.

4.2.4 Morphological characterization of skeletal muscle

Soleus and EDL muscles were assessed for global and fibre type-specific histological features (i.e., FCSA, myosin isoform, capillarity, and fibrosis), as previously described (Al-Shammari *et al.*, 2019). Full details of all analyses are provided in Chapter 2 General methods: 2.8.

4.2.5 Statistical analyses

Following appropriate checks of normality, between-group differences were assessed by one-way ANOVA followed by Bonferroni *post hoc* test. Differences

between lean controls and HFpEF were analysed by unpaired two-tailed Student t-tests. Analyses were performed in GraphPad Prism v.8. Data are presented as mean±SD, and the level of significance was set at $P < 0.05$ for all analyses.

4.3 Results

4.3.1 Cardiometabolic phenotype in untreated obese ZSF1 rats

As previously noted (Leite *et al.*, 2015; Bowen *et al.*, 2017b; Espino-Gonzalez *et al.*, 2020; Schauer *et al.*, 2020), untreated obese ZSF1 rats (i.e., HFpEF+Ve) showed evidence of typical metabolic signs associated with HFpEF including obesity (Figure 4.2a) and hyperglycaemia (Figure 4.2b) although systolic blood pressure was not different between groups (Figure 4.2c). Compared with controls, HFpEF rats developed cardiac hypertrophy represented as increased heart weight, heart weight /tibia length and ventricular mass (Figure 4.2d-f). The ratio between the early maximal ventricular filling velocity and the late filling velocity (E/A; an index of diastolic dysfunction) was lower in HFpEF rats (Figure 4.2g). Lean and obese-HFpEF rats had preserved left ventricular ejection fraction (LVEF) (Figure 4.2h). HFpEF rats developed cardiac dysfunction, which was confirmed by non-invasive and invasive measurements of stroke volume and cardiac output (Figure 4.2i-l).

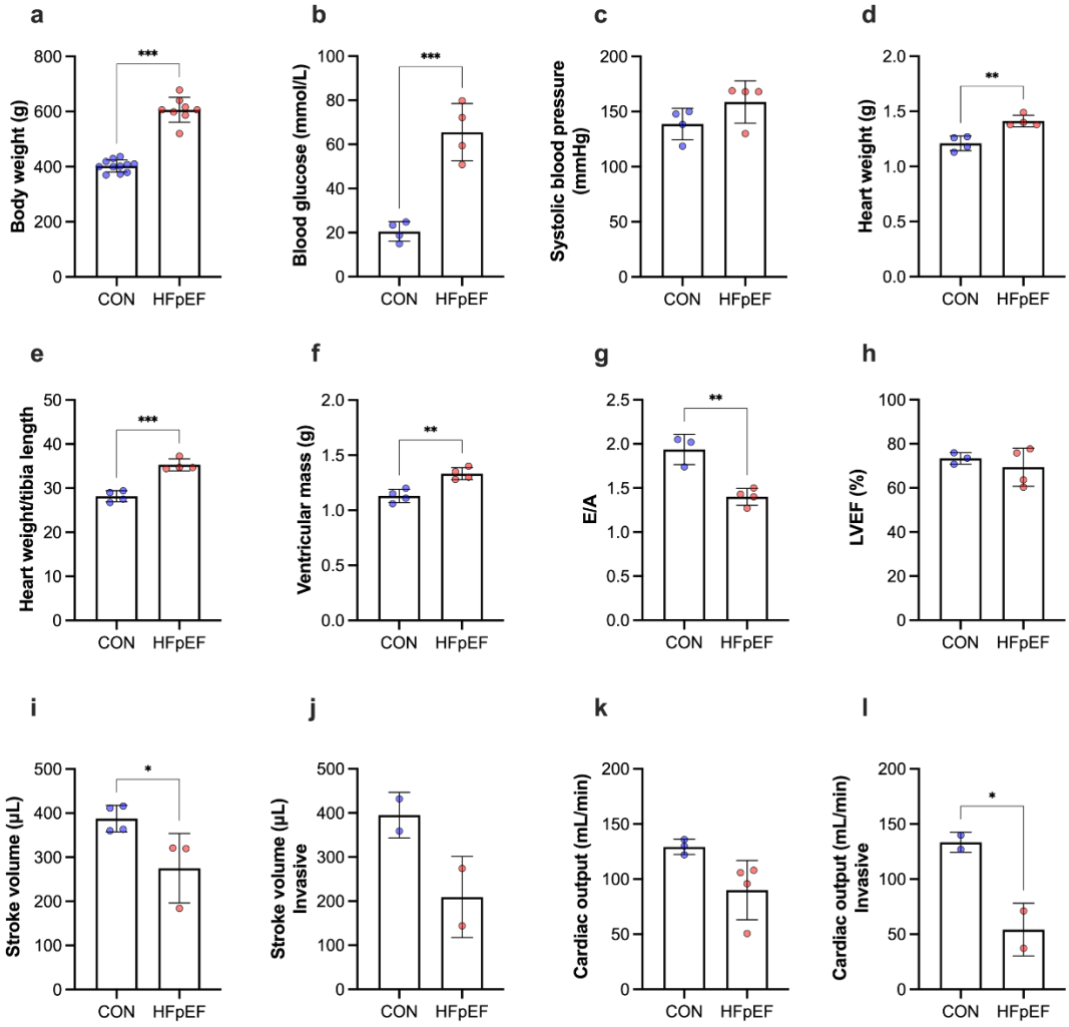

Figure 4.2. Cardio-metabolic characteristics. HFpEF rats developed obesity ($P < 0.001$) **(a)** and hyperglycaemia ($P < 0.001$) **(b)** with no significant changes in systolic blood pressure ($P = 0.14$) **(c)**. Obese-HFpEF rats also had cardiac hypertrophy represented as increased heart weight ($P = 0.003$) **(d)**, heart weight /tibia length ($P < 0.001$) **(e)** and ventricular mass ($P = 0.002$) **(f)**. The ratio between the ratio between the early maximal ventricular filling velocity and the late filling velocity (E/A) was lower in HFpEF rats ($P = 0.003$) **(g)**, whereas left ventricular ejection fraction (LVEF) was similar between groups ($P = 0.48$) **(h)**. Non-invasive and invasive measurements of stroke volume and cardiac output showed that HFpEF rats developed diastolic dysfunction: stroke volume ($P = 0.04$) **(i)**, stroke volume - invasive ($P = 0.13$) **(j)**, cardiac output ($P = 0.06$) **(k)** and cardiac output - invasive ($P = 0.05$) **(l)**.

4.3.2 Effects of Entresto and Vastiras on cardiac measures

Ten weeks of medication with Entresto or Entresto+Vastiras did not significantly affected body weight, blood glucose levels and systolic blood pressure in HFpEF rats (Figure 4.3a-c). In contrast, however, HFpEF-induced impairments in heart weight and E/A were ameliorated by Entresto and/or Vastiras (Figure 4.3d-g).

Similarly, invasive measurements of cardiac output showed that both Entresto and Entresto+Vastiras improved cardiac function (Figure 4.3l). In addition, invasive and non-invasive measurements of stroke volume showed this tended to be lower in HFpEF+Ve rats, which was attenuated by medications (Figure 4.3i, j). LVEF was reduced in the HFpEF+En+Va group (Figure 4.3h). Taken together, these data suggest that Entresto and Vastiras partly ameliorate cardiac impairments induced by HFpEF.

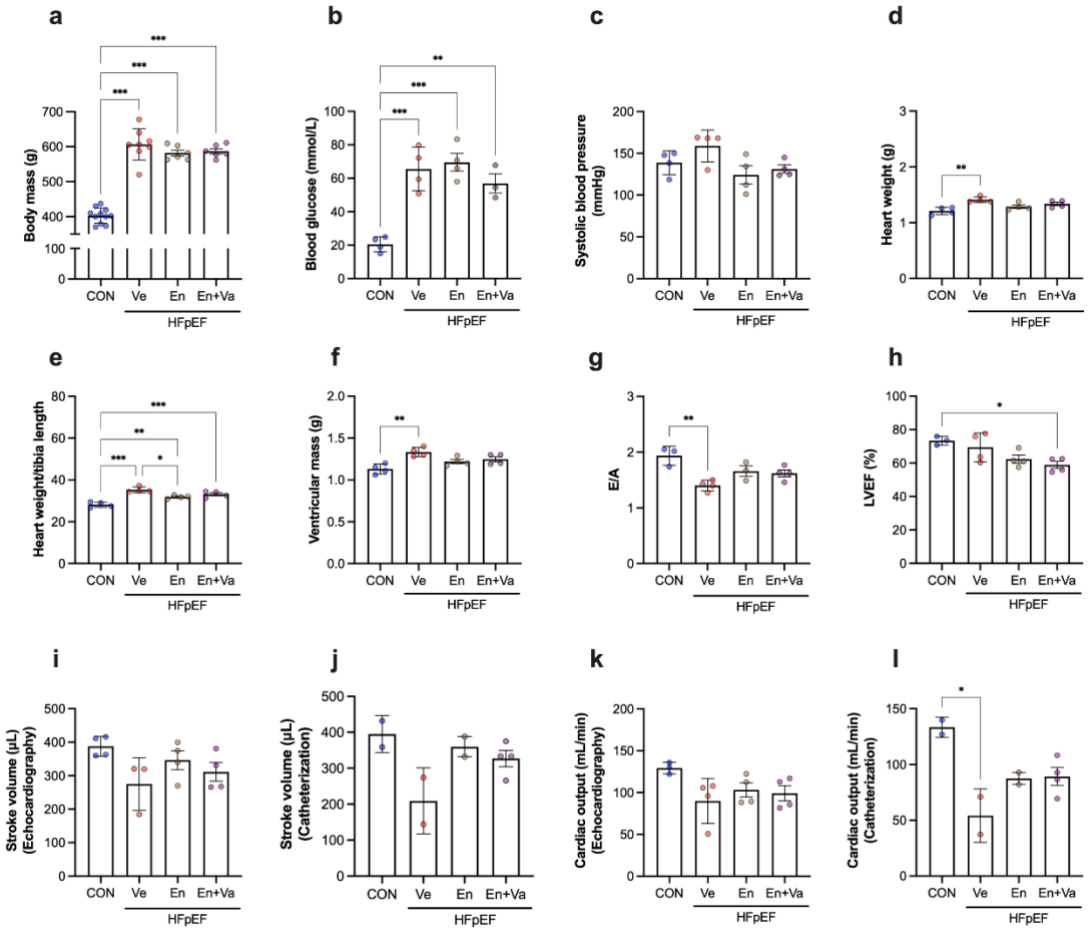

Figure 4.3. Effects of Entresto and Vastiras in metabolic features and cardiac function and morphology. Compared to controls, HFpEF rats with or without treatments had increased body weight (all $P < 0.001$) **(a)** and blood glucose levels (all $P < 0.05$) **(b)**. Systolic blood pressure was similar between groups (all $P > 0.05$) **(c)**. HFpEF-induced cardiac hypertrophy was improved by Entresto, as values were similar to those observed in controls ($P = 0.23$) **(d)**; however, after normalisation to tibia length, heart weight was increased in HFpEF rats with or without treatments (all $P < 0.05$) **(e)**. Ventricular mass was similar between controls and HFpEF+Entresto ($P = 0.10$) **(f)**. Similarly, HFpEF-induced impairments in E/A were rescued by Entresto and/or Vastiras ($p = 0.08$) **(g)**.

Compared to lean controls, LVEF was reduced in HFpEF+En+Va (P = 0.02) **(h)**. Invasive and non-invasive measurements of stroke volume showed that this tended to be lower in HFpEF+Ve rats (P = 0.10 and P = 0.13, respectively), which was rescued by medications (all p > 0.05) **(i, j)**. Cardiac output, measured by non-invasive methods, was similar between groups (p > 0.05) **(k)**. In contrast, however, invasive measures of cardiac output showed that this was lower in HFpEF+Ve (P = 0.006), which was rescued by medications (P > 0.05) **(l)**.

4.3.3 Effects of Entresto and Vastiras on skeletal muscle remodelling

Compared with lean controls, HFpEF rats with or without treatments had lower EDL wet-mass and FCSA, which was more prominent in Type IIb/IIx fibres (Figure 4.4a-c). Proportion of Type I, IIa and IIb/IIx fibres was similar between groups (Figure 4.4d). HFpEF induced a reduction in C:F, which was not rescued by Entresto or Entresto+Vastiras (Figure 4.4e). No significant differences were observed in CD (Figure 4.4f). Fibre type-specific histological analysis showed that, compared to controls, LCFR of Type I fibres was lower in HFpEF, with no significant changes in treated groups (Figure 4.4g). Impairments in LCFR were more prominent in Type IIb/IIx (fast/glycolytic) fibres, which were not rescued by medications (Figure 4.4g). LCD (Type I, IIa and IIb/IIx fibres) was similar between groups (Figure 4.4h).

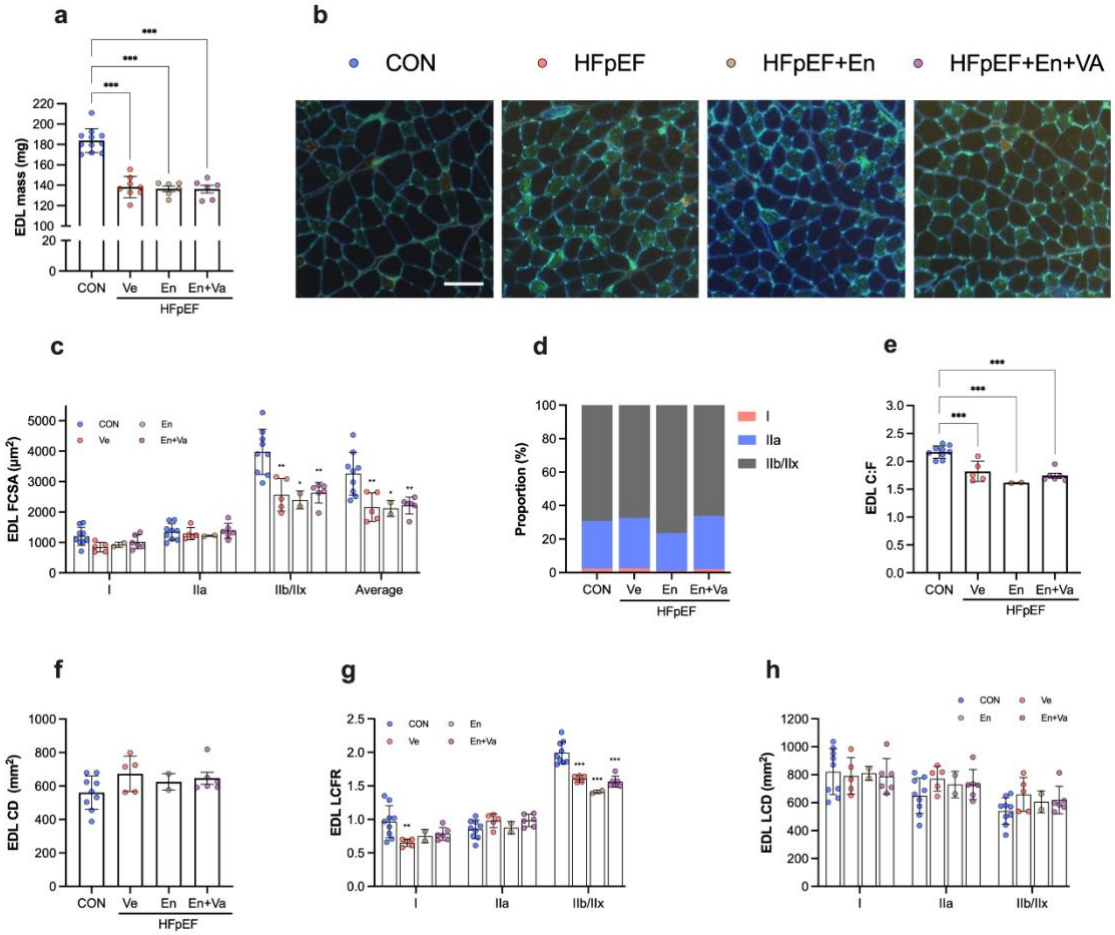

Figure 4.4. Effects of Entresto and Vastiras in EDL morphology. Compared to lean controls, obese-HFpEF rats with or without treatments had reduced wet-mass (all $P < 0.001$) **(a)** and cross-sectional area (CSA) of Type IIb/IIx fibres ($P < 0.05$) **(b, c)**. The numerical proportion of Type I, IIa and IIb/IIx fibres was similar between groups ($P > 0.05$) **(d)**. Compared to controls, non-treated and treated obese-HFpEF rats had reduced capillary-to-fibre (C:F) ratio (all < 0.05) **(e)**. In contrast, capillary density (CD) was similar between groups ($P > 0.05$) **(f)**. Obese-HFpEF rats with or without treatments had reduced local capillary-to-fibre ratio (LCFR) in Type IIb/IIx fibres ($P < 0.001$) **(g)**, while local capillary density (LCD) of Type I, IIa and IIb/IIx fibres was similar between groups ($P > 0.05$) **(h)**. Scale bar represents 100 μm.

The EDL is a highly glycolytic muscle. To compare morphological changes between mixed and oxidative muscles, we also analysed global and local histological features of the soleus muscle. While soleus wet-mass was lower in all obese-HFpEF groups (Figure 4.5a), this did not reach significance in terms of FCSA (Figure 4.5b, c). Fibre type composition was also not different between groups (Figure 4.5d). In contrast to the EDL muscle, global and local

measurements of C:F, CD, LCFR and LCD showed that these were not significantly affected by HFpEF or medications (Figure 4.5e-h). Similarly, percentage of fibrosis was comparable between groups (Figure 4.5i, j).

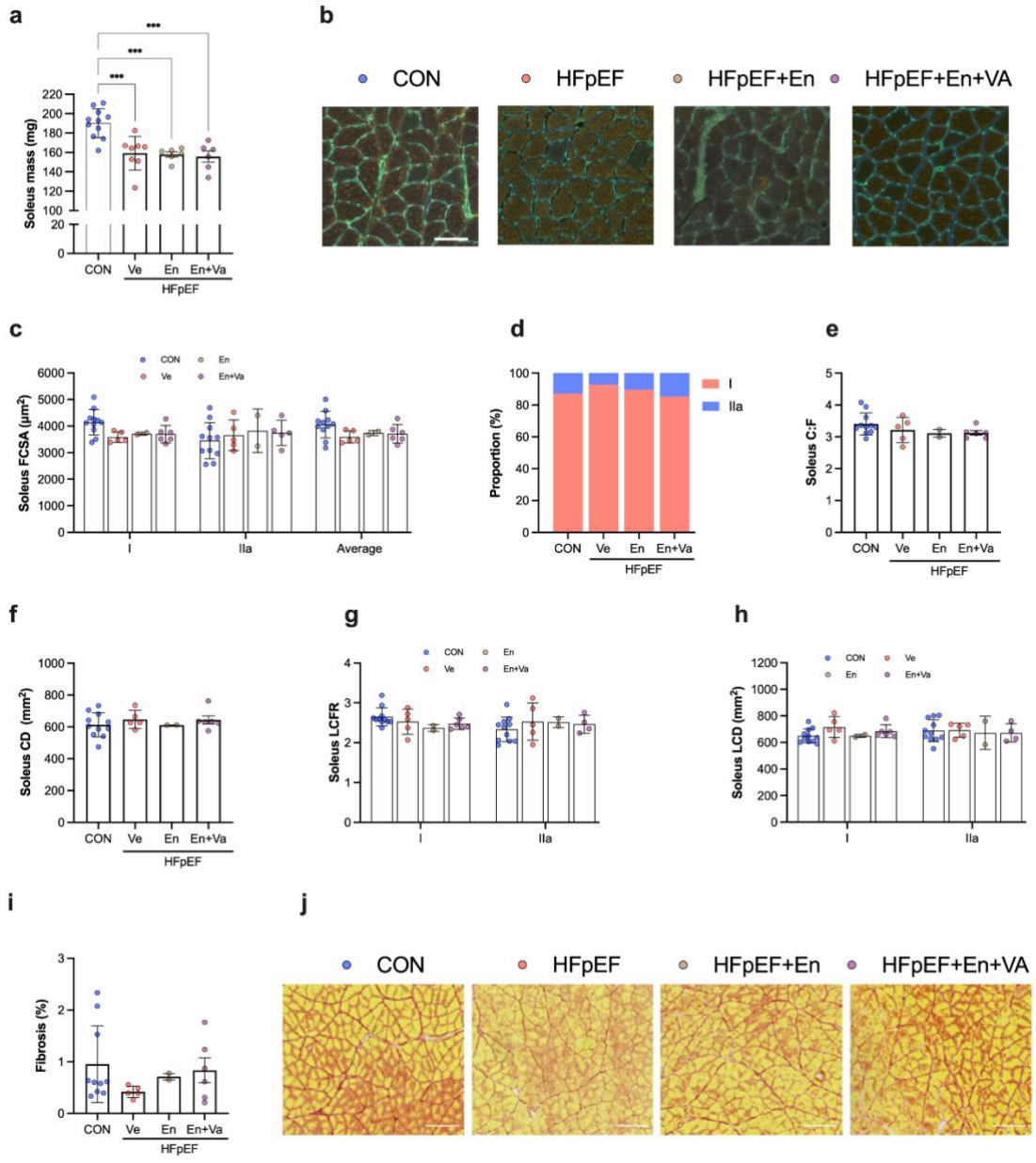

Figure 4.5. Effects of Entresto and Vastiras in soleus morphology. Compared to controls, HFpEF rats with or without treatments had lower muscle mass (all $P < 0.001$) **(a)**. In contrast, fibre cross-sectional area (FCSA) **(b, c)**, fibre type proportion **(d)**, capillary-to-fibre (C:F) ratio **(e)**, capillary density (CD) **(f)**, local capillary-to-fibre ratio (LCFR) **(g)**, local capillary density (LCD) **(h)**, and percentage of fibrosis **(i, j)** were comparable between groups (all $P > 0.05$). Scale bar represents 100 μm.

4.4 Discussion

This study, using a well-established rat model of HFpEF, provides novel data to confirm that improvements in global cardiac function do not reverse skeletal muscle atrophy and capillary rarefaction. Our data adds new data to confirm this is relevant at the myofiber level and across various fibre-types. Thus these findings supports past research that indicated Entresto improved cardiac function independent to changes skeletal muscle wet-mass and function (Schauer *et al.*, 2021). We also provide additional evidence that Entresto alone or in combination with Vastiras can enhance cardiac function but with no impact on HFpEF-induced skeletal muscle remodelling. Our data may have important implications for treating HFpEF-associated skeletal muscle deficits, suggesting that alternative approaches beyond a cardio-centric view are likely necessary.

4.4.1 Experimental models for HFpEF

Increasing evidence indicates that rather than central (cardiac) factors, peripheral skeletal muscle alterations play a key role in the pathogenesis of exercise intolerance in HFpEF (Haykowsky *et al.*, 2014; Kitzman *et al.*, 2014). However, treatments for HFpEF-associated muscle deficits remain poorly explored and this has been compounded by almost all pharmacological treatments having limited clinical benefits (Anderson *et al.*, 2022). Identification of animal models that closely replicate the human condition is a critical step in developing and testing new treatments, which has been challenging for HFpEF. Compared to other animal models, such as the Dahl salt-sensitive rat (DSS) and the transverse aortic constriction surgery/deoxycorticosterone mouse (TAC/DOCA), the ZSF1 rat has shown the highest overlap to the human condition with regards to skeletal muscle alterations (Goto *et al.*, 2020), thus making this a suitable model for exploring

therapeutic interventions for HFpEF-associated muscle alterations. Specifically, ZSF1 rats have shown to develop muscle atrophy, impaired contractile function, and reduced capillary supply (Bowen *et al.*, 2017b; Bowen *et al.*, 2018; Espino-Gonzalez *et al.*, 2020; Schauer *et al.*, 2020). We found that obese-ZSF1 rats also have impaired blood flow response to contractions that implies a perfusive oxygen delivery limitation (Chapter 3 Results I). In the present study, HFpEF rats developed muscle wasting (represented as lower wet-mass and fibre atrophy) and reduced capillarity, thus supporting the concept of HFpEF being characterised by a skeletal muscle pathology.

4.4.2 Fast-twitch glycolytic fibres are more vulnerable than slow-twitch oxidative fibres to HFpEF-induced muscle atrophy

It has been suggested that skeletal muscle remodelling in HFpEF is fibre-type dependent. Compared to slow-twitch soleus (oxidative muscle), the EDL (glycolytic muscle) shows greater susceptibility to impairments in fibre size and capillarisation (Bowen *et al.*, 2018). In contrast to past studies (Schauer *et al.*, 2021), the present study used fibre type-specific histological analysis to directly confirm new evidence that HFpEF-induced atrophy and reduced capillary supply of the EDL muscle are more prominent in Type IIb/IIx (fast/glycolytic) fibres. Compared to slow-twitch oxidative fibres, fast-twitch glycolytic fibres have shown to be more vulnerable under a variety of atrophic disorders associated with enhanced proteasome-mediated degradation through activation of MuRF1 (Wang & Pessin, 2013). In line with this, increased expression of MuRF1 has been observed in EDL muscles of ZSF1-HFpEF rats as well patient muscle (quadriceps) (Goto *et al.*, 2020). The resistance of oxidative fibres may be explained, at least in part, by increased activity of peroxisome proliferator-

activated receptor gamma coactivator 1-alpha (PGC-1α), a well-described factor required for mitochondrial biogenesis, oxidative metabolism, and slow-twitch fibre formation (Sandri *et al.*, 2006; Wang & Pessin, 2013). PGC-1α protects skeletal muscle from atrophy by inhibiting transcriptional activity of FOXO, which suppresses atrogene (MuRF1) expression and protein degradation (Sandri *et al.*, 2006). While PGC-1α expression was not measured in the present study, we did not observe fibre atrophy in the soleus muscle, which compared to mixed muscles, is known to have higher levels of PGC-1α (Lin *et al.*, 2002). Collectively, therefore, our data suggest that muscle groups composed of fast-twitch fibres should be primarily targeted during rehabilitation in HFpEF patients, as these may be more vulnerable to impairments and this aligns to past data in HFrEF (Li *et al.*, 2007).

4.4.3 Entresto and Vastiras do not influence skeletal muscle but improve cardiac indices

Therapeutic treatments for HFpEF have been a major challenge and largely limited thus far to exercise and nutritional interventions (Kitzman *et al.*, 2016). However, exercise may not be a practical option, as patients with this syndrome frequently have severe functional limitations; thus development of new pharmacological treatments represents an unmet medical need. To date, Empagliflozin, a SGLT2I, is the only treatment that has been able to reduce the risk of cardiovascular death or hospitalization in HFpEF patients (Anker *et al.*, 2021); yet, several therapies have shown promising results that could benefit functional status. Entresto (Sacubitril/Valsartan), an ARNI, improved diastolic function, cardiac remodelling, and endothelial function in HFpEF (Gori *et al.*, 2019; Schauer *et al.*, 2021) but was unable to improve skeletal muscle wet mass

and contractile function in obese-HFpEF rats (Schauer *et al.*, 2021). In the present study, we evaluated the therapeutic potential of Entresto alone and in combination with Vastiras ($proANP_{31-67}$), a novel compound derived from the linear fragment of atrial natriuretic peptide (ANP) that attenuated cardiac hypertrophy, reduce fibrosis and improve cardiac function in hypertensive Dahl/Salt sensitive rats (Altara *et al.*, 2020), but its effects on skeletal muscle remained unexplored. Ten weeks of Entresto alone or in combination with Vastiras did not improve the observed atrophy and reduced capillarisation of HFpEF EDL muscles. Similarly histological analyses of fibre type distribution, capillarisation and fibrosis of soleus muscle did not reveal beneficial effects of the treatments, suggesting that both mixed (EDL) and oxidative (soleus) muscles are not influenced by Entresto or Vastiras. In contrast, both medications improved cardiac morphology and function in obese-HFpEF rats. Specifically, treatments were able to partially ameliorate the observed impartments in heart weight, E/A and stroke volume in HFpEF rats. While a deeper exploration of the mechanisms underlying cardiac benefits induced by Entresto and/or Vastiras was outside the scope of this study, the reduction in heart/ventricular mass may be a consequence of blood pressure control, as this tended to be normalised in treated rats, which is known to ameliorate myocyte hypertrophy (Schauer *et al.*, 2021). It is also likely that treatments reduced myocardial fibrosis and restored titin phosphorylation, thereby preserving left ventricular elasticity, as previously observed in ZSF1-HFpEF rats and both HFpEF and HFrEF patients (Cunningham *et al.*, 2020; Schauer *et al.*, 2021). Overall, this also suggest two key conclusions: 1) increasing global blood flow alone did not reverse skeletal muscle abnormities in HFpEF; and 2) the medications unlikely have direct

beneficial effects on skeletal muscle (albeit a longer time period may be required to see effects of both).

4.4.4 Limitations

The present study is subject to some limitations. Our experiments were performed in male rats only, thus, sex-dependent differences cannot be excluded. Further, this study lacks assessments of skeletal muscle contractile properties, therefore, the effects of Entresto+Vastiras in HFpEF muscle function remains to be critically evaluated although changes are unlikely based on past studies showing no effects using Entresto only (Schauer *et al.*, 2021). Furthermore, only two rats from the HFpEF+Entresto group were included for histological analyses due to transportation issues which may limit conclusions.

4.5 Conclusions

Obese-HFpEF rats develop skeletal muscle histological alterations that are more prominent in fast-twitch glycolytic fibres. However, increasing cardiac function *per se*, *via* targeted cardiovascular drugs, had no impact on skeletal muscle morphology in HFpEF rats. Overall, this suggests alternative skeletal muscle-specific interventions are required to overcome peripheral musculature deficits in HFpEF rather than simply targeting improvements in global cardiac function.

Chapter 5 Results III. Overload-induced skeletal muscle hypertrophy is impaired in HFpEF

5.1 Introduction

Impaired exercise capacity ($\dot{V}O_{2peak}$) is one of the central manifestations of HF and closely associated with decreased patient survival and poor of quality of life (Nadruz *et al.*, 2017). Growing evidence suggest that skeletal muscle (peripheral) alterations play a more dominant role in explaining exercise intolerance in HFpEF rather than cardiac (central) dysfunction (Haykowsky & Kitzman, 2014; Mohammed *et al.*, 2014). HFpEF-associated skeletal muscle alterations in both patients and experimental models confirm lower skeletal muscle strength (Bekfani *et al.*, 2016), fat infiltration (Haykowsky *et al.*, 2014; Zamani *et al.*, 2020), fibre atrophy (Bowen *et al.*, 2018), reduced capillarization (Kitzman *et al.*, 2014; Bowen *et al.*, 2018), mitochondrial dysfunction (Bowen *et al.*, 2015; Molina *et al.*, 2016; Bowen *et al.*, 2017b), augmented high-energy phosphate depletion during exercise (Bhella *et al.*, 2011a; Weiss *et al.*, 2017), lower O_2 extraction (Dhakal *et al.*, 2015; Houstis *et al.*, 2018; Zamani *et al.*, 2020), impaired muscle mechanics and reduced functional hyperaemia (Espino-Gonzalez *et al.*, 2020).

While there is a lack of effective treatments for HFpEF, exercise training is associated with prognostic benefits in patients (Kitzman *et al.*, 2010; Dieberg *et al.*, 2015; Pandey *et al.*, 2015; Chan *et al.*, 2016). Exercise training improves $\dot{V}O_{2peak}$ and quality of life in HFpEF, in part by enhancing arterial-venous O_2 content (ΔAVO_2) and augmenting peripheral oxygen extraction, without significantly altering cardiac function or structure (Kitzman *et al.*, 2010; Haykowsky *et al.*, 2012; Smart *et al.*, 2012; Tucker *et al.*, 2016). Importantly, however, exercise trials have mainly focused on cardiorespiratory function, while

little is known about exercise-induced skeletal muscle adaptations. In HFrEF patients, exercise training studies (endurance or resistance) are well established to reverse many skeletal muscle alterations such as lower muscle mass, fibre atrophy, fibre type shift, reduced C:F, lower mitochondrial density and impaired blood flow (Gielen *et al.*, 2003; Esposito *et al.*, 2018; Engineer *et al.*, 2019; Tryfonos *et al.*, 2021). Interestingly, recent data from obese-HFpEF rats indicated that endurance training was unable to overcome several histological, mitochondrial and functional skeletal muscle impairments (Bowen *et al.*, 2017b; Bowen *et al.*, 2018), while patient studies addressing this issue remain elusive. Thus, at present there remains a gap in knowledge whether HFpEF impairs skeletal muscle remodelling to response to adequate stimuli.

Muscle adaptation to mechanical overload (exercise) is typically characterized by increases in muscle wet-mass and FCSA (Ianuzzo & Chen, 1979; Timson *et al.*, 1985), which are dependent on changes in protein synthesis and/or addition of new myonuclei (Blaauw & Reggiani, 2014). Further, exercise-induced muscle adaptations can be affected by intrinsic (e.g., mitochondrial dysfunction) and/or extrinsic skeletal muscle alterations (e.g., impaired flood flow). For example, decreased mitochondrial ATP production can limit protein synthesis (Carafoli *et al.*, 1964; Hyatt & Powers, 2021), which directly affects skeletal muscle hypertrophy. On the other hand, adequate blood flow and capillarisation is critical for anabolic stimuli to increase protein synthesis and fibre size (Timmerman *et al.*, 2010; Snijders *et al.*, 2017; Moro *et al.*, 2019) as this allows the delivery of oxygen, nutrients, and growth factors. We recently demonstrated that HFpEF rats have an impaired blood flow response to contractions that implies a perfusive oxygen delivery limitation (Espino-Gonzalez *et al.*, 2020). However, whether this

affects exercise-induced skeletal muscle adaptations remains unclear, with only preliminary patient data suggesting that exercise training may improve vasodilation (measured by non-invasive methods) (Hearon *et al.*, 2022).

The experimental model of mechanical overload is widely used as a method to study skeletal muscle hypertrophy, often induced by synergist ablation (Terena *et al.*, 2017). This model provides a unique opportunity to study myofiber cellular changes and underlying mechanisms that are often difficult to observe in humans as well as under conditions of modest hypertrophy such as exercise training (Lowe & Alway, 2002; Egginton, 2011). The present study, therefore, aimed to determine whether HFpEF affects the ability of skeletal muscle to undergo muscle hypertrophy in response to adequate stimuli. Specifically, the TA was surgically removed to evaluate the compensatory response of the EDL muscle. Skeletal muscle morphology, contractile properties, mitochondrial respiration, and functional hyperaemia were also measured. A better understanding of mechanisms limiting skeletal muscle hypertrophy in HFpEF could help direct future experiments and therapeutic approaches to target muscle wasting and weakness.

5.2 Methods

5.2.1 Ethical approval

All experimental procedures were performed in accordance with the UK Scientific Procedures (Animals) Act 1986 and local approval was given by the University of Leeds Animal Welfare and Ethical Review Committee.

5.2.2 Animals

Obese and lean ZSF1 rats were compared at 20 weeks of age, after 15 days of surgically induced functional overload on the EDL muscle. HFpEF cardio-metabolic phenotype was confirmed by diffusion tensor magnetic resonance imaging (DT-MRI) and invasive hemodynamics (Espino-Gonzalez *et al.*, 2020). *In situ* muscle function, functional hyperaemia, *in situ* mitochondrial respiration and skeletal muscle morphology were assessed (Figure 5.1).

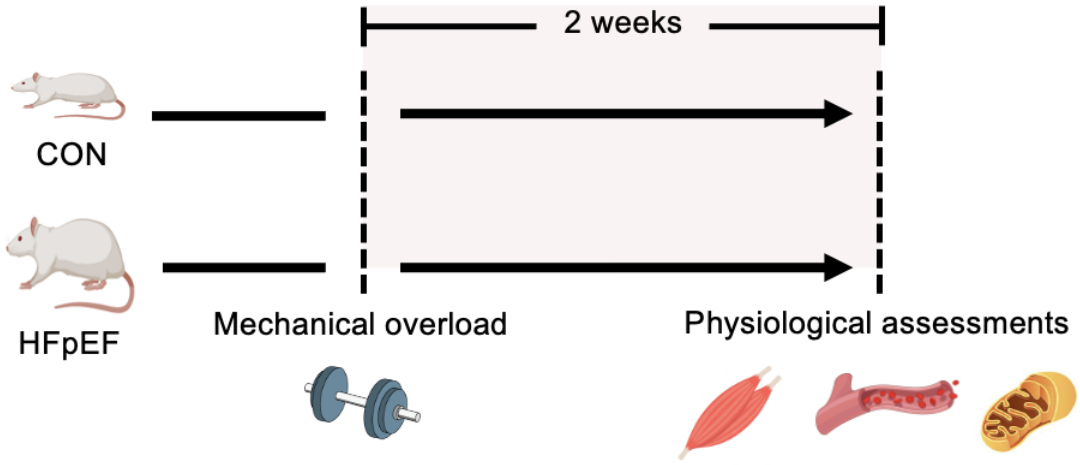

Figure 5.1. Study design. Male obese (n = 8) and lean (n = 8) ZSF1 rats were compared at 20 weeks of age, after 15 days of surgically induced functional overload on the EDL muscle. *In situ* muscle function and femoral artery blood, *in situ* mitochondrial respiration and skeletal muscle morphology were assessed.

5.2.3 Overload protocol

To induce EDL hypertrophy, unilateral synergistic surgical ablation of the TA muscle was performed as previously described (Frischknecht & Vrbova, 1991). The contralateral limb was sham-operated to serve as an intra-animal control. Full details of synergist ablation surgery are provided in Chapter 2 General methods: 2.4.

5.2.4 *In situ* muscle performance and femoral artery blood flow

In situ assessments of EDL muscle performance (isometric twitch and maximal forces and fatigability) and femoral artery blood flow were determined as previously described (Espino-Gonzalez *et al.*, 2020). Full details are provided in Chapter 2 General methods: 2.5.

5.2.5 Tissue analyses

In situ mitochondrial respiration was assessed in permeabilised EDL muscle fibres using high resolution respirometry, as described elsewhere (Bowen *et al.*, 2015). Analyses of fibre type-specific CSA, fibre type composition, C:F, CD, LCFR, LCD and *In silico* muscle PO_2 were performed on EDL cryosections, as previously described (Al-Shammari *et al.*, 2019). Citrate synthase was assessed photometrically in homogenates by commercially available kits. Western blot was used to quantify the expression of mitochondrial proteins. Full details of all measurement procedures are provided in Chapter II General methods.

5.2.6 Statistical analyses

After appropriate checks of normality, differences between and within groups were assessed by Two-way analysis of variance (ANOVA) followed by Bonferroni *post hoc* test. A three-way ANOVA was used to determine whether there is a

three-way relationship among HFpEF, overload and fibre type. Analyses were performed in GraphPad Prism v.8. Data are presented as mean±SD, and the level of significance was accepted as $P < 0.05$ for all analyses.

5.3 Results

5.3.1 Cardio-metabolic phenotype

Cardio-metabolic phenotype of the animal model is shown in Chapter 3 Results I. At 20 weeks of age, obese-ZSF1 rats developed metabolic comorbidities and cardiac changes typically associated with HFpEF. These included obesity, hyperglycaemia, hypertension and increased right ventricular wall thickness (Espino-Gonzalez *et al.*, 2020).

5.3.2 Skeletal muscle morphology

Representative muscle sections of the EDL muscle are presented in Figure 5.2a. Compared to controls, contralateral and overloaded muscles of HFpEF rats had reduced FCSA (Figure 5.2b). After 15 days of overload, total FCSA showed an increase of 29% in the control group, whereas this was unchanged in HFpEF rats (Figure 5.2b). The overload-induced fibre hypertrophy observed in the control group occurred primarily in Type IIb/IIx fibres (Figure 5.2e), with no significant changes in Type I (Figure 5.2c) and Type IIa (Figure 5.2d). There was a significant interaction between HFpEF, overload and fibre type ($P = 0.04$). Contralateral muscles of HFpEF rats showed a lower percentage of Type I fibres (Figure 5.2f). Contralateral and overloaded muscles of HFpEF rats also had lower C:F, although both groups showed a similar increase in this after overload (Figure 5.2g). In contrast, only HFpEF rats showed a significant increase in CD after overload (Figure 5.2h). Fibre type-specific analysis of capillary distribution

revealed that, after overload, LCFR of Type IIb/IIx fibres was increased in both groups (Figure 5.2k), whereas this remained unchanged in Type I (Figure 5.2i) and Type IIa fibres (Figure 5.2j). HFpEF rats showed an increased overload-induced response in LCD of Type IIb/IIx fibres (Figure 5.2n), with no significant changes in LCD of Type I (Figure 5.2l) and Type IIa fibres (Figure 5.2m). Simulations of muscle PO_2 at maximal rate of oxygen consumption revealed that, compared to lean controls, the overloaded muscles of HFpEF rats had higher muscle oxygen tension (Figure 5.2o, p).

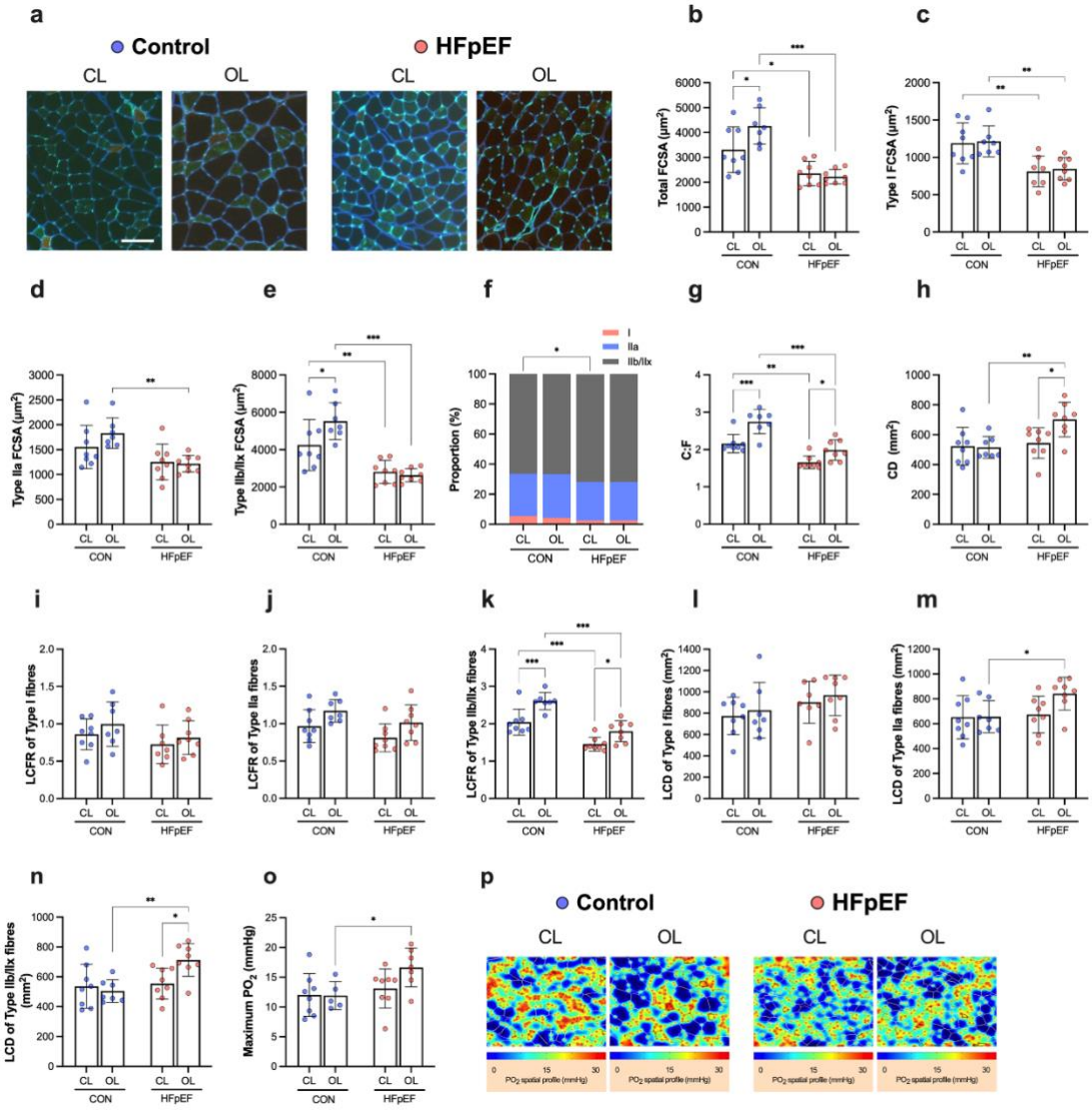

Figure 5.2. Histological features of the EDL muscle. Representative EDL sections **(a)**. Compared to CON, contralateral (CL) and overloaded (OL) muscles

of HFpEF rats had reduced FCSA ($P < 0.05$) **(b)**. After overload, total FCSA increased in CON rats ($P = 0.02$), whereas this was unchanged in HFpEF ($P > 0.99$) **(b)**; this response occurred primarily in Type IIb/IIx fibres ($P = 0.02$) **(e)**, with no significant changes in Type I **(c)** and Type IIa (all $P > 0.05$) **(d)**. Contralateral muscles of HFpEF rats had a lower percentage of Type I fibres ($P = 0.03$) **(f)**. Contralateral and overloaded muscles of HFpEF rats also had lower C:F (all $P < 0.05$), although both groups showed a similar increase in this after overload (all $P < 0.05$) **(g)**. In contrast, only HFpEF rats showed a significant increase in CD after overload ($P = 0.01$) **(h)**. Overload increased LCFR of Type IIb/IIx fibres in both groups (all $P < 0.05$) **(k)**, whereas this remained unchanged in Type I **(i)** and Type IIa fibres (all $P > 0.05$) **(j)**. After overload, HFpEF rats showed an increased in LCD of Type IIb/IIx fibres ($P = 0.02$) **(n)**, with no significant changes in LCD of Type I **(l)** and Type IIa fibres (all $P > 0.05$) **(m)**. Compared to CON, overloaded muscles of HFpEF rats had higher PO_2 at maximal rate of oxygen consumption ($P = 0.04$) **(o, p)**. Scale bar represents 100 μm.

5.3.3 *In situ* muscle function and femoral artery blood flow

Compared to lean controls, HFpEF rats had lower skeletal muscle mass (Figure 5.3a); yet, both groups showed a significant increase in this after 2 weeks of overload (Figure 5.3a). Absolute twitch and maximal forces were increased in the control group after overload, while these remained similar in the HFpEF group (Figure 5.3b and Figure 5.3c, respectively). However, when normalised to muscle mass, specific twitch and maximal forces were not different between or within groups (Figure 5.3d and Figure 5.3e, respectively). Muscle fatigue was significantly improved in both groups after overload (Figure 5.3f). No significant differences between or within groups were observed in resting blood flow (Figure 5.3g). In contrast, overloaded muscles of lean rats showed a lower functional hyperaemic response compared to their respective contralateral muscles (Figure 5.3h). Functional hyperaemia was also impaired in the contralateral muscles of HFpEF rats when compared to those in controls (Figure 5.3h).

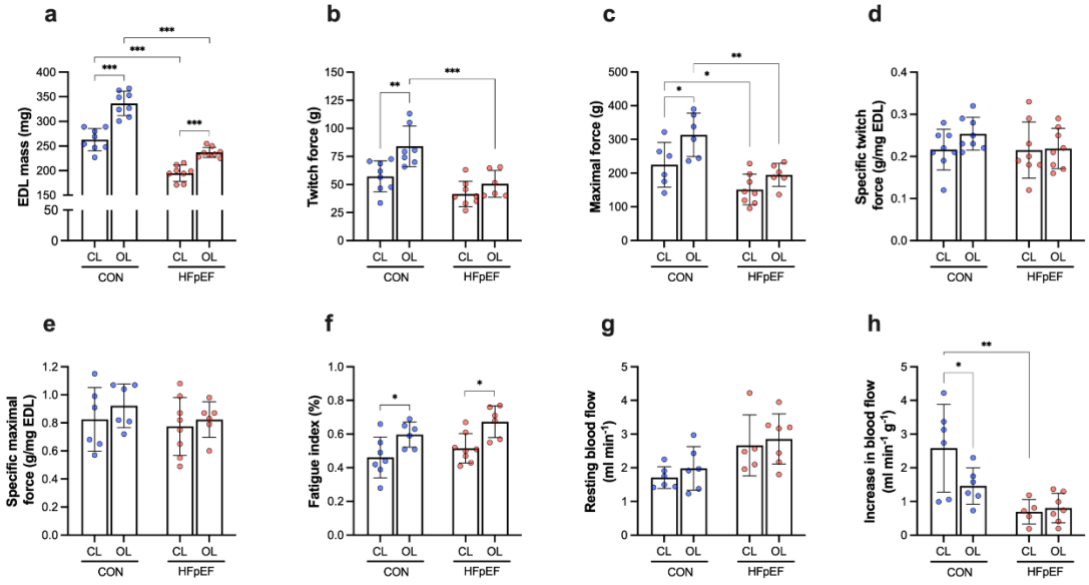

Figure 5.3. *In situ* EDL contractile function and femoral artery blood flow. Compared to CON, HFpEF rats had lower muscle mass ($P < 0.05$), although both groups had a significant increase in this after overload (all $P < 0.05$) **(a)**. Absolute twitch **(b)** and maximal forces **(c)** were increased in the control group after overload (all $P < 0.05$), while these remained similar in HFpEF (all $P > 0.05$). In contrast, specific twitch **(d)** and maximal forces **(e)** were not different between or within groups (all $P > 0.05$). Overload improved muscle fatigue in both groups (all $P < 0.05$) **(f)**. No significant differences between or within groups were observed in resting blood flow (all $P > 0.05$) **(g)**. In contrast, overloaded muscles of lean rats showed a lower functional hyperaemic response compared to their contralateral muscles ($P = 0.04$). Compared to CON, contralateral muscles of HFpEF rats had an impaired increase in blood flow during stimulation ($P = 0.001$) **(h)**.

5.3.4 Mitochondrial function

High-resolution respirometry experiments revealed that, after overload, all mitochondrial respiratory states tended to be lower in HFpEF, although only oxidative phosphorylation with complex I substrates (P_I) reached significance (Figure 5.4a). After normalisation to complex IV activity (C_{IV}) (a marker of mitochondrial content), no significant differences were found for any of the respiratory states (Figure 5.4b). In contrast, however, after overload, the respiratory control ratio (RCR) was significantly increased by 51% in the control group, with no significant changes (7%) in HFpEF (Figure 5.4c), indicating an impaired response in mitochondrial coupling efficiency. No significant differences

were found in citrate synthase activity (Figure 5.4d). Similarly, markers of mitochondrial function and morphology, such as OPA1, PGC-1α, Drp1, ACC and ACL, were comparable between CON and HFpEF (Figure 5.4e-p).

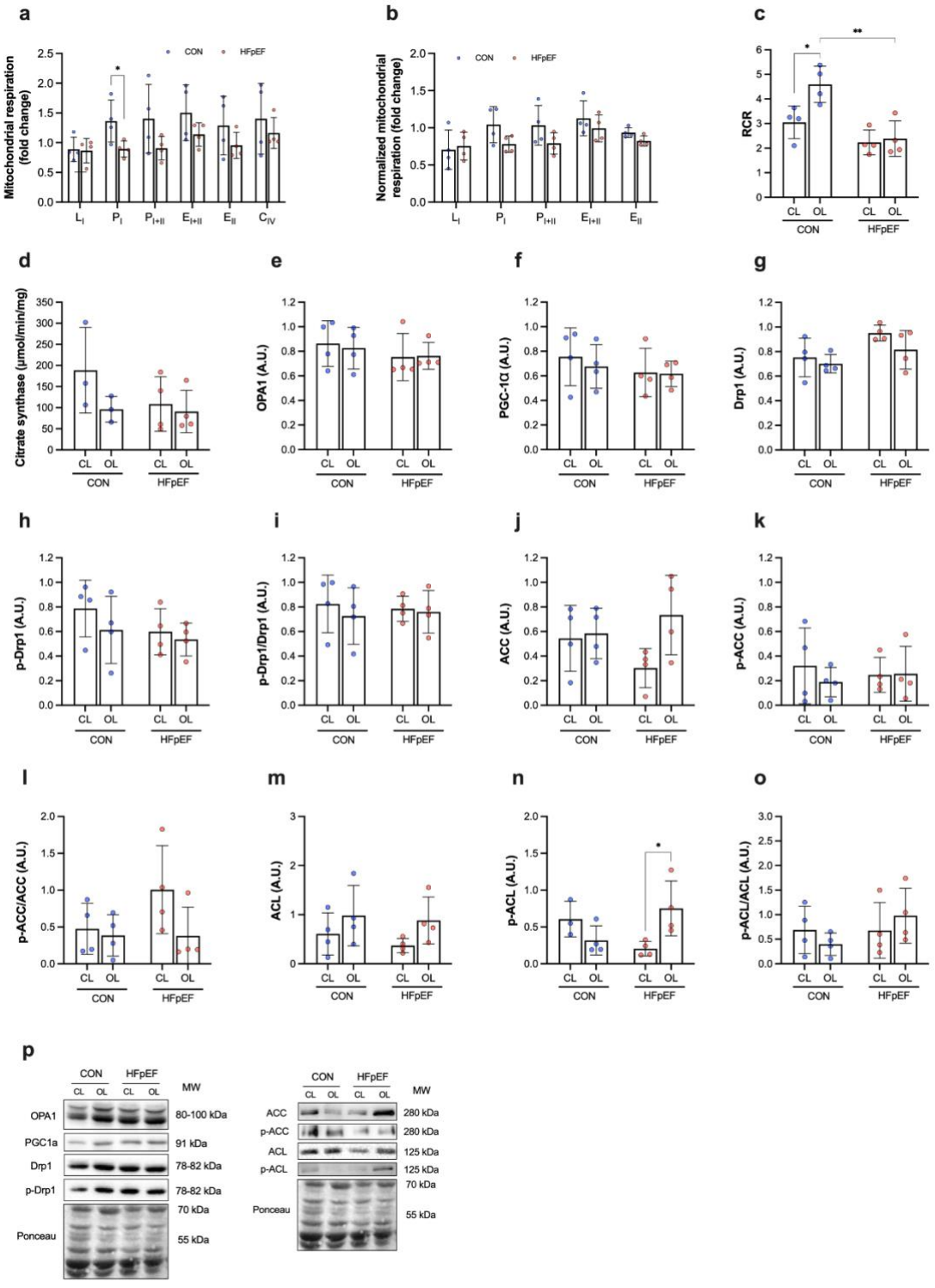

Figure 5.4. *In situ* mitochondrial respiration of permeabilized EDL muscle fibres. After overload, all mitochondrial respiratory states tended to be lower in

HFpEF, but only P_I reached significance (P = 0.04) **(a)**. After normalisation to complex IV activity (C_{IV}), no significant differences were found (P > 0.05) **(b)**. In contrast, after overload, the respiratory control ratio (RCR) was increased in CON rats (P = 0.01), with no significant changes in HFpEF (P > 0.99) **(c)**. No significant differences were found in citrate synthase activity (All P > 0.05) **(d)**. Similarly, protein contents of OPA1, PGC-1α, Drp1, ACC and ACL, were comparable between groups (P > 0.05) **(e-p)**.

5.4 Discussion

The main finding from the present study was that functional overload for two weeks increased myofiber size, specifically Type IIb/IIx FCSA, in lean but not obese-HFpEF rats indicative of anabolic resistance. Mechanistically, overload significantly increased mitochondrial coupling efficiency in lean but not obese-HFpEF rats, while vascular function was well preserved in both groups. This indicates for the first time HFpEF is associated with a deficit in myofiber hypertrophy that may be linked to mitochondrial abnormalities.

5.4.1 Mechanisms of muscle hypertrophy

Muscle adaptation to mechanical overload is typically characterized by increases in muscle wet-mass and FCSA (Ianuzzo & Chen, 1979; Timson *et al.*, 1985), which is determined by elevated rates of protein synthesis *via* improved translational efficiency and/or addition of new myonuclei *via* SC (Blaauw & Reggiani, 2014). While measurements of protein synthesis and myonuclei accretion were outside the scope of this study, we did observe that, compared to lean controls, obese-HFpEF rats had a similar increase in muscle wet-mass, whereas FCSA remained unchanged after two weeks of overload. A similar overload-induced hypertrophic response has been observed in old mice (Dungan *et al.*, 2022) and mice lacking inflammatory cytokine interleukin-6 (IL-6), and may be explained, at least in part, by a greater accumulation of collagen content and

fibrosis (White *et al.*, 2009). Alternatively, muscle hypertrophy can also be attributed to the longitudinal “branching”, “fragmenting”, or “splitting” of existing muscle fibres, which may result in the presence of new muscle fibres (hyperplasia) (Murach *et al.*, 2019). This phenomenon has been observed during “extreme” loading in disease models, and typically occurs concomitant with signs of regeneration, thus being considered as pathological hypertrophy (Isaacs *et al.*, 1973; Schmalbruch, 1984; Faber *et al.*, 2014). However, whether hypertrophy in HFpEF is mediated *via* muscle fibre splitting, and/or associated with increased fibrosis, remain to be determined.

5.4.2 Role of vascular function to limit muscle hypertrophy in HFpEF

The vascular system is responsible for the delivery of oxygen, nutrients and growth factors, and removal of waste products to/from muscles, which is orchestrated by several mechanisms, including mechanical stimulation, local and regional metabolic responses, circulating substances and neural signals (Egginton, 2011). Adequate blood flow and capillarisation is therefore critical for anabolic stimuli, such as insulin and exercise, to increase protein synthesis and fibre size (Timmerman *et al.*, 2010; Snijders *et al.*, 2017; Moro *et al.*, 2019). We previously demonstrated that obese-HFpEF rats have an impaired blood flow response to contractions that implies a perfusive oxygen delivery limitation (Espino-Gonzalez *et al.*, 2020). In this study, however, resting femoral artery blood flow and functional hyperaemia in HFpEF rats were not impaired after overload. In addition, both lean and HFpEF rats showed a similar overload-induced increase in C:F with no impairments in muscle PO_2 at maximal exercise, which indicates adequate oxygenation. These responses are consistent with previous experiments in rats, where two weeks of overload did not impair resting

and maximal EDL muscle blood flow, but increased C:F; in addition, similar to our results in lean rats, functional hyperaemia was reduced in overloaded muscles compared to contralateral muscles (Egginton *et al.*, 1998). However, whether these findings will translate to humans remains unclear.

To date, only few studies have investigated the effect of exercise training on skeletal muscle function in HFpEF patients (Haykowsky *et al.*, 2012; Fu *et al.*, 2016; Hearon *et al.*, 2022). A recent study showed that 8 weeks of isolated knee extension exercise training improved exercise capacity, skeletal muscle vasodilation and blood flow in HFpEF patients (Hearon *et al.*, 2022). Collectively, therefore, it is unlikely that exercise- or loading-induced skeletal muscle responses in HFpEF are limited by changes in vascular function. However, this remains to be confirmed by direct measurements of skeletal muscle function, morphology (e.g., FCSA, fibre type distribution and capillarity) and blood flow in patients with HFpEF.

5.4.3 Role of mitochondrial dysfunction to limit muscle hypertrophy in HFpEF

Several muscle wasting disorder, including HF, are associated with mitochondrial dysfunction and impaired ability to produce ATP (Max, 1972; Romanello *et al.*, 2010; Calvani *et al.*, 2013; Rosca & Hoppel, 2013; Hyatt & Powers, 2021). Here, we observed that the impaired overload-induced hypertrophic response in HFpEF rats was associated with reduced mitochondrial coupling efficiency. Specifically, after overload, the respiratory control ratio (RCR) was increased in lean controls (51%), with no significant changes in HFpEF rats (7%). Decreased mitochondrial ATP production can limit protein synthesis and accelerate protein degradation

(Carafoli *et al.*, 1964; Hyatt & Powers, 2021). ATP is required for protein synthesis and, therefore, low levels could depress the synthesis of new proteins, thereby contributing to muscle atrophy. Low levels of ATP in skeletal muscle have been associated with increased AMPK activity and subsequent inhibition of mTOR, a major regulator of multiple components involved in protein synthesis, including initiation and elongation factors, and ribosome biogenesis (Thomson, 2018). Increased AMPK activity can also activate FoxO3, which triggers the expression of proteins involved in the ubiquitin proteasome system (e.g., MAFbx and MuRF1) and autophagy (e.g., LC3) (Greer *et al.*, 2007). While we did not measure the expression of atrogenes, obese-ZSF1 rats and HFpEF patients have shown an increased expression of MuRF1, MuRF2 and MAFbx in skeletal muscle (Bowen *et al.*, 2017b; Goto *et al.*, 2020). However, the activity of these pathways during mechanical overload (exercise) in HFpEF remains to be determined.

Muscle atrophy has also been associated with impaired mitochondrial fusion and fission, as evidenced by lower expression of the fusion protein OPA1 and the fission protein DRP1. In the present study, however, OPA1 and Drp1 were not significantly affected by HFpEF or overload. Similarly, no significant differences between or within groups were observed in PGC-1α, a key mitochondrial regulator that protects skeletal muscle atrophy by suppressing transcriptional activity of FOXO, atrophy-specific gene expression and protein degradation (Sandri *et al.*, 2006). Moreover, ACC and ACL, two mitochondrial players that regulate fatty acid oxidation (Vavvas *et al.*, 1997), and satellite cell differentiation and muscle regeneration (Das *et al.*, 2017), respectively, were not significantly affected by HFpEF or overload. Collectively, therefore, our data suggest that impaired overload-induced hypertrophy in HFpEF may be explained, at least in

part, by limitations in mitochondrial ATP production *via* a signalling pathway not yet characterised in this disease.

5.4.4 Limitations

Lean and obese-HFpEF rats were compared at a relatively early time point (20 weeks), which may limit translation of our findings to more advanced stages of HFpEF. However, this rat model has been shown to develop metabolic impairments associated with typical signs of HFpEF as well as muscle dysfunction developing as early as 10-15 weeks of age (Schauer *et al.*, 2020). Further, our experiments were performed in male rats only, thus, it remains unclear whether similar findings would be observed in females. Furthermore, physical activity levels between groups were not measured and cannot be ruled out as having an impact on our experimental measures. However, it is well established that low physical activity fails to account for the skeletal muscle deficits induced by HF (Simonini *et al.*, 1996; Miller *et al.*, 2009).

5.5 Conclusions

Mechanical overload significantly increased muscle force and myofiber size in controls but not in obese-HFpEF rats, which was linked to impaired mitochondrial and not vascular function.

Chapter 6 Results IV. Impaired overload-induced skeletal muscle hypertrophy in obese-HFpEF rats is rescued by caloric restriction

6.1 Introduction

Heart failure (HF) with preserved ejection fraction (HFpEF) has become the dominant form of HF in many parts of the world (Dunlay *et al.*, 2017). An optimal evidence-based strategy to manage this syndrome is unclear and is often complicated by comorbidities and non-cardiac 'peripheral' impairments, such as skeletal muscle and vascular dysfunction (Sharma & Kass, 2014; Silverman & Shah, 2019; Mishra & Kass, 2021b). SGLT2I (Anker *et al.*, 2021), exercise training (Pandey *et al.*, 2015) and recently dietary modifications (i.e., caloric restriction) (Kitzman *et al.*, 2016) have been some of the few treatments to improve outcomes in HFpEF patients. Caloric restriction (CR) in particular has widespread benefits, improving lifespan and homeostasis in multiple cells and tissues (Brandhorst *et al.*, 2015) including skeletal muscle (Hwee & Bodine, 2009; Cerletti *et al.*, 2012). CR improved cardiac function, exercise capacity and glucose metabolism, and induced weight loss, while increasing quality of life and survival in obese HF patients (with both reduced and preserved LVEF) (Rider *et al.*, 2013; Bonilla-Palomas *et al.*, 2016; Kitzman *et al.*, 2016; Bianchi, 2020).

To date, only one study has examined the effects of CR on skeletal muscle in HFpEF patients (Kitzman *et al.*, 2016) and none in experimental models. Specifically, twenty weeks of CR improved skeletal muscle function and exercise capacity (i.e., peak VO_2) while reducing body weight and fat mass (Kitzman *et al.*, 2016). In addition, CR in combination with aerobic exercise training showed additive benefits, which was positively correlated with the change in thigh muscle

to intermuscular fat ratio (Kitzman *et al.*, 2016). We demonstrated that HFpEF affects the ability of skeletal muscle to undergo hypertrophy in response to mechanical overload in an obese-HFpEF rats (Chapter 5 Results III). Interestingly, evidence from aged rats showed long-term CR is capable of reversing blunted myofiber hypertrophy during mechanical overload (Hwee & Bodine, 2009).

Myofiber growth is generally determined by two nonexclusive mechanisms: 1) elevated rates of protein synthesis *via* improved translational efficiency and capacity *via* Akt-mTORC1 signalling; and/or 2) addition of new myonuclei that is dependent upon muscle SC (Blaauw & Reggiani, 2014). Studies suggest that activation of SC to support myonuclear accretion is required during overload-induced muscle hypertrophy (Rosenblatt & Parry, 1992; Rosenblatt *et al.*, 1994; Adams *et al.*, 2002; Egner *et al.*, 2016). However, contradictory evidence exists, where hypertrophy in some cases can occur without SC activation and subsequent myonuclei accretion due to increased protein synthesis signalling alone (Rosenblatt & Parry, 1993; Lowe & Alway, 1999; McCarthy & Esser, 2007). In HFpEF, a knowledge gap exists in understanding the anabolic signalling pathways that regulate muscle hypertrophy. Previous experiments have shown that insulin resistance or other related comorbidities may impair the ability of skeletal muscle to activate mTOR signalling and undergo load-induced muscle hypertrophy (Katta *et al.*, 2010; Paturi *et al.*, 2010). Collectively, whether load-induced myofiber hypertrophy in HFpEF is impaired due to decreased myonuclear accretion and/or protein synthesis signalling is unknown, but CR rejuvenate myofiber growth especially given evidence it can normalise SC

function, anabolic signalling, and myofiber hypertrophy in aged rodents (Hwee & Bodine, 2009).

The present study, therefore, aimed to examine the effects of CR on skeletal muscle at baseline and during stimulated hypertrophy in HFpEF, by applying functional, histological and molecular approaches to obese-HFpEF rats and lean controls. Specifically, we performed global and local fibre-type specific phenotyping of FCSA, isoform, and capillarity. In parallel, we further assessed myonuclear accretion and protein synthesis *via* relevant anabolic signalling proteins. A better understanding of the mechanisms by which CR ameliorates skeletal muscle deficits induced HFpEF could help direct future patients experiments and therapeutic approaches.

6.2 Methods

6.2.1 Ethical approval

All experimental procedures were performed in accordance with the UK Scientific Procedures (Animals) Act 1986 and local approval was given by the University of Leeds Animal Welfare and Ethical Review Committee.

6.2.2 Animals

Lean, HFpEF and HFpEF+CR rats were compared after 14 days of surgically induced functional overload on the EDL muscle. CR over 4 weeks was initiated at week 1 with 10% restriction, increased to 25% at week 2, and maintained at 40% restriction after functional overload in the last two weeks. Body weight was monitored every ~5 days to not exceed a loss of >10%. Controls were fed ad

libitum. *In vitro* muscle function, skeletal muscle morphology and anabolic and catabolic signalling pathways were evaluated (Figure 6.1).

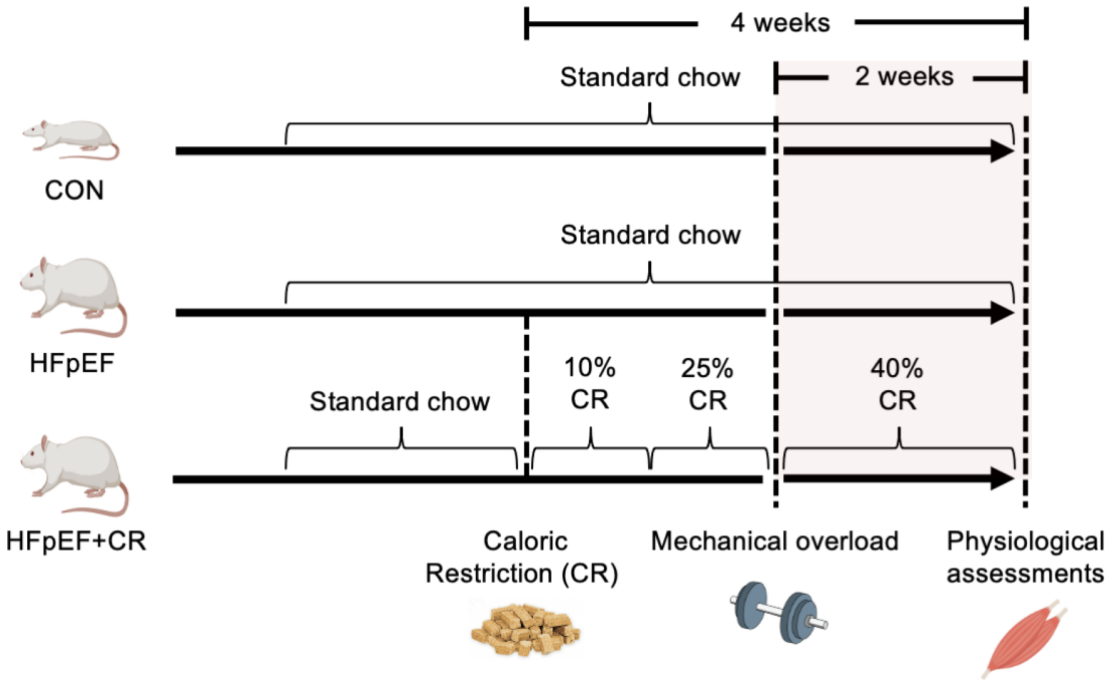

Figure 6.1. Study design. Lean (n = 4), HFpEF (n = 4) and HFpEF+CR (n = 4) rats were compared after 14 days of functional overload on the EDL muscle. CR was initiated at 10% restriction, increased to 25% in the second week, and maintained at 40% restriction after overload in the last two weeks.

6.2.3 Overload protocol

To induce EDL hypertrophy, unilateral synergistic surgical ablation of the TA muscle was performed as previously described (Frischknecht & Vrbova, 1991). The contralateral limb was sham-operated and served as a relative control. Full details of synergist ablation surgery are provided in Chapter 2 General methods: 2.4.

6.2.4 *In vitro* functional assessment

The soleus muscle was mounted vertically in a buffer-filled organ bath between a hook and force transducer for measurement of *in vitro* isometric and isotonic

contractile properties (absolute and specific forces, time to peak tension, half relaxation time, and power), as previously described (Espino-Gonzalez *et al.*, 2020). Full details are provided in Chapter 2 General methods: 2.6.

6.2.5 Tissue analyses

Analyses of FCSA, fibre type composition, C:F, CD, LCFR and LCD were performed on EDL and soleus cryosections, as previously described (Al-Shammari *et al.*, 2019). EDL cryosections were also stained with DAPI to quantify the number of nuclei per fibre (i.e., nuclei residing within laminin stained myofibers). Western blot was used to quantify the expression of proteins involved in anabolic and catabolic signalling pathways. Full details of all measurement procedures are provided in Chapter II General methods.

6.2.6 Statistical analyses

After appropriate checks of normality, differences between and within groups were assessed by Two-way analysis of variance (ANOVA) followed by Bonferroni *post hoc* test. Analyses were performed in GraphPad Prism v.8. Data are presented as mean±SD, and the level of significance was accepted as $P < 0.05$ for all analyses.

6.3 Results

6.3.1 Body weight and blood glucose levels

Compared to lean controls, obese-HFpEF rats with or without CR had increased body weight (Figure 6.2a), which was monitored every ~5 days. HFpEF rats developed hyperglycaemia, and this was reduced by CR (Figure 6.2b).

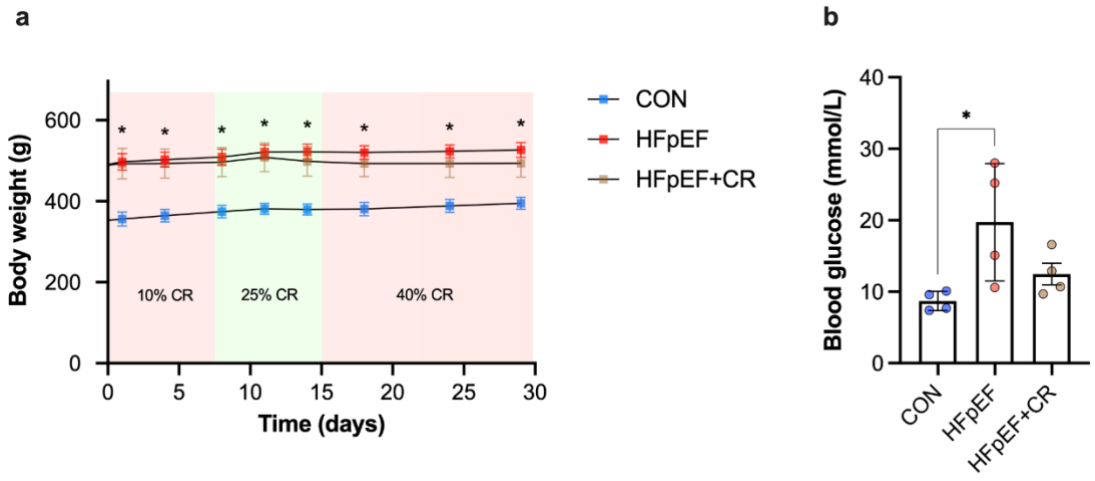

Figure 6.2. Metabolic phenotype. Compared to lean controls, obese-HFpEF rats with or without CR had increased body weight (all P > 0.05), which was monitored every ~5 days **(a)**. HFpEF rats had higher blood glucose levels (P = 0.04), which were reduced by CR (P = 0.97) **(b)**.

6.3.2 EDL morphology

After functional overload, EDL muscle mass was significantly increased in lean controls, but not in obese-HFpEF rats with or without CR (Figure 6.3a). Overload increased fibre number in HFpEF rats only, while this was increased in contralateral muscles of HFpEF+CR rats comparing to those of obese rats with ad libitum diet (Figure 6.3c). Lean rats showed an increase of 27% in FCSA, while this was increased by 9% and 35% in HFpEF and HFpEF+CR rats, respectively (Figure 6.3b, d). Fibre type-specific analysis revealed that Type I FCSA was significantly increased in HFpEF+CR rats only (Figure 6.3e); Type IIa FCSA was increased in CON and HFpEF+CR but not in HFpEF rats (Figure 6.3f), and Type IIb/IIx FCSA was significantly increased in lean controls, remained unchanged in HFpEF rats and tended to increase in HFpEF+CR rats (Figure 6.3g). Compared to overloaded EDLs in HFpEF rats, those of HFpEF+CR rats increased percentage of Type IIa fibres with a lower percentage of Type IIb/IIx (Figure 6.3h).

For capillarity, C:F increased in overloaded muscles of lean controls but not in HFpEF rats with or without CR (Figure 6.3i). Compared to contralateral muscles of lean and HFpEF rats, HFpEF+CR rats had increased CD (Figure 6.3j). Overload induced no significant changes in LCFR of Type I fibres in all groups, although this tended to be increased in HFpEF+CR rats (Figure 6.3k). No significant differences between or within groups were observed in LCFR of Type IIa fibres (Figure 6.3l), whereas LCFR of Type IIb/IIx fibres was increased in lean controls (Figure 6.3m). Overload did not induce changes in LCD of Type I, Type IIa and Type IIb/IIx fibres in all groups (Figure 6.3n-p). However, LCD of Type IIa and Type IIb/IIx fibres were increased in contralateral muscles of HFpEF+CR rats (Figure 6.3o, p). Importantly after overload, the number of nuclei per fibre (i.e., myonuclear accretion) was increased in lean and HFpEF+CR rats, but this was unchanged in HFpEF (Figure 6.3q, r).

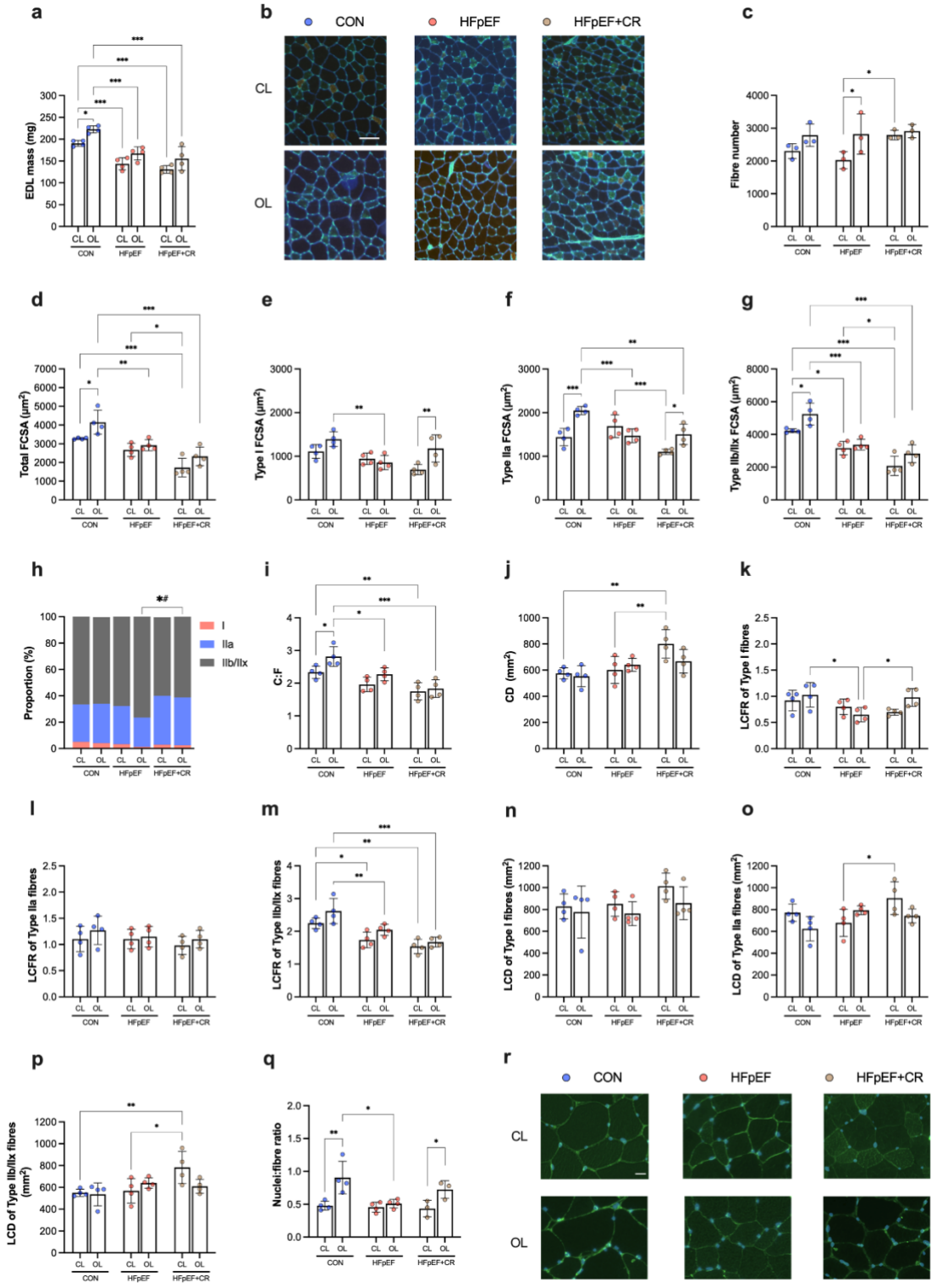

Figure 6.3. Histological features of the EDL muscle. After overload, EDL muscle mass was significantly increased in lean controls (p = 0.02), but not in HFpEF rats with or without CR (all P > 0.05) **(a)**. Overload increased fibre number in HFpEF rats (P > 0.04), while this was increased in contralateral muscles of HFpEF+CR rats comparing to those of obese rats with ad libitum diet (P = 0.05) **(c)**. Lean rats showed an increase of 27% in FCSA (P = 0.03), while this was increased by 9% (P > 0.05) and 35% (P = 0.19) in HFpEF and HFpEF+CR rats, respectively **(b, d)**. Overload increased Type I FCSA in HFpEF+CR rats only (P < 0.05) **(e)**. Type IIa FCSA was increased in CON (P < 0.05) and HFpEF+CR (P

= 0.02) but not in HFpEF rats (P = 0.32) **(f)**, while Type IIb/IIx FCSA was significantly increased in lean controls (P = 0.02), remained unchanged in HFpEF rats (P > 0.05) and tended to bed increased in HFpEF+CR rats (P = 0.12) **(g)**. Compared to overloaded muscles of HFpEF rats, those of HFpEF+CR rats showed an increased percentage of Type IIa fibres with a lower percentage of Type IIb/IIx (all P < 0.05) **(h)**. C:F was increased in overloaded muscles of lean controls, compared to those in HFpEF rats with or without CR (all P < 0.05) **(i)**. Only lean controls showed an overload-induced increase in C:F (P = 0.04) **(h)**. Compared to contralateral muscles of lean and HFpEF rats, those of HFpEF+CR rats had increased CD (P < 0.05) **(j)**. No significant differences between or within groups were observed in LCFR of Type I and Type IIa fibres (all P > 0.05) **(k, i)**, whereas LCFR of Type IIb/IIx fibres was increased in contralateral and overloaded muscles of lean controls (all P < 0.05) **(m)**. Overload did not induce changes in LCD of Type I, Type IIa and Type IIb/IIx fibres in all groups (P > 0.05) **(n-p)**; yet, LCD of Type IIa and Type IIb/IIx fibres were increased in contralateral muscles of HFpEF+CR rats (all P < 0.05) **(o, p)**. After overload, the number of nuclei per fibre was increased in CON and HFpEF+CR rats (P < 0.05) but not in HFpEF rats (P > 0.05) **(q, r)**. Scale bar represents 100 µm **(b)** and 30 µm **(r)**.

6.3.3 Overload-induced changes in protein synthesis and degradation

SUnSET analysis revealed that protein synthesis, based on the incorporation of puromycin, was not different between or within groups (Figure 6.4a). In all groups, downstream targets of mTOR that affect protein synthesis, such as 4E-BP1, S6 (except p-S6) and AMPK, were not significantly affected by overload (Figure 6.4b-k). Overloaded muscles of lean and HFpEF+CR rats showed a higher content of total 4E-BP1 compared to those of HFpEF rats (Figure 6.4b). Overload increased p-S6 in HFpEF+CR rats only (Figure 6.4f). Proteins related to catabolic pathways, including MuRF1 and p62, were not different between or within groups (Figure 6.4l-n). Overall, these data suggest that the mTOR signalling pathway as well catabolic signalling axis (i.e., the ubiquitin-proteosome and autophagy) were not affected by two weeks of overload.

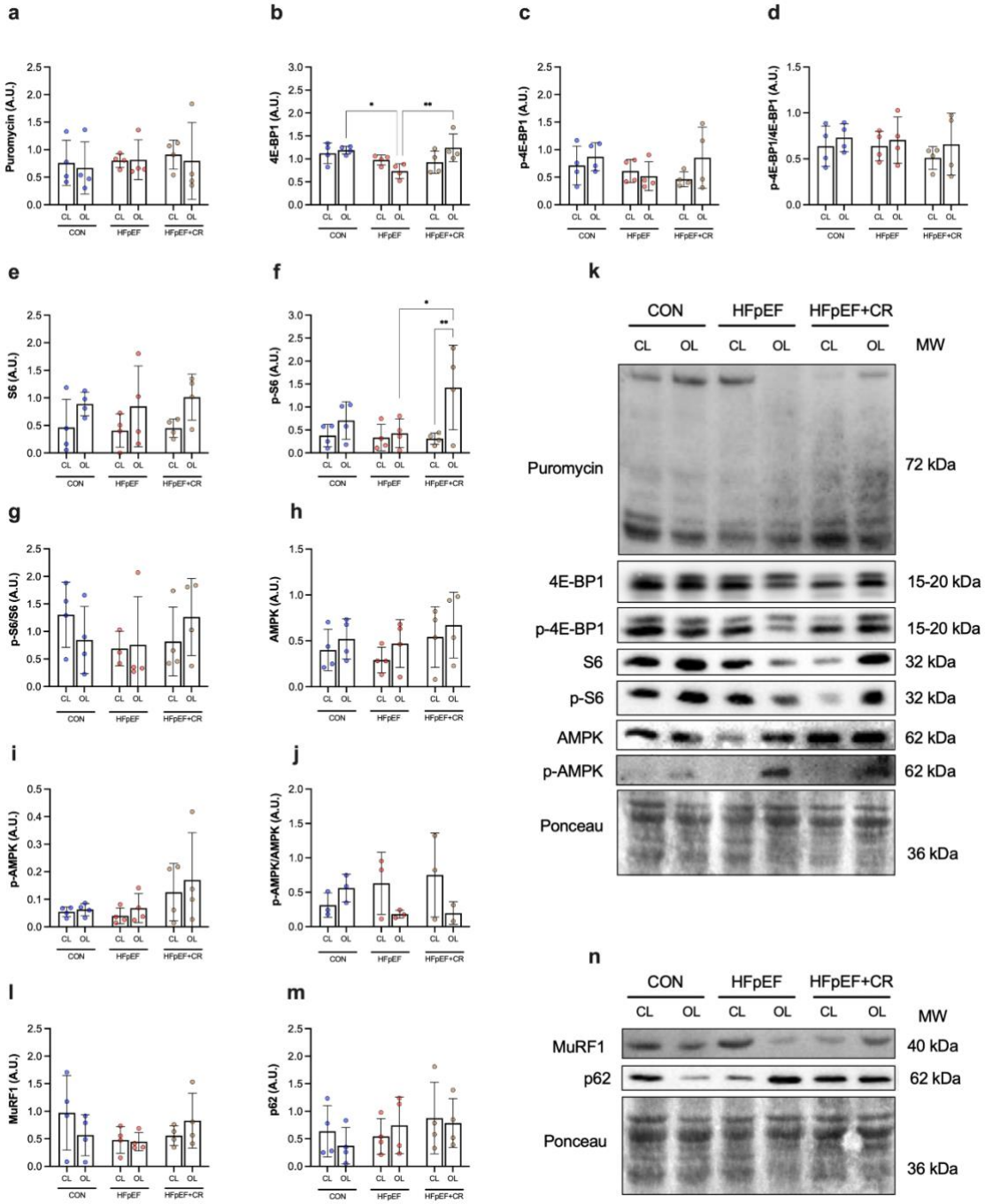

Figure 6.4. Overload-induced response in protein synthesis and degradation. Protein synthesis, based on the incorporation of puromycin, was not different between or within groups (P > 0.05) **(a)**. 4E-BP1, S6 (except p-S6) and AMPK protein contents were not significantly affected by overload (P > 0.05**) (b-k)**. Overloaded muscles of lean and HFpEF+CR rats showed a higher content of total 4E-BP1 compared to those of HFpEF rats (P < 0.05) **(b)**. Overload increased p-S6 in HFpEF+CR rats only (P < 0.05) **(f)**. MuRF1 and p62 protein contents were not different between or within groups (P > 0.05) **(l-n)**.

6.3.4 Soleus morphology and function

Compared to lean controls, soleus muscle mass tended to be reduced in obese-HFpEF rats with or without CR (Figure 6.5a). Similarly, FCSA tended to be reduced in HFpEF rats, which was increased by CR although it did not reach statistical significance (P = 0.51) (Figure 6.5b, c). Skeletal muscle fibre type distribution was not different between groups (Figure 6.5d). Compared to HFpEF rats, HFpEF+CR rats showed an increase in C:F (Figure 6.5e), whereas no significant differences were observed in CD (Figure 6.5f). Fibre type-specific analysis of capillary distribution revealed that the increase in capillarity observed in HFpEF+CR rats occurred primarily in Type IIa fibres (Figure 6.5g), while no significant differences were found in LCD of Type I or Type IIa fibres (Figure 6.5h).

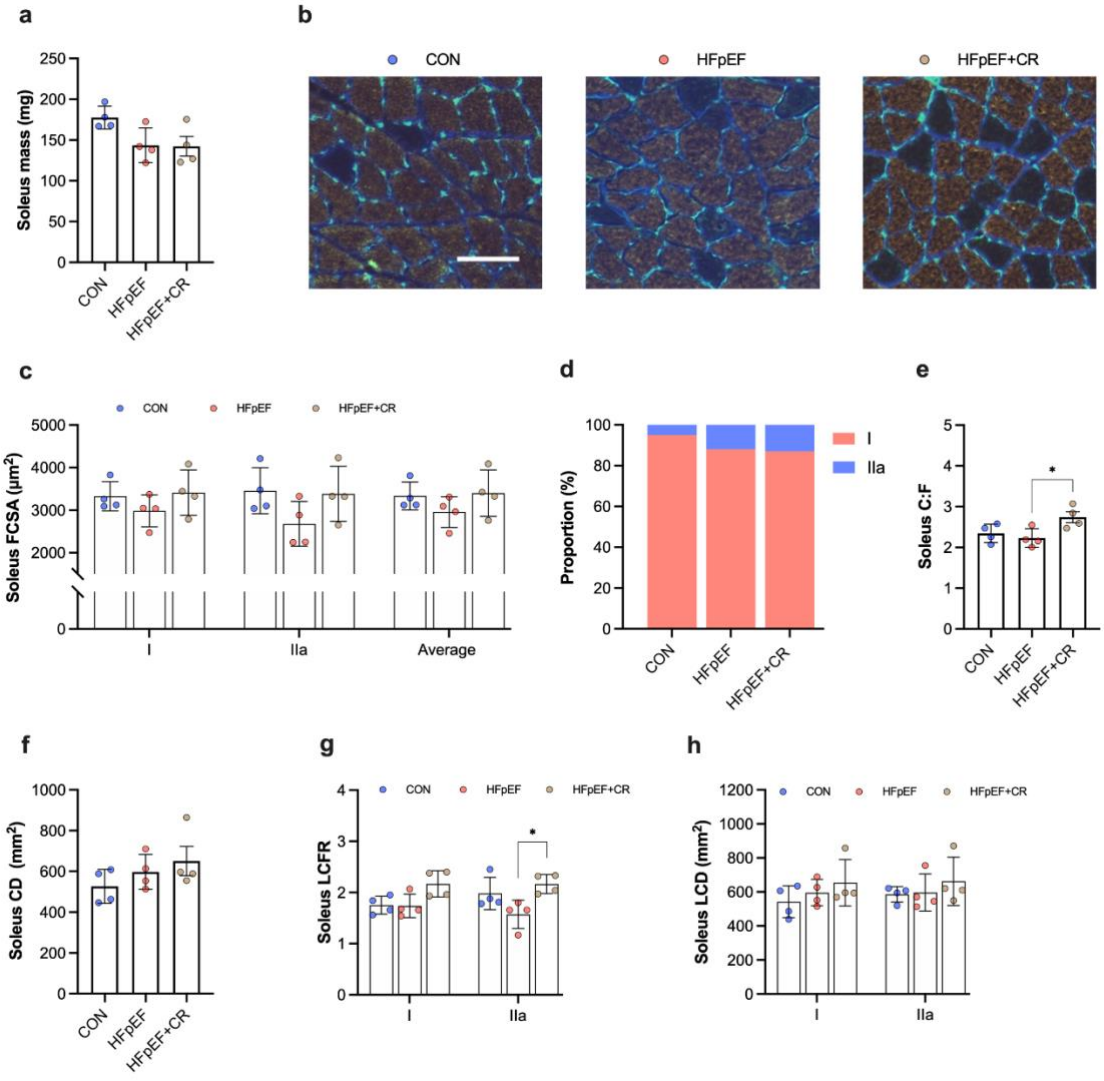

Figure 6.5. Histological features of the soleus muscle. Soleus muscle mass, FCSA and fibre type distribution were not significantly different between groups (all P > 0.05) **(a-d)**. Compared to HFpEF rats, HFpEF+CR rats had increased C:F (P = 0.04) **(e)**, whereas CD was not different between groups (all P > 0.05) **(f)**. Compared to HFpEF rats, HFpEF+CR rats had increased LCFR of Type IIa fibres (P = 0.03) **(g)**. No significant differences were found in LCD of Type I or Type IIa fibres (all P > 0.05) **(h)**. Scale bar represents 100 μm.

Soleus absolute twitch and maximal forces were lower in HEpEF rats with or without CR (Figure 6.6a, b). However, mass-specific twitch and maximal forces were comparable between groups (Figure 6.6c, d). No significant differences were observed in time to peak tension, half relaxation time, shortening velocity and fatigue plotted as percentage initial force (Figure 6.6e-h). Compared to lean and HFpEF+CR rats, muscle power was ~15% lower in HFpEF rats, although it

did not reach significance (P = 0.34) (Figure 6.6i). As protein synthesis is highly time-sensitive, acute changes in protein synthesis were also assessed after *in vitro* muscle contractions. We measured 4E-BP1, S6 and AMPK (downstream targets of mTOR) protein contents in stimulated (ST) and non-stimulated (NST) muscles and found that these were not significantly affected by HFpEF or CR (Figure 6.6j-s).

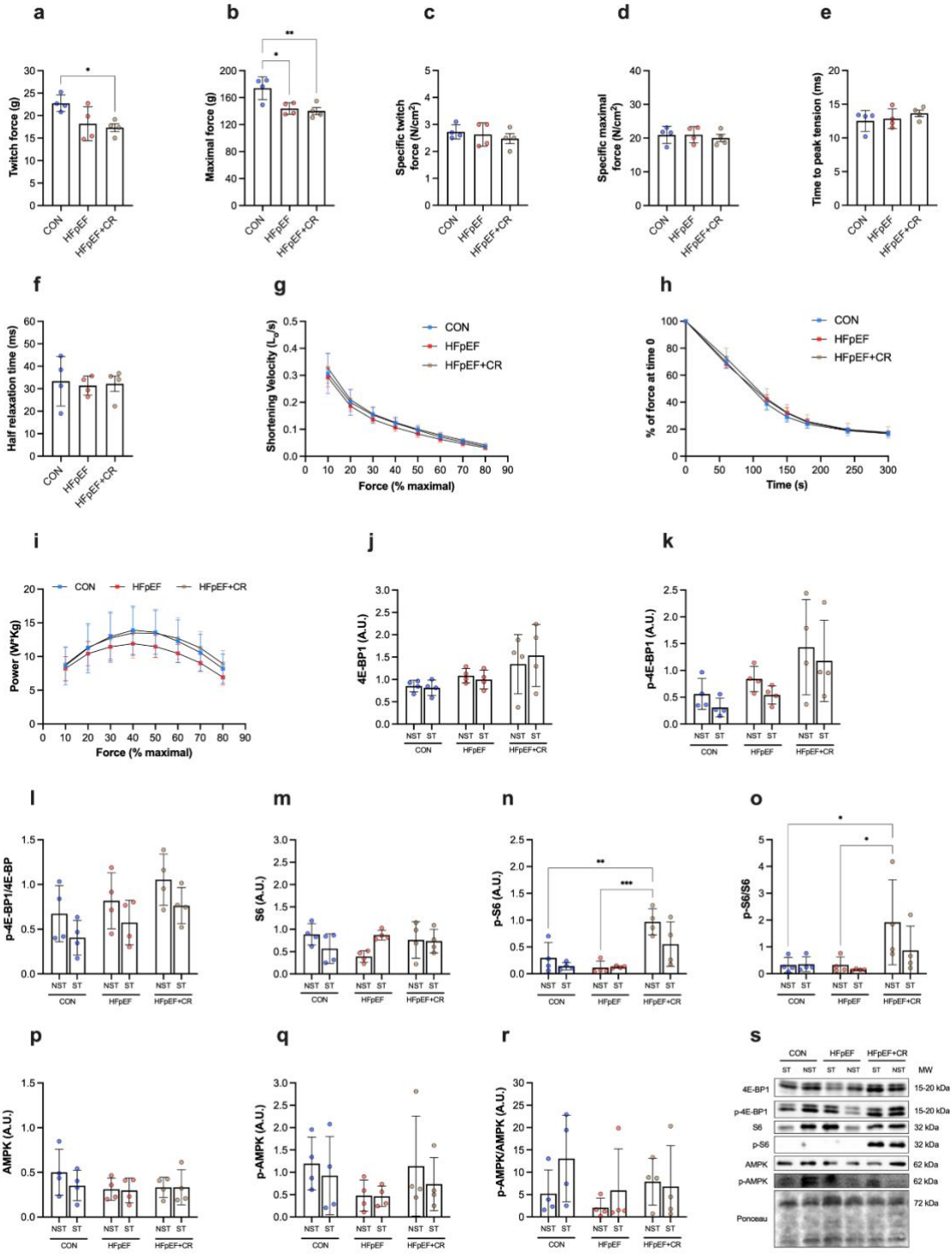

Figure 6.6. ***In vitro*** **skeletal muscle function.** Soleus absolute twitch and maximal forces were lower in HEpEF rats with or without CR (all $P < 0.05$) **(a, b)**, whereas mass-specific twitch and maximal forces were comparable between groups (all $P > 0.05$) **(c, d)**. No significant differences were observed in time to peak tension, half relaxation time, shortening velocity, fatigue and muscle power (all $P > 0.05$) **(e-i)**. 4E-BP1, S6 and AMPK protein contents in stimulated (ST) and non-stimulated (NST) muscles were not different between groups (all $P > 0.05$) **(j-s)**.

6.4 Discussion

We previously demonstrated that overload-induced skeletal muscle hypertrophy is impaired in obese-HFpEF rats (Chapter 5 Results III). Here we provide new evidence that myofiber hypertrophy can be partially rescued *via* acute CR treatment. The underlying mechanism for this seems related to improved myonuclear accretion (possibly *via* enhanced muscle stem cell function) rather than increased protein synthesis signalling. We also show that CR affected skeletal muscle remodelling in a fibre type-specific manner and benefits baseline muscle phenotype in HFpEF. These data are the first to show that CR rejuvenates myofiber growth in the setting of HFpEF and highlight novel mechanistic targets that may help develop therapies.

6.4.1 Effects of caloric restriction in HFpEF on metabolic and muscle phenotype

CR has consistently demonstrated to reduced body weight in HF patients (Rider *et al.*, 2013; Kitzman *et al.*, 2016; Bianchi, 2020) and HF animal models (Yan *et al.*, 2013; de Lucia *et al.*, 2018). Here, body weight of caloric-restricted rats was maintained throughout the intervention period (four weeks), which contrasts a previous study where CR (four weeks) reduced body weight in obese HF rats (Takatsu *et al.*, 2013); this discrepancy may be related to the lower percentage of CR used in our study (10-40% vs 65%). Our study also showed that blood glucose levels were normalised in HFpEF rats with CR compared to untreated HFpEF rats. Regulation of glucose homeostasis by CR has been consistently demonstrated in different cohorts (Soare *et al.*, 2014) and animal models (Colman *et al.*, 1998; Colman *et al.*, 2009; Mitchell *et al.*, 2016; Velingkaar *et al.*, 2020; Ham *et al.*, 2022).

In relation to skeletal muscle, little is known about the effects of CR in HFpEF and no experimental animal studies have focused on this. DEXA and MRI measures of body composition have shown that CR reduces lean body mass and thigh skeletal muscle (cm^2) in HFpEF patients, but increases percent lean body mass and muscle quality (leg power divided by thigh muscle) (Kitzman *et al.*, 2016). Here, HFpEF rats showed lower EDL and soleus muscle mass but this was not affected by CR. In contrast, CR exacerbated fibre atrophy in the EDL muscles and this response was more prominent in fast-twitch glycolytic fibres. We (Chapter 4 Results II) and others have previously demonstrated that fast-twitch glycolytic fibres are more prone to be affected by atrophic conditions than slow-twitch oxidative fibres (Wang & Pessin, 2013; Talbot & Maves, 2016). In support, we also observed that CR did not aggravate but tended to increase FCSA, and increased C:F in the soleus muscle, which consists almost entirely of slow-twitch oxidative fibres. Further, CR restriction tended to increase muscle power, which further supports previous observations in HFpEF patients (Kitzman *et al.*, 2016). Overall it seems CR may improve muscle quality to benefit overall function at the expense of some baseline reductions in muscle mass.

6.4.2 Regulation of muscle hypertrophy and effects of CR in HFpEF

Skeletal muscle mass is regulated by changes in the balance between rates of protein synthesis and protein degradation, which is orchestrated by anabolic (e.g., the mTOR pathway) and catabolic pathways (e.g., the ubiquitin-proteasome system and autophagy). This balance is tightly governed by upstream factors related to hormonal, metabolic, mechanical and neural activity (Schiaffino *et al.*, 2013), which explains why CR, physical inactivity and several diseases can cause substantial loss of skeletal muscle mass and strength. In this study, downstream

targets of mTOR, such as 4E-BP1, S6 and AMPK, as well as key regulators of the ubiquitin-proteosome system and autophagy (MuRF1 and p62, respectively) were not significantly affected by CR or HFpEF. This contradicts previous studies suggesting that CR suppresses mTOR activity and activates autophagy to maintain proper cell function and promote cell survival (Margolis *et al.*, 2016; Chen *et al.*, 2019; Chung & Chung, 2019) although our study was only for an acute time period not long term. Further, skeletal muscles of obese-ZSF1 rats and HFpEF patients have shown increased levels of MuRF1, leading to an increase of ubiquitinylated proteins, which are subsequently degraded by the proteasome system (Goto *et al.*, 2020). Taken together, CR seems to affect skeletal muscle remodelling in a fibre type-specific manner, while its mechanisms of action remain to be fully established.

We confirmed that CR rescued blunted myofiber hypertrophy in obese-HFpEF rats. Specifically, after overload, total FCSA was increased by 27% and 35% in lean controls and caloric-restricted HFpEF rats, respectively, but increased by only 9% in HFpEF rats with ad libitum diet. Interestingly, CR caused a greater overload-induced hypertrophic response in oxidative fibres (Type I and Type IIa), suggesting that fast-twitch glycolytic fibres are not only more vulnerable to atrophy, as previously discussed, but also have a reduced hypertrophic response. It is suggested that during hypertrophy SC undergo proliferation, differentiation and fusion with existing myofibers in order to provide new myonuclei for growing muscle cells and maintain an optimal myonuclear domain size (Petrella *et al.*, 2006; Petrella *et al.*, 2008; Phillips, 2014; Snijders *et al.*, 2015). This is supported by experiments where overload-induced muscle hypertrophy was prevented in SC-deficient rodents (Rosenblatt & Parry, 1992;

Rosenblatt *et al.*, 1994; Adams *et al.*, 2002; Egner *et al.*, 2016). However, findings from other studies have yielded contradictory results (Rosenblatt & Parry, 1993; Lowe & Alway, 1999), and techniques for SC depletion where DNA replication is inhibited either pharmacologically or by γ-irradiation, have been questioned (McCarthy & Esser, 2007).

In our study, the impaired hypertrophic response observed in HFpEF rats was associated with a lower number of nuclei per fibre, while the improved hypertrophy after CR occurred in line with increased myonuclear accretion. Thus, our data support the concept that increased SC function and subsequent myonuclear accretion play an important role in muscle hypertrophy, while providing new evidence that HFpEF impairs myonuclear accretion in response to mechanical overload, which can be ameliorated by CR. What specific mechanisms related to SC dysfunction exists in HFpEF remain unclear, but CR has been well document to increase SC number, function and myogenic progression in mouse studies alongside accelerating regeneration after injury (Cerletti *et al.*, 2012). Other mechanisms for the improved hypertrophic response observed in HFpEF rats with CR may also be related to improvements in mitochondrial ATP production (which are important for both protein synthesis during hypertrophy (Carafoli *et al.*, 1964; Hyatt & Powers, 2021) but also SC homeostasis). CR is known to increase mitochondrial function in both permeabilized muscle fibres (Lanza *et al.*, 2012) and isolated SC of mice. However, this remains to be directly confirmed by future experiments.

In lean “control” rodents, muscle adaptation to mechanical overload is typically characterized by an increase in protein synthesis, represented as total protein content (White *et al.*, 2009), myofibrillar protein content (Almurshed & Grunewald, 2000) or increased puromycin incorporation (Pereira *et al.*, 2017). A previous study showed that this is not affected by CR. Specifically, muscle mass, total protein, and myofibrillar protein contents were increased in overloaded muscles of both caloric restricted rats and rats with ad libitum diet (Almurshed & Grunewald, 2000). In contrast, our data showed that protein synthesis, measured by puromycin incorporation, was not affected by overload, HFpEF or CR. In addition, mTOR-related signalling (i.e., 4E-BP1, S6 and AMPK) was not different between or within groups, which contrast previous observations where overload increased phosphorylation of mTOR, p70S6k and S6 in lean controls but not in obese rats with insulin resistance (Katta *et al.*, 2010; Paturi *et al.*, 2010). These discrepancies may be explained by differences between animal models, time period of the overload, and methods for measuring protein synthesis. To the best of our knowledge, this is the first study where ZSF1 rats are subjected to synergist ablation-induced mechanical overload, and the time point when protein synthesis is supposed to increase remains to be established. This has been examined in different animal models and can differ across overload periods and diseases/comorbidities. For example, lean rats have shown an increase of 37% and 17% in phosphorylation of mTOR after 7 and 21 days of overload, respectively, whereas this increased by 18% in obese rats after 7 days of overload but remained unchanged after 21 days (Katta *et al.*, 2010). It is possible, therefore, that we missed or did not reach the point where protein synthesis increases in response to overload. We did perform acute experiments and measured protein synthesis immediately after muscle contractions and similarly

found no differences between groups/conditions. However, muscles were frozen immediately after contractions and past studies have shown it may take >3 h to see peak effects on protein synthesis (Atherton *et al.*, 2005). Future studies examining multiple time points are therefore required to clarify this issue.

6.4.3 Limitations

We did not confirm that obese rats developed a clinical HFpEF phenotype. However, we (Espino-Gonzalez *et al.*, 2020) and others have consistently demonstrated that this rat model develops key features of HFpEF as early as 10-15 weeks of age (Schauer *et al.*, 2020), including diastolic dysfunction, preserved ejection fraction, myocardial remodelling, hypercalcemia, obesity and exercise intolerance (Hamdani *et al.*, 2013; Leite *et al.*, 2015; Franssen *et al.*, 2016; van Dijk *et al.*, 2016; Bowen *et al.*, 2017b). Further, our experiments were performed in male rats only, thus, it remains unclear whether similar results would be replicated in females. We also only assessed a single time point after overload and may have missed earlier or later transient changes in protein synthesis and myonuclear accretion.

Clinically, the long-term effects of CR on improving clinical outcomes in HF patients may be complex. For example, some HF patients are susceptible to develop sarcopenia and frailty, thus, the benefits of caloric restriction must be counterbalanced by the risks it may impose as it may compromise vital nutrition in elderly or debilitated patients. Further, paradoxically, while obesity increases the risk of HF, obese HF patients in general have shown better survival outcomes than those who are normal or underweight as assessed *via* body mass index (Haass *et al.*, 2011).

6.5 Conclusions

Acute CR restored overload-induced fibre hypertrophy in HFpEF rats, which was associated with increased myonuclear accretion and not protein synthesis signalling. This indicates CR could rejuvenate muscle stem cell function to support myofiber growth, which may offer a novel and viable non-pharmacological treatment to enhance muscle mass in patients with HFpEF.

Chapter 7 General discussion

HFpEF is no longer considered a simple syndrome of cardiac dysfunction but includes several skeletal muscle abnormalities that limit exercise capacity and quality of life (Anderson *et al.*, 2022). To date, HFpEF-related muscle deficits remain poorly understood and available treatments are limited. This thesis, using a well-characterised cardiometabolic rat model (Franssen *et al.*, 2016; Bowen *et al.*, 2017b; Schauer *et al.*, 2020), provides new evidence that:

i) HFpEF induced multiple skeletal muscle alterations including contractile dysfunction, fibre atrophy, capillary loss, and impaired blood flow.

ii) Cardiovascular pharmacological treatments of Entresto and Vastiras improved heart function in HFpEF but had no impact on skeletal muscle remodelling.

iii) Skeletal muscle hypertrophy following mechanical overload in HFpEF was attenuated and this was associated with mitochondrial but not vascular impairments.

iv) Impaired skeletal muscle hypertrophy was partially rescued following acute caloric restriction in HFpEF and linked increased myonuclear accretion.

7.1 Skeletal muscle alterations in HFpEF

HFpEF is associated with several skeletal muscle alterations that are closely associated with exercise intolerance and poor quality of life, with one major feature a loss of muscle mass and strength (Bekfani *et al.*, 2016). Here, we confirmed that compared to controls, obese-ZSF1 rats developed muscle atrophy and contractile dysfunction alongside impaired vascular structure and function. In addition, we provide new evidence that soleus shortening velocity and mechanical power were impaired in HFpEF rats, which occurred in the absence of any fibre type shift to suggest slowed cross-bridge kinetics as previously reported in HFrEF (Coirault *et al.*, 2007; Miller *et al.*, 2010). Further, we performed the first direct measures of leg (muscle) arterial blood flow in HFpEF and reveal that functional hyperaemia was impaired in HFpEF rats, which is consistent with some (Lee *et al.*, 2016b; Maréchaux *et al.*, 2016; Kishimoto *et al.*, 2017) but not all (Hundley *et al.*, 2007; Haykowsky *et al.*, 2013b; Lee *et al.*, 2016a; Zamani *et al.*, 2020) non-invasive measurements in patients with HFpEF. The disparity in findings between studies is likely explained by differences in the muscle studied, non-invasive and different measurements techniques, and patient heterogeneity. Our data, however, supports the potential for perfusive oxygen delivery limitations in HFpEF, which likely contributes to exercise intolerance in this disease (Poole *et al.*, 2018). We also performed fibre-type specific histological analyses to confirm that HFpEF rats had a Type II fibre-type shift and lower C:F ratio, which supports previous data from HFpEF patients in the vastus lateralis (Kitzman *et al.*, 2014). Finally, we revealed that fibre atrophy in HFpEF was more prominent in fast-twitch glycolytic fibres (Chapter 4 Results II and Chapter 6 Results IV), which supports previous research suggesting that fast-twitch glycolytic fibres are

more prone to be affected by atrophic conditions than slow-twitch oxidative fibres (Wang & Pessin, 2013; Talbot & Maves, 2016).

In addition to limb skeletal muscle, the thesis contributes novel data in relation to diaphragm plasticity in HFpEF. We showed that compared to controls, obese-HFpEF rats have increased Type I/IIa FCSA and reduced Type IIb/IIx FCSA, alongside increased fibre capillary supply and estimated levels of oxygenation. These data indicate compensatory adaptations in slow-twitch fibres and correspond to diaphragmatic alterations similar to those caused by denervation – atrophy in fast-twitch glycolytic fibres and hypertrophy in slow-twitch oxidative fibres (Aravamudan *et al.*, 2006) alongside increased CD (Paudyal *et al.*, 2018). The increased hypertrophy in oxidative fibres may be related to obesity and its associated chronic respiratory loading, which can act as a training stimulus to increase fibre size and fatigue-resistance (Farkas *et al.*, 1994; Powers *et al.*, 1996). In support, isometric, isotonic and cyclical contractile properties were well preserved in HFpEF rats. Taken together, our data suggest that obese-HFpEF induces functional, morphological and vascular alterations in limb skeletal muscle that likely contributes to exercise intolerance. In contrast, diaphragm phenotype remained well preserved. This animal model, therefore, may be suitable to further explore the mechanisms and treatments for the muscle pathology developed in HFpEF.

7.2 Impact of cardiovascular medications in HFpEF skeletal muscle

Given our findings of a muscle pathology in HFpEF, we next examined if Entresto alone or in combination with Vastiras could be used as a rescue treatment.

Entresto (Sacubitril/Valsartan) and Vastiras (proANP$_{31-67}$) can improve diastolic function, cardiac remodelling, endothelial function and glomerular filtration rate in HFpEF (Gori *et al.*, 2019; Altara *et al.*, 2020; Schauer *et al.*, 2021), but their effects on skeletal muscle in HFpEF remain poorly tested (Schauer *et al.*, 2021). In our study, ten weeks of Entresto alone or in combination with Vastiras did not rescue the observed atrophy and reduced capillarisation of HFpEF EDL muscles. Similarly histological analyses of fibre type distribution, capillarisation and fibrosis of soleus muscle did not reveal beneficial effects of the treatments, suggesting that both mixed (EDL) and oxidative (soleus) muscles are not influenced by Entresto or Vastiras. In contrast, both medications improved cardiac morphology and function (E/A and stroke volume) in obese-HFpEF rats, in line with past evidence (Schauer *et al.*, 2021). Taken together, these findings suggest that cardio-centric medications in HFpEF do not impact skeletal muscle remodelling and highlight the need for alternative approaches.

7.3 Impaired skeletal muscle hypertrophy in HFpEF

Muscle atrophy is a major feature in HFpEF that causes worse symptoms and limits quality of life (Bekfani *et al.*, 2020). Since cardiovascular medications did not influence HFpEF-induced skeletal muscle phenotype, we used a local intervention to directly induce muscle hypertrophy - the surgical synergist ablation model (compensatory overload) (Ianuzzo & Chen, 1979; Timson *et al.*, 1985). One major findings was that only controls showed an increased in muscle force and fibre size but not in HFpEF as previously observed in old mice and rats (Blough & Linderman, 2000; Dungan *et al.*, 2022). Impaired response to anabolic stimuli has been detected in several conditions in addition to ageing, including cancer and metabolic disorders. Anabolic resistance is often touted as an

underlying cause of muscle wasting in disease and this can ultimately reduce functional capacity and whole-body health i.e., blood glucose homeostasis, protein metabolism, and fat oxidation (Paulussen *et al.*, 2021). As such, one major question from this thesis is what limits muscle growth in HFpEF?

Skeletal muscle hypertrophy is generally determined by elevated protein synthesis *via* Akt-mTOR signalling and/or increased myonuclei accretion *via* SC (Blaauw & Reggiani, 2014). Our data show that protein synthesis, measured by puromycin incorporation, was not affected by overload or HFpEF. In addition, mTOR-related signalling (i.e., 4E-BP1, S6 and AMPK) was not different between or within groups. The reason for detecting no differences is somewhat surprising, but could be related to no change in protein synthesis or the time period of increased rates had returned to normal as is sometimes reported (Katta *et al.*, 2010; Fortes *et al.*, 2015). In contrast, the number of nuclei per muscle fibre (i.e., myonuclear accretion) was increased after overload in lean controls but not HFpEF. Adequate blood flow and capillarisation is critical for anabolic stimuli, such as insulin and exercise, to increase protein synthesis and fibre size (Timmerman *et al.*, 2010; Snijders *et al.*, 2017; Moro *et al.*, 2019). Our data show that resting femoral artery blood flow and functional hyperaemia in HFpEF rats were well preserved after overload. In addition, both lean and HFpEF rats showed a similar overload-induced increase in C:F with no impairments in muscle PO_2 at maximal exercise, which indicates adequate oxygenation. Alternatively, the impaired overload-induced hypertrophic response in HFpEF rats was associated with reduced mitochondrial coupling efficiency (impaired respiratory control ratio), which could pose a limit to protein synthesis (Carafoli *et al.*, 1964; Hyatt & Powers, 2021) and normal SC function (Wang *et al.*, 2013; Zhang *et al.*, 2016;

Karatzaferi *et al.*, 2019). Overall, therefore, our data suggest that overload-induced hypertrophy is impaired in HFpEF rats, which is associated with mitochondrial dysfunction and reduced myonuclear accretion rather than vascular dysfunction and reduced protein synthesis signalling.

7.4 Effects of caloric restriction on skeletal muscle phenotype in HFpEF

Caloric restriction (CR) is among the few treatments that have shown beneficial outcomes in HFpEF patients that may include skeletal muscle (Kitzman *et al.*, 2016). Here we provide new evidence that impaired overload-induced muscle hypertrophy in HFpEF rats can be partially rescued *via* acute CR treatment. Specifically, after overload, fibre size was increased in lean controls and HFpEF with CR but not in HFpEF on a normal diet. Mechanistically, improved fibre hypertrophy after CR occurred in line with increased myonuclear accretion. This supports the concept that acute CR improves SC function (Cerletti *et al.*, 2012), which contribute new myonuclei to muscle fibres to support muscle growth (Murach *et al.*, 2021) . Our data also support the concept that increased SC function and subsequent myonuclear accretion play an important role in muscle hypertrophy (Rosenblatt & Parry, 1992; Rosenblatt *et al.*, 1994; Adams *et al.*, 2002; Egner *et al.*, 2016), which has been questioned (Rosenblatt & Parry, 1993; Lowe & Alway, 1999; McCarthy & Esser, 2007). Interestingly, CR caused a greater hypertrophic response in oxidative fibres (Type I and Type IIa) but reduced Type IIb/IIx fibre size in non-overloaded EDL muscles. Further, CR tended to increase fibre size and C:F in the soleus, which primarily consists of slow-twitch oxidative fibres. Collectively, these findings suggest that fast-twitch glycolytic fibres are not only more vulnerable to atrophy, as previously reported

(Wang & Pessin, 2013; Talbot & Maves, 2016), but also have a reduced hypertrophic response in HFpEF.

CR may also increase muscle contractile function given our data showing this increased muscle power in HFpEF, which further supports previous observations in HFpEF patients (Kitzman *et al.*, 2016). Additionally, blood glucose levels were normalised in HFpEF rats with CR compared to untreated HFpEF rats, which has been consistently demonstrated in different cohorts (Soare *et al.*, 2014) and animal models (Colman *et al.*, 1998; Colman *et al.*, 2009; Mitchell *et al.*, 2016; Velingkaar *et al.*, 2020; Ham *et al.*, 2022). Taken together, therefore, CR may increase skeletal muscle hypertrophy (possibly *via* enhanced muscle stem cell function to increase myonuclear accretion), increase contractile function, and improve glucose homeostasis in HFpEF.

7.5 Experimental considerations and limitations

The present thesis is subject to some limitations. Overall, the findings must be interpreted with caution given they were performed in an animal model and may not directly translate to humans. The experiments were also performed in male rats only meaning sex-dependent differences cannot be excluded especially as many patients with HFpEF are female. We also used a relatively early time point in the progression of HFpEF, which may limit translation of our findings to more advanced stages of the disease and older patients. However, this rat model has been shown to develop metabolic impairments associated with typical signs of HFpEF as well as muscle dysfunction developing as early as 10-15 weeks of age (Schauer *et al.*, 2020).

Physical activity levels between groups were also not evaluated and cannot be ruled out as having an impact on our experimental measures, although it is established that low physical activity levels cannot account for muscle impairments induced by HF (Simonini *et al.*, 1996; Miller *et al.*, 2009). Furthermore, our experiments with cardiovascular medications lack assessments of skeletal muscle contractile properties, therefore, their effects on muscle function remain to be evaluated but seem unlikely (Schauer *et al.*, 2021). We also only assessed a single time point after overload and may have missed earlier or later transient changes in protein synthesis and myonuclear accretion, which should be considered when interpreting our major findings on limited muscle hypertrophy in HFpEF. This thesis also examined the acute effects of CR but the long-term effects in HFpEF remain uncertain. For example, some HF patients are susceptible to develop sarcopenia and frailty (Kinugasa & Yamamoto, 2017) while obese HF patients in general show better survival than normal or underweight patients (Haass *et al.*, 2011), meaning the effects of CR must be carefully considered .

7.6 Outlook and future studies

This thesis supports several muscle-specific changes reported to occur in HFpEF patients (e.g., muscle dysfunction, fibre atrophy predominantly in Type II fibres, a fibre-type shift, reduced capillarity, mitochondrial dysfunction and impaired blood flow (Kitzman *et al.*, 2014; Lee *et al.*, 2016b; Bekfani *et al.*, 2020)). As such, muscle groups composed of fast-twitch fibres should be primarily targeted during rehabilitation in HFpEF patients. This thesis also demonstrates that increasing

cardiac function *per se*, *via* targeted cardiovascular drugs (Entresto and Vastiras), had no impact on skeletal muscle morphology in HFpEF rats; thus, alternative skeletal muscle-specific interventions may be required to overcome peripheral muscle deficits in HFpEF rather than increasing global blood flow. Further, given that HFpEF rats showed anabolic resistance (i.e., impaired overload-induced muscle hypertrophy) associated with mitochondrial dysfunction, exercise training in combination with other treatments that target the mitochondria may be an alternative approach to treat the muscle pathology in HFpEF. We also found that CR increased muscle power and the hypertrophy response (possibly *via* enhanced SC function to increase myonuclear accretion) in HFpEF, which further supports previous observations in HFpEF patients (Kitzman *et al.*, 2016). However, although exercise and CR improve the quality of life of this population, studies have mainly been focused on the cardiorespiratory function and little is known about how they directly affect skeletal muscle. A more comprehensive characterisation of CR and exercise-induced muscle adaptations in HFpEF patients (including functional and histological analyses of fibre size, type, and capillarity as well as multi-omics approaches) will help to identify novel mechanistic targets and therapies.

7.7 Thesis conclusions

The studies outlined in this thesis have revealed novel findings related to the mechanisms and treatments of the skeletal muscle pathology in HFpEF. Using a multi-level characterisation, these experiments demonstrated that obese HFpEF rats develop vascular, functional, structural and mitochondrial skeletal muscle alterations, including fibre atrophy to cause muscle weakness and fatigue. Regarding treatments, this thesis showed that while cardio-centric

pharmacological medications improved heart function they did not impact skeletal muscle remodelling in HFpEF. This suggested skeletal muscle-specific interventions could be an optimal approach to restore muscle health in HFpEF and led us to our next experiment using mechanical overload. Mechanical overload increased fibre hypertrophy in healthy controls but not in obese-HFpEF rats, which was linked to impaired mitochondrial but not vascular function. As previous research showed CR improves clinical and functional outcomes in patients with HFpEF, we next showed acute CR restored overload-induced fibre hypertrophy in HFpEF rats that may have been underpinned by increased myonuclear accretion. This indicates CR could be an approach that rejuvenates muscle stem cell function to support myofiber growth. Overall, CR in combination with exercise training may offer a novel non-pharmacological treatment to improve skeletal muscle health in patients with HFpEF.

References

Abudiab MM, Redfield MM, Melenovsky V, Olson TP, Kass DA, Johnson BD & Borlaug BA. (2013). Cardiac output response to exercise in relation to metabolic demand in heart failure with preserved ejection fraction. *Eur J Heart Fail* **15,** 776-785.

Adams GR, Caiozzo VJ, Haddad F & Baldwin KM. (2002). Cellular and molecular responses to increased skeletal muscle loading after irradiation. *Am J Physiol Cell Physiol* **283,** C1182-1195.

Adams V, Linke A & Winzer E. (2017). Skeletal muscle alterations in HFrEF vs. HFpEF. *Curr Heart Fail Rep* **14,** 489-497.

Adams V, Schauer A, Augstein A, Kirchhoff V, Draskowski R, Jannasch A, Goto K, Lyall G, Männel A, Barthel P, Mangner N, Winzer EB, Linke A & Labeit S. (2022). Targeting MuRF1 by small molecules in a HFpEF rat model improves myocardial diastolic function and skeletal muscle contractility. *J Cachexia Sarcopenia Muscle* **13,** 1565-1581.

Adams V, Wunderlich S, Mangner N, Hommel J, Esefeld K, Gielen S, Halle M, Ellingsen Ø, Van Craenenbroeck EM, Wisløff U, Pieske B, Linke A & Winzer EB. (2021). Ubiquitin-proteasome-system and enzymes of energy metabolism in skeletal muscle of patients with HFpEF and HFrEF. *ESC Heart Fail* **8,** 2556-2568.

Al-Shammari AA, Kissane RWP, Holbek S, Mackey AL, Andersen TR, Gaffney EA, Kjaer M & Egginton S. (2019). Integrated method for quantitative morphometry and oxygen transport modeling in striated muscle. *J Appl Physiol (1985)* **126,** 544-557.

Almurshed K & Grunewald K. (2000). The effects of dietary energy restriction on overloaded skeletal muscle in rats. *Br J Nutr* **84,** 697-704.

Altara R, da Silva GJJ, Frisk M, Spelta F, Zouein FA, Louch WE, Booz GW & Cataliotti A. (2020). Cardioprotective Effects of the Novel Compound Vastiras in a Preclinical Model of End-Organ Damage. *Hypertension* **75,** 1195-1204.

Anderson M, Parrot CF, Haykowsky MJ, Brubaker PH, Ye F & Upadhya B. (2022). Skeletal muscle abnormalities in heart failure with preserved ejection fraction. *Heart Fail Rev*.

Anker SD, Butler J, Filippatos G, Ferreira JP, Bocchi E, Böhm M, Brunner-La Rocca HP, Choi DJ, Chopra V, Chuquiure-Valenzuela E, Giannetti N, Gomez-Mesa JE, Janssens S, Januzzi JL, Gonzalez-Juanatey JR, Merkely B, Nicholls SJ, Perrone SV, Piña IL, Ponikowski P, Senni M, Sim

D, Spinar J, Squire I, Taddei S, Tsutsui H, Verma S, Vinereanu D, Zhang J, Carson P, Lam CSP, Marx N, Zeller C, Sattar N, Jamal W, Schnaidt S, Schnee JM, Brueckmann M, Pocock SJ, Zannad F & Packer M. (2021). Empagliflozin in Heart Failure with a Preserved Ejection Fraction. *N Engl J Med* **385,** 1451-1461.

Anker SD, Negassa A, Coats AJ, Afzal R, Poole-Wilson PA, Cohn JN & Yusuf S. (2003). Prognostic importance of weight loss in chronic heart failure and the effect of treatment with angiotensin-converting-enzyme inhibitors: an observational study. *Lancet* **361,** 1077-1083.

Aquilani R, Opasich C, Gualco A, Verri M, Testa A, Pasini E, Viglio S, Iadarola P, Pastoris O, Dossena M & Boschi F. (2008). Adequate energy-protein intake is not enough to improve nutritional and metabolic status in muscle-depleted patients with chronic heart failure. *European journal of heart failure* **10,** 1127-1135.

Aravamudan B, Mantilla CB, Zhan WZ & Sieck GC. (2006). Denervation effects on myonuclear domain size of rat diaphragm fibers. *J Appl Physiol (1985)* **100,** 1617-1622.

Atherton PJ, Babraj J, Smith K, Singh J, Rennie MJ & Wackerhage H. (2005). Selective activation of AMPK-PGC-1alpha or PKB-TSC2-mTOR signaling can explain specific adaptive responses to endurance or resistance training-like electrical muscle stimulation. *Faseb j* **19,** 786-788.

Barroso MC, Kramer F, Greene SJ, Scheyer D, Köhler T, Karoff M, Seyfarth M, Gheorghiade M & Dinh W. (2016). Serum insulin-like growth factor-1 and its binding protein-7: potential novel biomarkers for heart failure with preserved ejection fraction. *BMC Cardiovasc Disord* **16,** 199.

Bekfani T, Bekhite Elsaied M, Derlien S, Nisser J, Westermann M, Nietzsche S, Hamadanchi A, Fröb E, Westphal J, Haase D, Kretzschmar T, Schlattmann P, Smolenski UC, Lichtenauer M, Wernly B, Jirak P, Lehmann G, Möbius-Winkler S & Schulze PC. (2020). Skeletal Muscle Function, Structure, and Metabolism in Patients With Heart Failure With Reduced Ejection Fraction and Heart Failure With Preserved Ejection Fraction. *Circ Heart Fail* **13,** e007198.

Bekfani T, Bekhite M, Neugebauer S, Derlien S, Hamadanchi A, Nisser J, Hilse MS, Haase D, Kretzschmar T, Wu MF, Lichtenauer M, Kiehntopf M, von Haehling S, Schlattmann P, Lehmann G, Franz M, Möbius-Winkler S & Schulze C. (2022). Metabolomic Profiling in Patients with Heart Failure and Exercise Intolerance: Kynurenine as a Potential Biomarker. *Cells* **11**.

Bekfani T, Pellicori P, Morris DA, Ebner N, Valentova M, Steinbeck L, Wachter R, Elsner S, Sliziuk V, Schefold JC, Sandek A, Doehner W, Cleland JG, Lainscak M, Anker SD & von Haehling S. (2016). Sarcopenia in patients

with heart failure with preserved ejection fraction: Impact on muscle strength, exercise capacity and quality of life. *Int J Cardiol* **222,** 41-46.

Benson AP, Bernus O, Dierckx H, Gilbert SH, Greenwood JP, Holden AV, Mohee K, Plein S, Radjenovic A, Ries ME, Smith GL, Sourbron S & Walton RD. (2011). Construction and validation of anisotropic and orthotropic ventricular geometries for quantitative predictive cardiac electrophysiology. *Interface Focus* **1,** 101-116.

Benson AP, Gilbert SH, Li P, Newton SM & Holden AV. (2008). Reconstruction and Quantification of Diffusion Tensor Imaging-Derived Cardiac Fibre and Sheet Structure in Ventricular Regions used in Studies of Excitation Propagation. *Math Model Nat Phenom* **3,** 101-130.

Bhella PS, Prasad A, Heinicke K, Hastings JL, Arbab-Zadeh A, Adams-Huet B, Pacini EL, Shibata S, Palmer MD, Newcomer BR & Levine BD. (2011a). Abnormal haemodynamic response to exercise in heart failure with preserved ejection fraction. *Eur J Heart Fail* **13,** 1296-1304.

Bhella PS, Prasad A, Heinicke K, Hastings JL, Arbab-Zadeh A, Adams-Huet B, Pacini EL, Shibata S, Palmer MD, Newcomer BR & Levine BD. (2011b). Abnormal haemodynamic response to exercise in heart failure with preserved ejection fraction. *Eur J Heart Fail* **13,** 1296-1304.

Bianchi VE. (2020). Caloric restriction in heart failure: A systematic review. *Clin Nutr ESPEN* **38,** 50-60.

Blaauw B & Reggiani C. (2014). The role of satellite cells in muscle hypertrophy. *J Muscle Res Cell Motil* **35,** 3-10.

Blough ER & Linderman JK. (2000). Lack of skeletal muscle hypertrophy in very aged male Fischer 344 x Brown Norway rats. *J Appl Physiol (1985)* **88,** 1265-1270.

Bodine SC, Latres E, Baumhueter S, Lai VK, Nunez L, Clarke BA, Poueymirou WT, Panaro FJ, Na E, Dharmarajan K, Pan ZQ, Valenzuela DM, DeChiara TM, Stitt TN, Yancopoulos GD & Glass DJ. (2001a). Identification of ubiquitin ligases required for skeletal muscle atrophy. *Science* **294,** 1704-1708.

Bodine SC, Stitt TN, Gonzalez M, Kline WO, Stover GL, Bauerlein R, Zlotchenko E, Scrimgeour A, Lawrence JC, Glass DJ & Yancopoulos GD. (2001b). Akt/mTOR pathway is a crucial regulator of skeletal muscle hypertrophy and can prevent muscle atrophy in vivo. *Nat Cell Biol* **3,** 1014-1019.

Bonilla-Palomas JL, Gámez-López AL, Castillo-Domínguez JC, Moreno-Conde M, López Ibáñez MC, Alhambra Expósito R, Ramiro Ortega E, Anguita-

Sánchez MP & Villar-Ráez A. (2016). Nutritional Intervention in Malnourished Hospitalized Patients with Heart Failure. *Arch Med Res* **47,** 535-540.

Bottinelli R, Schiaffino S & Reggiani C. (1991). Force-velocity relations and myosin heavy chain isoform compositions of skinned fibres from rat skeletal muscle. *J Physiol* **437,** 655-672.

Bowen TS, Adams V, Werner S, Fischer T, Vinke P, Brogger MN, Mangner N, Linke A, Sehr P, Lewis J, Labeit D, Gasch A & Labeit S. (2017a). Small-molecule inhibition of MuRF1 attenuates skeletal muscle atrophy and dysfunction in cardiac cachexia. *J Cachexia Sarcopenia Muscle* **8,** 939-953.

Bowen TS, Brauer D, Rolim NPL, Baekkerud FH, Kricke A, Ormbostad Berre AM, Fischer T, Linke A, da Silva GJ, Wisloff U & Adams V. (2017b). Exercise Training Reveals Inflexibility of the Diaphragm in an Animal Model of Patients With Obesity-Driven Heart Failure With a Preserved Ejection Fraction. *J Am Heart Assoc* **6**.

Bowen TS, Herz C, Rolim NPL, Berre AO, Halle M, Kricke A, Linke A, da Silva GJ, Wisloff U & Adams V. (2018). Effects of Endurance Training on Detrimental Structural, Cellular, and Functional Alterations in Skeletal Muscles of Heart Failure With Preserved Ejection Fraction. *J Card Fail* **24,** 603-613.

Bowen TS, Rolim NP, Fischer T, Baekkerud FH, Medeiros A, Werner S, Bronstad E, Rognmo O, Mangner N, Linke A, Schuler G, Silva GJ, Wisloff U, Adams V & Optimex Study G. (2015). Heart failure with preserved ejection fraction induces molecular, mitochondrial, histological, and functional alterations in rat respiratory and limb skeletal muscle. *Eur J Heart Fail* **17,** 263-272.

Brandhorst S, Choi IY, Wei M, Cheng CW, Sedrakyan S, Navarrete G, Dubeau L, Yap LP, Park R, Vinciguerra M, Di Biase S, Mirzaei H, Mirisola MG, Childress P, Ji L, Groshen S, Penna F, Odetti P, Perin L, Conti PS, Ikeno Y, Kennedy BK, Cohen P, Morgan TE, Dorff TB & Longo VD. (2015). A Periodic Diet that Mimics Fasting Promotes Multi-System Regeneration, Enhanced Cognitive Performance, and Healthspan. *Cell Metab* **22,** 86-99.

Bruno C, Favuzzi AMR, Vergani E, Venuti A, Nicolazzi MA, Fuorlo M, Landolfi R & Mancini A. (2018). Multi-hormonal deficits in heart failure with preserved ejection Fraction: prevalence and impact on diastolic dysfunction. *Endocrine Abstracts*

Bruno C, Silvestrini A, Calarco R, Favuzzi AMR, Vergani E, Nicolazzi MA, d'Abate C, Meucci E, Mordente A, Landolfi R & Mancini A. (2020). Anabolic Hormones Deficiencies in Heart Failure With Preserved Ejection Fraction:

Prevalence and Impact on Antioxidants Levels and Myocardial Dysfunction. *Front Endocrinol (Lausanne)* **11,** 281.

Burke MA, Katz DH, Beussink L, Selvaraj S, Gupta DK, Fox J, Chakrabarti S, Sauer AJ, Rich JD, Freed BH & Shah SJ. (2014). Prognostic importance of pathophysiologic markers in patients with heart failure and preserved ejection fraction. *Circulation Heart failure* **7,** 288-299.

Butler J, Fonarow GC, Zile MR, Lam CS, Roessig L, Schelbert EB, Shah SJ, Ahmed A, Bonow RO, Cleland JG, Cody RJ, Chioncel O, Collins SP, Dunnmon P, Filippatos G, Lefkowitz MP, Marti CN, McMurray JJ, Misselwitz F, Nodari S, O'Connor C, Pfeffer MA, Pieske B, Pitt B, Rosano G, Sabbah HN, Senni M, Solomon SD, Stockbridge N, Teerlink JR, Georgiopoulou VV & Gheorghiade M. (2014). Developing therapies for heart failure with preserved ejection fraction: current state and future directions. *JACC Heart Fail* **2,** 97-112.

Calvani R, Joseph AM, Adhihetty PJ, Miccheli A, Bossola M, Leeuwenburgh C, Bernabei R & Marzetti E. (2013). Mitochondrial pathways in sarcopenia of aging and disuse muscle atrophy. *Biol Chem* **394,** 393-414.

Carafoli E, Margreth A & Buffa P. (1964). Early biochemical changes in mitochondria from denervated muscle and their relation to the onset of atrophy. *Exp Mol Pathol* **3,** 171-181.

Carnac G, Vernus B & Bonnieu A. (2007). Myostatin in the pathophysiology of skeletal muscle. *Current genomics* **8,** 415-422.

Cerletti M, Jang YC, Finley LW, Haigis MC & Wagers AJ. (2012). Short-term calorie restriction enhances skeletal muscle stem cell function. *Cell Stem Cell* **10,** 515-519.

Chan E, Giallauria F, Vigorito C & Smart NA. (2016). Exercise training in heart failure patients with preserved ejection fraction: a systematic review and meta-analysis. *Monaldi archives for chest disease = Archivio Monaldi per le malattie del torace* **86,** 759.

Chauvin C, Koka V, Nouschi A, Mieulet V, Hoareau-Aveilla C, Dreazen A, Cagnard N, Carpentier W, Kiss T, Meyuhas O & Pende M. (2014). Ribosomal protein S6 kinase activity controls the ribosome biogenesis transcriptional program. *Oncogene* **33,** 474-483.

Chen CN, Liao YH, Tsai SC & Thompson LV. (2019). Age-dependent effects of caloric restriction on mTOR and ubiquitin-proteasome pathways in skeletal muscles. *Geroscience* **41,** 871-880.

Chung KW & Chung HY. (2019). The Effects of Calorie Restriction on Autophagy: Role on Aging Intervention. *Nutrients* **11**.

Cleland JG, Tendera M, Adamus J, Freemantle N, Polonski L & Taylor J. (2006). The perindopril in elderly people with chronic heart failure (PEP-CHF) study. *Eur Heart J* **27,** 2338-2345.

Close RI. (1972). Dynamic properties of mammalian skeletal muscles. *Physiol Rev* **52,** 129-197.

Coats AJS, Forman DE, Haykowsky M, Kitzman DW, McNeil A, Campbell TS & Arena R. (2017). Physical function and exercise training in older patients with heart failure. *Nat Rev Cardiol* **14,** 550-559.

Coirault C, Guellich A, Barbry T, Samuel JL, Riou B & Lecarpentier Y. (2007). Oxidative stress of myosin contributes to skeletal muscle dysfunction in rats with chronic heart failure. *Am J Physiol Heart Circ Physiol* **292,** H1009-1017.

Colman RJ, Anderson RM, Johnson SC, Kastman EK, Kosmatka KJ, Beasley TM, Allison DB, Cruzen C, Simmons HA, Kemnitz JW & Weindruch R. (2009). Caloric restriction delays disease onset and mortality in rhesus monkeys. *Science* **325,** 201-204.

Colman RJ, Roecker EB, Ramsey JJ & Kemnitz JW. (1998). The effect of dietary restriction on body composition in adult male and female rhesus macaques. *Aging (Milano)* **10,** 83-92.

Cunningham JW, Claggett BL, O'Meara E, Prescott MF, Pfeffer MA, Shah SJ, Redfield MM, Zannad F, Chiang LM, Rizkala AR, Shi VC, Lefkowitz MP, Rouleau J, McMurray JJV, Solomon SD & Zile MR. (2020). Effect of Sacubitril/Valsartan on Biomarkers of Extracellular Matrix Regulation in Patients With HFpEF. *J Am Coll Cardiol* **76,** 503-514.

Das S, Morvan F, Morozzi G, Jourde B, Minetti GC, Kahle P, Rivet H, Brebbia P, Toussaint G, Glass DJ & Fornaro M. (2017). ATP Citrate Lyase Regulates Myofiber Differentiation and Increases Regeneration by Altering Histone Acetylation. *Cell Rep* **21,** 3003-3011.

de Lucia C, Gambino G, Petraglia L, Elia A, Komici K, Femminella GD, D'Amico ML, Formisano R, Borghetti G, Liccardo D, Nolano M, Houser SR, Leosco D, Ferrara N, Koch WJ & Rengo G. (2018). Long-Term Caloric Restriction Improves Cardiac Function, Remodeling, Adrenergic Responsiveness, and Sympathetic Innervation in a Model of Postischemic Heart Failure. *Circ Heart Fail* **11,** e004153.

Denies MS, Johnson J, Maliphol AB, Bruno M, Kim A, Rizvi A, Rustici K & Medler S. (2014). Diet-induced obesity alters skeletal muscle fiber types of male but not female mice. *Physiol Rep* **2,** e00204.

Dhakal BP, Malhotra R, Murphy RM, Pappagianopoulos PP, Baggish AL, Weiner RB, Houstis NE, Eisman AS, Hough SS & Lewis GD. (2015). Mechanisms of exercise intolerance in heart failure with preserved ejection fraction: the role of abnormal peripheral oxygen extraction. *Circ Heart Fail* **8,** 286-294.

Dieberg G, Ismail H, Giallauria F & Smart NA. (2015). Clinical outcomes and cardiovascular responses to exercise training in heart failure patients with preserved ejection fraction: a systematic review and meta-analysis. *Journal of applied physiology (Bethesda, Md : 1985)* **119,** 726-733.

Dmitrieva RI, Lelyavina TA, Komarova MY, Galenko VL, Ivanova OA, Tikanova PA, Khromova NV, Golovkin AS, Bortsova MA, Sergushichev A, Sitnikova MY & Kostareva AA. (2019). Skeletal Muscle Resident Progenitor Cells Coexpress Mesenchymal and Myogenic Markers and Are Not Affected by Chronic Heart Failure-Induced Dysregulations. *Stem Cells Int* **2019,** 5690345.

Dungan CM, Figueiredo VC, Wen Y, VonLehmden GL, Zdunek CJ, Thomas NT, Mobley CB, Murach KA, Brightwell CR, Long DE, Fry CS, Kern PA, McCarthy JJ & Peterson CA. (2022). Senolytic treatment rescues blunted muscle hypertrophy in old mice. *Geroscience*.

Dunlay SM, Roger VL & Redfield MM. (2017). Epidemiology of heart failure with preserved ejection fraction. *Nat Rev Cardiol* **14,** 591-602.

Edelmann F, Gelbrich G, Dungen HD, Frohling S, Wachter R, Stahrenberg R, Binder L, Topper A, Lashki DJ, Schwarz S, Herrmann-Lingen C, Loffler M, Hasenfuss G, Halle M & Pieske B. (2011). Exercise training improves exercise capacity and diastolic function in patients with heart failure with preserved ejection fraction: results of the Ex-DHF (Exercise training in Diastolic Heart Failure) pilot study. *Journal of the American College of Cardiology* **58,** 1780-1791.

Edelmann F, Wachter R, Schmidt AG, Kraigher-Krainer E, Colantonio C, Kamke W, Duvinage A, Stahrenberg R, Durstewitz K, Löffler M, Düngen HD, Tschöpe C, Herrmann-Lingen C, Halle M, Hasenfuss G, Gelbrich G & Pieske B. (2013). Effect of spironolactone on diastolic function and exercise capacity in patients with heart failure with preserved ejection fraction: the Aldo-DHF randomized controlled trial. *Jama* **309,** 781-791.

Egginton S. (2011). Physiological factors influencing capillary growth. *Acta physiologica (Oxford, England)* **202,** 225-239.

Egginton S & Hudlicka O. (1999). Early changes in performance, blood flow and capillary fine structure in rat fast muscles induced by electrical stimulation. *The Journal of physiology* **515 (Pt 1),** 265-275.

Egginton S, Hudlická O, Brown MD, Walter H, Weiss JB & Bate A. (1998). Capillary growth in relation to blood flow and performance in overloaded rat skeletal muscle. *J Appl Physiol (1985)* **85,** 2025-2032.

Egner IM, Bruusgaard JC & Gundersen K. (2016). Satellite cell depletion prevents fiber hypertrophy in skeletal muscle. *Development* **143,** 2898-2906.

Elliott JE, Greising SM, Mantilla CB & Sieck GC. (2016). Functional impact of sarcopenia in respiratory muscles. *Respir Physiol Neurobiol* **226,** 137-146.

Engineer A, Albers SS & Kucey AS. (2019). The role of submaximal exercise-induced skeletal muscle remodelling in heart failure with reduced ejection fraction patients. *J Physiol* **597,** 669-671.

Espino-Gonzalez E, Tickle PG, Benson AP, Kissane RWP, Askew GN, Egginton S & Bowen TS. (2020). Abnormal skeletal muscle blood flow, contractile mechanics and fibre morphology in a rat model of obese-HFpEF. *J Physiol*.

Esposito F, Mathieu-Costello O, Wagner PD & Richardson RS. (2018). Acute and chronic exercise in patients with heart failure with reduced ejection fraction: evidence of structural and functional plasticity and intact angiogenic signalling in skeletal muscle. *J Physiol* **596,** 5149-5161.

Faber RM, Hall JK, Chamberlain JS & Banks GB. (2014). Myofiber branching rather than myofiber hyperplasia contributes to muscle hypertrophy in mdx mice. *Skelet Muscle* **4,** 10.

Farkas GA, Gosselin LE, Zhan WZ, Schlenker EH & Sieck GC. (1994). Histochemical and mechanical properties of diaphragm muscle in morbidly obese Zucker rats. *Journal of applied physiology (Bethesda, Md : 1985)* **77,** 2250-2259.

Faxén UL, Hage C, Benson L, Zabarovskaja S, Andreasson A, Donal E, Daubert JC, Linde C, Brismar K & Lund LH. (2017). HFpEF and HFrEF Display Different Phenotypes as Assessed by IGF-1 and IGFBP-1. *J Card Fail* **23,** 293-303.

Fernández-Solà J, Lluis M, Sacanella E, Estruch R, Antúnez E & Urbano-Márquez A. (2011). Increased myostatin activity and decreased myocyte proliferation in chronic alcoholic cardiomyopathy. *Alcohol Clin Exp Res* **35,** 1220-1229.

Ferreira LF, Moylan JS, Gilliam LA, Smith JD, Nikolova-Karakashian M & Reid MB. (2010). Sphingomyelinase stimulates oxidant signaling to weaken skeletal muscle and promote fatigue. *Am J Physiol Cell Physiol* **299,** C552-560.

Fortes MA, Pinheiro CH, Guimarães-Ferreira L, Vitzel KF, Vasconcelos DA & Curi R. (2015). Overload-induced skeletal muscle hypertrophy is not impaired in STZ-diabetic rats. *Physiol Rep* **3**.

Franssen C, Chen S, Unger A, Korkmaz HI, De Keulenaer GW, Tschöpe C, Leite-Moreira AF, Musters R, Niessen HW, Linke WA, Paulus WJ & Hamdani N. (2016). Myocardial Microvascular Inflammatory Endothelial Activation in Heart Failure With Preserved Ejection Fraction. *JACC Heart Fail* **4,** 312-324.

Frischknecht R & Vrbova G. (1991). Adaptation of rat extensor digitorum longus to overload and increased activity. *Pflugers Archiv : European journal of physiology* **419,** 319-326.

Frontera WR & Ochala J. (2015). Skeletal muscle: a brief review of structure and function. *Calcif Tissue Int* **96,** 183-195.

Fu TC, Yang NI, Wang CH, Cherng WJ, Chou SL, Pan TL & Wang JS. (2016). Aerobic Interval Training Elicits Different Hemodynamic Adaptations Between Heart Failure Patients with Preserved and Reduced Ejection Fraction. *Am J Phys Med Rehabil* **95,** 15-27.

Fukuta H, Goto T, Wakami K & Ohte N. (2016). Effects of drug and exercise intervention on functional capacity and quality of life in heart failure with preserved ejection fraction: A meta-analysis of randomized controlled trials. *Eur J Prev Cardiol* **23,** 78-85.

Fulster S, Tacke M, Sandek A, Ebner N, Tschope C, Doehner W, Anker SD & von Haehling S. (2013). Muscle wasting in patients with chronic heart failure: results from the studies investigating co-morbidities aggravating heart failure (SICA-HF). *Eur Heart J* **34,** 512-519.

Gevaert AB, Lemmens K, Vrints CJ & Van Craenenbroeck EM. (2017). Targeting Endothelial Function to Treat Heart Failure with Preserved Ejection Fraction: The Promise of Exercise Training. *Oxid Med Cell Longev* **2017,** 4865756-4865756.

Gielen S, Adams V, Möbius-Winkler S, Linke A, Erbs S, Yu J, Kempf W, Schubert A, Schuler G & Hambrecht R. (2003). Anti-inflammatory effects of exercise training in the skeletal muscle of patients with chronic heart failure. *J Am Coll Cardiol* **42,** 861-868.

Gielen S, Sandri M, Kozarez I, Kratzsch J, Teupser D, Thiery J, Erbs S, Mangner N, Lenk K, Hambrecht R, Schuler G & Adams V. (2012). Exercise training attenuates MuRF-1 expression in the skeletal muscle of patients with chronic heart failure independent of age: the randomized Leipzig Exercise Intervention in Chronic Heart Failure and Aging catabolism study. *Circulation* **125,** 2716-2727.

Gingras AC, Gygi SP, Raught B, Polakiewicz RD, Abraham RT, Hoekstra MF, Aebersold R & Sonenberg N. (1999). Regulation of 4E-BP1 phosphorylation: a novel two-step mechanism. *Genes Dev* **13,** 1422-1437.

Goodman CA. (2014). The role of mTORC1 in regulating protein synthesis and skeletal muscle mass in response to various mechanical stimuli. *Rev Physiol Biochem Pharmacol* **166,** 43-95.

Goodman CA. (2019). Role of mTORC1 in mechanically induced increases in translation and skeletal muscle mass. *J Appl Physiol (1985)* **127,** 581-590.

Gori M, D'Elia E & Senni M. (2019). Sacubitril/valsartan therapeutic strategy in HFpEF: Clinical insights and perspectives. *Int J Cardiol* **281,** 158-165.

Goto K, Schauer A, Augstein A, Methawasin M, Granzier H, Halle M, Craenenbroeck EMV, Rolim N, Gielen S, Pieske B, Winzer EB, Linke A & Adams V. (2020). Muscular changes in animal models of heart failure with preserved ejection fraction: what comes closest to the patient? *ESC Heart Fail*.

Grassi B, Majerczak J, Bardi E, Buso A, Comelli M, Chlopicki S, Guzik M, Mavelli I, Nieckarz Z, Salvadego D, Tyrankiewicz U, Skórka T, Bottinelli R, Zoladz JA & Pellegrino MA. (2017). Exercise training in Tgα(q)*44 mice during the progression of chronic heart failure: cardiac vs. peripheral (soleus muscle) impairments to oxidative metabolism. *J Appl Physiol (1985)* **123,** 326-336.

Greer EL, Oskoui PR, Banko MR, Maniar JM, Gygi MP, Gygi SP & Brunet A. (2007). The energy sensor AMP-activated protein kinase directly regulates the mammalian FOXO3 transcription factor. *J Biol Chem* **282,** 30107-30119.

Grundy D. (2015). Principles and standards for reporting animal experiments in The Journal of Physiology and Experimental Physiology. *J Physiol* **593,** 2547-2549.

Gruson D, Ahn SA, Ketelslegers JM & Rousseau MF. (2011). Increased plasma myostatin in heart failure. *Eur J Heart Fail* **13,** 734-736.

Guazzi M, Borlaug B, Metra M, Losito M, Bandera F, Alfonzetti E, Boveri S & Sugimoto T. (2021). Revisiting and Implementing the Weber and

Ventilatory Functional Classifications in Heart Failure by Cardiopulmonary Imaging Phenotyping. *J Am Heart Assoc* **10,** e018822.

Gutierrez G & Vincent JL. (1991). *Tissue Oxygen Utilization*. Springer-Verlag Berlin Heidelberg, Berlin

Haass M, Kitzman DW, Anand IS, Miller A, Zile MR, Massie BM & Carson PE. (2011). Body mass index and adverse cardiovascular outcomes in heart failure patients with preserved ejection fraction: results from the Irbesartan in Heart Failure with Preserved Ejection Fraction (I-PRESERVE) trial. *Circ Heart Fail* **4,** 324-331.

Ham DJ, Börsch A, Chojnowska K, Lin S, Leuchtmann AB, Ham AS, Thürkauf M, Delezie J, Furrer R, Burri D, Sinnreich M, Handschin C, Tintignac LA, Zavolan M, Mittal N & Rüegg MA. (2022). Distinct and additive effects of calorie restriction and rapamycin in aging skeletal muscle. *Nat Commun* **13,** 2025.

Hamazaki N, Kamiya K, Matsuzawa R, Nozaki K, Ichikawa T, Tanaka S, Nakamura T, Yamashita M, Maekawa E, Noda C, Yamaoka-Tojo M, Matsunaga A, Masuda T & Ako J. (2020). Prevalence and prognosis of respiratory muscle weakness in heart failure patients with preserved ejection fraction. *Respir Med* **161,** 105834.

Hamdani N, Franssen C, Lourenço A, Falcão-Pires I, Fontoura D, Leite S, Plettig L, López B, Ottenheijm CA, Becher PM, González A, Tschöpe C, Díez J, Linke WA, Leite-Moreira AF & Paulus WJ. (2013). Myocardial titin hypophosphorylation importantly contributes to heart failure with preserved ejection fraction in a rat metabolic risk model. *Circ Heart Fail* **6,** 1239-1249.

Han HQ & Mitch WE. (2011). Targeting the myostatin signaling pathway to treat muscle wasting diseases. *Current opinion in supportive and palliative care* **5,** 334-341.

Hannan KM, Brandenburger Y, Jenkins A, Sharkey K, Cavanaugh A, Rothblum L, Moss T, Poortinga G, McArthur GA, Pearson RB & Hannan RD. (2003). mTOR-dependent regulation of ribosomal gene transcription requires S6K1 and is mediated by phosphorylation of the carboxy-terminal activation domain of the nucleolar transcription factor UBF. *Mol Cell Biol* **23,** 8862-8877.

Hara K, Yonezawa K, Kozlowski MT, Sugimoto T, Andrabi K, Weng QP, Kasuga M, Nishimoto I & Avruch J. (1997). Regulation of eIF-4E BP1 phosphorylation by mTOR. *J Biol Chem* **272,** 26457-26463.

Haun CT, Vann CG, Roberts BM, Vigotsky AD, Schoenfeld BJ & Roberts MD. (2019). A Critical Evaluation of the Biological Construct Skeletal Muscle

Hypertrophy: Size Matters but So Does the Measurement. *Front Physiol* **10,** 247.

Haykowsky MJ, Brubaker PH, John JM, Stewart KP, Morgan TM & Kitzman DW. (2011). Determinants of exercise intolerance in elderly heart failure patients with preserved ejection fraction. *Journal of the American College of Cardiology* **58,** 265-274.

Haykowsky MJ, Brubaker PH, Morgan TM, Kritchevsky S, Eggebeen J & Kitzman DW. (2013a). Impaired aerobic capacity and physical functional performance in older heart failure patients with preserved ejection fraction: role of lean body mass. *The journals of gerontology Series A, Biological sciences and medical sciences* **68,** 968-975.

Haykowsky MJ, Brubaker PH, Stewart KP, Morgan TM, Eggebeen J & Kitzman DW. (2012). Effect of endurance training on the determinants of peak exercise oxygen consumption in elderly patients with stable compensated heart failure and preserved ejection fraction. *J Am Coll Cardiol* **60,** 120-128.

Haykowsky MJ, Herrington DM, Brubaker PH, Morgan TM, Hundley WG & Kitzman DW. (2013b). Relationship of flow-mediated arterial dilation and exercise capacity in older patients with heart failure and preserved ejection fraction. *J Gerontol A Biol Sci Med Sci* **68,** 161-167.

Haykowsky MJ & Kitzman DW. (2014). Exercise physiology in heart failure and preserved ejection fraction. *Heart Fail Clin* **10,** 445-452.

Haykowsky MJ, Kouba EJ, Brubaker PH, Nicklas BJ, Eggebeen J & Kitzman DW. (2014). Skeletal muscle composition and its relation to exercise intolerance in older patients with heart failure and preserved ejection fraction. *Am J Cardiol* **113,** 1211-1216.

Hearon CM, Jr., Samels M, Dias KA, MacNamara JP, Levine BD & Sarma S. (2022). Isolated knee extensor exercise training improves skeletal muscle vasodilation, blood flow, and functional capacity in patients with HFpEF. *Physiol Rep* **10,** e15419.

Heidenreich PA, Bozkurt B, Aguilar D, Allen LA, Byun JJ, Colvin MM, Deswal A, Drazner MH, Dunlay SM, Evers LR, Fang JC, Fedson SE, Fonarow GC, Hayek SS, Hernandez AF, Khazanie P, Kittleson MM, Lee CS, Link MS, Milano CA, Nnacheta LC, Sandhu AT, Stevenson LW, Vardeny O, Vest AR & Yancy CW. (2022). 2022 AHA/ACC/HFSA Guideline for the Management of Heart Failure: Executive Summary: A Report of the American College of Cardiology/American Heart Association Joint Committee on Clinical Practice Guidelines. *Circulation* **145,** e876-e894.

Heineke J, Auger-Messier M, Xu J, Sargent M, York A, Welle S & Molkentin JD. (2010). Genetic deletion of myostatin from the heart prevents skeletal muscle atrophy in heart failure. *Circulation* **121,** 419-425.

Hernández N, Torres SH, Finol HJ, Sosa A & Cierco M. (1996). Capillary and muscle fiber type changes in DOCA-salt hypertensive rats. *Anat Rec* **246,** 208-216.

Hodson N, West DWD, Philp A, Burd NA & Moore DR. (2019). Molecular regulation of human skeletal muscle protein synthesis in response to exercise and nutrients: a compass for overcoming age-related anabolic resistance. *Am J Physiol Cell Physiol* **317,** C1061-c1078.

Houstis NE, Eisman AS, Pappagianopoulos PP, Wooster L, Bailey CS, Wagner PD & Lewis GD. (2018). Exercise Intolerance in Heart Failure With Preserved Ejection Fraction: Diagnosing and Ranking Its Causes Using Personalized O(2) Pathway Analysis. *Circulation* **137,** 148-161.

Hudlická O, Brown M, Cotter M, Smith M & Vrbová G. (1977). The effect of long-term stimulation of fast muscles on their blood flow, metabolism and ability to withstand fatigue. *Pflügers Archiv* **369,** 141-149.

Hultman E. (1995). Fuel selection, muscle fibre. *Proc Nutr Soc* **54,** 107-121.

Hundley WG, Bayram E, Hamilton CA, Hamilton EA, Morgan TM, Darty SN, Stewart KP, Link KM, Herrington DM & Kitzman DW. (2007). Leg flow-mediated arterial dilation in elderly patients with heart failure and normal left ventricular ejection fraction. *Am J Physiol Heart Circ Physiol* **292,** H1427-1434.

Hwee DT & Bodine SC. (2009). Age-related deficit in load-induced skeletal muscle growth. *J Gerontol A Biol Sci Med Sci* **64,** 618-628.

Hyatt HW & Powers SK. (2021). Mitochondrial Dysfunction Is a Common Denominator Linking Skeletal Muscle Wasting Due to Disease, Aging, and Prolonged Inactivity. *Antioxidants (Basel)* **10**.

Ianuzzo CD & Chen V. (1979). Metabolic character of hypertrophied rat muscle. *J Appl Physiol Respir Environ Exerc Physiol* **46,** 738-742.

Isaacs ER, Bradley WG & Henderson G. (1973). Longitudinal fibre splitting in muscular dystrophy: a serial cinematographic study. *J Neurol Neurosurg Psychiatry* **36,** 813-819.

Jasuja R & LeBrasseur NK. (2014). Regenerating skeletal muscle in the face of aging and disease. *Am J Phys Med Rehabil* **93,** S88-96.

Jiang WL, Gu HB, Zhang YF, Xia QQ, Qi J & Chen JC. (2016). Vitamin D Supplementation in the Treatment of Chronic Heart Failure: A Meta-analysis of Randomized Controlled Trials. *Clinical cardiology* **39,** 56-61.

Josephson RK. (1985). Mechanical Power output from Striated Muscle during Cyclic Contraction. *Journal of Experimental Biology* **114,** 493-512.

Kalogeropoulos A, Georgiopoulou V, Psaty BM, Rodondi N, Smith AL, Harrison DG, Liu Y, Hoffmann U, Bauer DC, Newman AB, Kritchevsky SB, Harris TB, Butler J & Health ABCSI. (2010). Inflammatory markers and incident heart failure risk in older adults: the Health ABC (Health, Aging, and Body Composition) study. *J Am Coll Cardiol* **55,** 2129-2137.

Karatzaferi C, Sandri M, Sakkas GK & Smith C. (2019). Effects of Redox Disturbances on Motility, Contractility and Muscle Tissue Pathogenesis. *Oxid Med Cell Longev* **2019,** 3272035.

Katta A, Kundla S, Kakarla SK, Wu M, Fannin J, Paturi S, Liu H, Addagarla HS & Blough ER. (2010). Impaired overload-induced hypertrophy is associated with diminished mTOR signaling in insulin-resistant skeletal muscle of the obese Zucker rat. *Am J Physiol Regul Integr Comp Physiol* **299,** R1666-1675.

Kelley RC, Betancourt L, Noriega AM, Brinson SC, Curbelo-Bermudez N, Hahn D, Kumar RA, Balazic E, Muscato DR, Ryan TE, van der Pijl RJ, Shen S, Ottenheijm CAC & Ferreira LF. (2022). Skeletal myopathy in a rat model of postmenopausal heart failure with preserved ejection fraction. *J Appl Physiol (1985)* **132,** 106-125.

Kennel PJ, Mancini DM & Schulze PC. (2015). Skeletal Muscle Changes in Chronic Cardiac Disease and Failure. *Compr Physiol* **5,** 1947-1969.

Kim MN & Park SM. (2021). Current Status of Pharmacologic and Nonpharmacologic Therapy in Heart Failure with Preserved Ejection Fraction. *Heart Fail Clin* **17,** 463-482.

Kinugasa Y & Yamamoto K. (2017). The challenge of frailty and sarcopenia in heart failure with preserved ejection fraction. *Heart* **103,** 184-189.

Kishimoto S, Kajikawa M, Maruhashi T, Iwamoto Y, Matsumoto T, Iwamoto A, Oda N, Matsui S, Hidaka T, Kihara Y, Chayama K, Goto C, Aibara Y, Nakashima A, Noma K & Higashi Y. (2017). Endothelial dysfunction and abnormal vascular structure are simultaneously present in patients with heart failure with preserved ejection fraction. *Int J Cardiol* **231,** 181-187.

Kissane RWP, Egginton S & Askew GN. (2018). Regional variation in the mechanical properties and fibre-type composition of the rat extensor digitorum longus muscle. *Exp Physiol* **103,** 111-124.

Kitzman DW, Brubaker P, Morgan T, Haykowsky M, Hundley G, Kraus WE, Eggebeen J & Nicklas BJ. (2016). Effect of Caloric Restriction or Aerobic Exercise Training on Peak Oxygen Consumption and Quality of Life in Obese Older Patients With Heart Failure With Preserved Ejection Fraction: A Randomized Clinical Trial. *Jama* **315,** 36-46.

Kitzman DW, Brubaker PH, Morgan TM, Stewart KP & Little WC. (2010). Exercise training in older patients with heart failure and preserved ejection fraction: a randomized, controlled, single-blind trial. *Circulation Heart failure* **3,** 659-667.

Kitzman DW, Nicklas B, Kraus WE, Lyles MF, Eggebeen J, Morgan TM & Haykowsky M. (2014). Skeletal muscle abnormalities and exercise intolerance in older patients with heart failure and preserved ejection fraction. *Am J Physiol Heart Circ Physiol* **306,** H1364-1370.

Lam CSP, Voors AA, de Boer RA, Solomon SD & van Veldhuisen DJ. (2018). Heart failure with preserved ejection fraction: from mechanisms to therapies. *Eur Heart J* **39,** 2780-2792.

Lanza IR, Zabielski P, Klaus KA, Morse DM, Heppelmann CJ, Bergen HR, 3rd, Dasari S, Walrand S, Short KR, Johnson ML, Robinson MM, Schimke JM, Jakaitis DR, Asmann YW, Sun Z & Nair KS. (2012). Chronic caloric restriction preserves mitochondrial function in senescence without increasing mitochondrial biogenesis. *Cell Metab* **16,** 777-788.

Larsen S, Nielsen J, Hansen CN, Nielsen LB, Wibrand F, Stride N, Schroder HD, Boushel R, Helge JW, Dela F & Hey-Mogensen M. (2012). Biomarkers of mitochondrial content in skeletal muscle of healthy young human subjects. *The Journal of physiology* **590,** 3349-3360.

Lavietes MH, Gerula CM, Fless KG, Cherniack NS & Arora RR. (2004). Inspiratory muscle weakness in diastolic dysfunction. *Chest* **126,** 838-844.

Lee JF, Barrett-O'Keefe Z, Garten RS, Nelson AD, Ryan JJ, Nativi JN, Richardson RS & Wray DW. (2016a). Evidence of microvascular dysfunction in heart failure with preserved ejection fraction. *Heart* **102,** 278-284.

Lee JF, Barrett-O'Keefe Z, Nelson AD, Garten RS, Ryan JJ, Nativi-Nicolau JN, Richardson RS & Wray DW. (2016b). Impaired skeletal muscle vasodilation during exercise in heart failure with preserved ejection fraction. *International journal of cardiology* **211,** 14-21.

Leite S, Oliveira-Pinto J, Tavares-Silva M, Abdellatif M, Fontoura D, Falcão-Pires I, Leite-Moreira AF & Lourenço AP. (2015). Echocardiography and invasive hemodynamics during stress testing for diagnosis of heart failure with preserved ejection fraction: an experimental study. *Am J Physiol Heart Circ Physiol* **308,** H1556-1563.

Lenk K, Erbs S, Höllriegel R, Beck E, Linke A, Gielen S, Winkler SM, Sandri M, Hambrecht R, Schuler G & Adams V. (2012). Exercise training leads to a reduction of elevated myostatin levels in patients with chronic heart failure. *Eur J Prev Cardiol* **19,** 404-411.

Li P, Waters RE, Redfern SI, Zhang M, Mao L, Annex BH & Yan Z. (2007). Oxidative phenotype protects myofibers from pathological insults induced by chronic heart failure in mice. *Am J Pathol* **170,** 599-608.

Lin J, Wu H, Tarr PT, Zhang CY, Wu Z, Boss O, Michael LF, Puigserver P, Isotani E, Olson EN, Lowell BB, Bassel-Duby R & Spiegelman BM. (2002). Transcriptional co-activator PGC-1 alpha drives the formation of slow-twitch muscle fibres. *Nature* **418,** 797-801.

Liu F, Fry CS, Mula J, Jackson JR, Lee JD, Peterson CA & Yang L. (2013). Automated fiber-type-specific cross-sectional area assessment and myonuclei counting in skeletal muscle. *J Appl Physiol (1985)* **115,** 1714-1724.

Liu GY & Sabatini DM. (2020). mTOR at the nexus of nutrition, growth, ageing and disease. *Nat Rev Mol Cell Biol* **21,** 183-203.

Loai S, Zhou YQ, Vollett KDW & Cheng HM. (2021). Skeletal Muscle Microvascular Dysfunction Manifests Early in Diabetic Cardiomyopathy. *Front Cardiovasc Med* **8,** 715400.

Lowe DA & Alway SE. (1999). Stretch-induced myogenin, MyoD, and MRF4 expression and acute hypertrophy in quail slow-tonic muscle are not dependent upon satellite cell proliferation. *Cell Tissue Res* **296,** 531-539.

Lowe DA & Alway SE. (2002). Animal models for inducing muscle hypertrophy: are they relevant for clinical applications in humans? *The Journal of orthopaedic and sports physical therapy* **32,** 36-43.

Marechaux S, Samson R, van Belle E, Breyne J, de Monte J, Dedrie C, Chebai N, Menet A, Banfi C, Bouabdallaoui N, Le Jemtel TH & Ennezat PV. (2016). Vascular and Microvascular Endothelial Function in Heart Failure With Preserved Ejection Fraction. *J Card Fail* **22,** 3-11.

Maréchaux S, Samson R, van Belle E, Breyne J, de Monte J, Dédrie C, Chebai N, Menet A, Banfi C, Bouabdallaoui N, Le Jemtel TH & Ennezat PV. (2016). Vascular and Microvascular Endothelial Function in Heart Failure With Preserved Ejection Fraction. *J Card Fail* **22,** 3-11.

Margolis LM, Rivas DA, Berrone M, Ezzyat Y, Young AJ, McClung JP, Fielding RA & Pasiakos SM. (2016). Prolonged Calorie Restriction Downregulates Skeletal Muscle mTORC1 Signaling Independent of Dietary Protein Intake and Associated microRNA Expression. *Front Physiol* **7,** 445.

Marsh RL & Bennett AF. (1986). Thermal dependence of contractile properties of skeletal muscle from the lizard Sceloporus occidentalis with comments on methods for fitting and comparing force-velocity curves. *J Exp Biol* **126,** 63-77.

Maskin CS, Forman R, Sonnenblick EH, Frishman WH & LeJemtel TH. (1983). Failure of dobutamine to increase exercise capacity despite hemodynamic improvement in severe chronic heart failure. *Am J Cardiol* **51,** 177-182.

Massie BM, Carson PE, McMurray JJ, Komajda M, McKelvie R, Zile MR, Anderson S, Donovan M, Iverson E, Staiger C & Ptaszynska A. (2008). Irbesartan in patients with heart failure and preserved ejection fraction. *N Engl J Med* **359,** 2456-2467.

Matsumura K, Teranaka W, Matsumoto H, Fujii K, Tsujimoto S, Otagaki M, Morishita S, Hashimoto K, Shibutani H, Yamamoto Y & Shiojima I. (2020). Loss of skeletal muscle mass predicts cardiac death in heart failure with a preserved ejection fraction but not heart failure with a reduced ejection fraction. *ESC Heart Fail* **7,** 4100-4107.

Max SR. (1972). Disuse atrophy of skeletal muscle: loss of functional activity of mitochondria. *Biochem Biophys Res Commun* **46,** 1394-1398.

Mayer C, Zhao J, Yuan X & Grummt I. (2004). mTOR-dependent activation of the transcription factor TIF-IA links rRNA synthesis to nutrient availability. *Genes Dev* **18,** 423-434.

McCarthy JJ & Esser KA. (2007). Counterpoint: Satellite cell addition is not obligatory for skeletal muscle hypertrophy. *J Appl Physiol (1985)* **103,** 1100-1102; discussion 1102-1103.

McDonagh STJ, Wylie LJ, Thompson C, Vanhatalo A & Jones AM. (2019). Potential benefits of dietary nitrate ingestion in healthy and clinical populations: A brief review. *European journal of sport science* **19,** 15-29.

McDonagh TA, Metra M, Adamo M, Gardner RS, Baumbach A, Böhm M, Burri H, Butler J, Čelutkienė J, Chioncel O, Cleland JGF, Coats AJS, Crespo-Leiro

MG, Farmakis D, Gilard M, Heymans S, Hoes AW, Jaarsma T, Jankowska EA, Lainscak M, Lam CSP, Lyon AR, McMurray JJV, Mebazaa A, Mindham R, Muneretto C, Francesco Piepoli M, Price S, Rosano GMC, Ruschitzka F & Kathrine Skibelund A. (2021). 2021 ESC Guidelines for the diagnosis and treatment of acute and chronic heart failure. *Eur Heart J* **42,** 3599-3726.

McHugh K, DeVore AD, Wu J, Matsouaka RA, Fonarow GC, Heidenreich PA, Yancy CW, Green JB, Altman N & Hernandez AF. (2019). Heart Failure With Preserved Ejection Fraction and Diabetes: JACC State-of-the-Art Review. *Journal of the American College of Cardiology* **73,** 602-611.

McMurray JJ, Ostergren J, Swedberg K, Granger CB, Held P, Michelson EL, Olofsson B, Yusuf S & Pfeffer MA. (2003). Effects of candesartan in patients with chronic heart failure and reduced left-ventricular systolic function taking angiotensin-converting-enzyme inhibitors: the CHARM-Added trial. *Lancet* **362,** 767-771.

McMurray JJ, Packer M, Desai AS, Gong J, Lefkowitz MP, Rizkala AR, Rouleau JL, Shi VC, Solomon SD, Swedberg K & Zile MR. (2014). Angiotensin-neprilysin inhibition versus enalapril in heart failure. *N Engl J Med* **371,** 993-1004.

Mehra MR, Lavie CJ, Ventura HO & Milani RV. (2006). Fish oils produce anti-inflammatory effects and improve body weight in severe heart failure. *J Heart Lung Transplant* **25,** 834-838.

Metra M & Teerlink JR. (2017). Heart failure. *Lancet* **390,** 1981-1995.

Meyer FJ, Borst MM, Zugck C, Kirschke A, Schellberg D, Kubler W & Haass M. (2001). Respiratory muscle dysfunction in congestive heart failure: clinical correlation and prognostic significance. *Circulation* **103,** 2153-2158.

Michels AA, Robitaille AM, Buczynski-Ruchonnet D, Hodroj W, Reina JH, Hall MN & Hernandez N. (2010). mTORC1 directly phosphorylates and regulates human MAF1. *Mol Cell Biol* **30,** 3749-3757.

Miller MS, VanBuren P, LeWinter MM, Braddock JM, Ades PA, Maughan DW, Palmer BM & Toth MJ. (2010). Chronic heart failure decreases cross-bridge kinetics in single skeletal muscle fibres from humans. *J Physiol* **588,** 4039-4053.

Miller MS, Vanburen P, Lewinter MM, Lecker SH, Selby DE, Palmer BM, Maughan DW, Ades PA & Toth MJ. (2009). Mechanisms underlying skeletal muscle weakness in human heart failure: alterations in single fiber myosin protein content and function. *Circ Heart Fail* **2,** 700-706.

Mishra S & Kass DA. (2021a). Cellular and molecular pathobiology of heart failure with preserved ejection fraction. *Nat Rev Cardiol*.

Mishra S & Kass DA. (2021b). Cellular and molecular pathobiology of heart failure with preserved ejection fraction. *Nat Rev Cardiol* **18,** 400-423.

Mitchell SJ, Madrigal-Matute J, Scheibye-Knudsen M, Fang E, Aon M, González-Reyes JA, Cortassa S, Kaushik S, Gonzalez-Freire M, Patel B, Wahl D, Ali A, Calvo-Rubio M, Burón MI, Guiterrez V, Ward TM, Palacios HH, Cai H, Frederick DW, Hine C, Broeskamp F, Habering L, Dawson J, Beasley TM, Wan J, Ikeno Y, Hubbard G, Becker KG, Zhang Y, Bohr VA, Longo DL, Navas P, Ferrucci L, Sinclair DA, Cohen P, Egan JM, Mitchell JR, Baur JA, Allison DB, Anson RM, Villalba JM, Madeo F, Cuervo AM, Pearson KJ, Ingram DK, Bernier M & de Cabo R. (2016). Effects of Sex, Strain, and Energy Intake on Hallmarks of Aging in Mice. *Cell Metab* **23,** 1093-1112.

Miyagi M, Kinugasa Y, Sota T, Yamada K, Ishisugi T, Hirai M, Yanagihara K, Haruki N, Matsubara K, Kato M & Yamamoto K. (2018). Diaphragm Muscle Dysfunction in Patients With Heart Failure. *J Card Fail* **24,** 209-216.

Mohammed SF, Borlaug BA, McNulty S, Lewis GD, Lin G, Zakeri R, Semigran MJ, LeWinter M, Hernandez AF, Braunwald E & Redfield MM. (2014). Resting ventricular-vascular function and exercise capacity in heart failure with preserved ejection fraction: a RELAX trial ancillary study. *Circ Heart Fail* **7,** 580-589.

Molina AJ, Bharadwaj MS, Van Horn C, Nicklas BJ, Lyles MF, Eggebeen J, Haykowsky MJ, Brubaker PH & Kitzman DW. (2016). Skeletal Muscle Mitochondrial Content, Oxidative Capacity, and Mfn2 Expression Are Reduced in Older Patients With Heart Failure and Preserved Ejection Fraction and Are Related to Exercise Intolerance. *JACC Heart Fail* **4,** 636-645.

Moro T, Brightwell CR, Phalen DE, McKenna CF, Lane SJ, Porter C, Volpi E, Rasmussen BB & Fry CS. (2019). Low skeletal muscle capillarization limits muscle adaptation to resistance exercise training in older adults. *Exp Gerontol* **127,** 110723.

Mourkioti F & Rosenthal N. (2008). NF-kappaB signaling in skeletal muscle: prospects for intervention in muscle diseases. *Journal of molecular medicine (Berlin, Germany)* **86,** 747-759.

Murach KA, Dungan CM, Peterson CA & McCarthy JJ. (2019). Muscle Fiber Splitting Is a Physiological Response to Extreme Loading in Animals. *Exerc Sport Sci Rev* **47,** 108-115.

Murach KA, Fry CS, Dupont-Versteegden EE, McCarthy JJ & Peterson CA. (2021). Fusion and beyond: Satellite cell contributions to loading-induced skeletal muscle adaptation. *Faseb j* **35,** e21893.

Nadruz W, Jr., West E, Sengelov M, Santos M, Groarke JD, Forman DE, Claggett B, Skali H & Shah AM. (2017). Prognostic Value of Cardiopulmonary Exercise Testing in Heart Failure With Reduced, Midrange, and Preserved Ejection Fraction. *J Am Heart Assoc* **6**.

Nagaya N, Moriya J, Yasumura Y, Uematsu M, Ono F, Shimizu W, Ueno K, Kitakaze M, Miyatake K & Kangawa K. (2004). Effects of ghrelin administration on left ventricular function, exercise capacity, and muscle wasting in patients with chronic heart failure. *Circulation* **110,** 3674-3679.

Nassif ME, Windsor SL, Borlaug BA, Kitzman DW, Shah SJ, Tang F, Khariton Y, Malik AO, Khumri T, Umpierrez G, Lamba S, Sharma K, Khan SS, Chandra L, Gordon RA, Ryan JJ, Chaudhry SP, Joseph SM, Chow CH, Kanwar MK, Pursley M, Siraj ES, Lewis GD, Clemson BS, Fong M & Kosiborod MN. (2021). The SGLT2 inhibitor dapagliflozin in heart failure with preserved ejection fraction: a multicenter randomized trial. *Nat Med* **27,** 1954-1960.

Nyitrai M, Rossi R, Adamek N, Pellegrino MA, Bottinelli R & Geeves MA. (2006). What limits the velocity of fast-skeletal muscle contraction in mammals? *J Mol Biol* **355,** 432-442.

Obokata M, Reddy YNV, Pislaru SV, Melenovsky V & Borlaug BA. (2017). Evidence Supporting the Existence of a Distinct Obese Phenotype of Heart Failure With Preserved Ejection Fraction. *Circulation* **136,** 6-19.

Owan TE, Hodge DO, Herges RM, Jacobsen SJ, Roger VL & Redfield MM. (2006). Trends in prevalence and outcome of heart failure with preserved ejection fraction. *The New England journal of medicine* **355,** 251-259.

Pandey A, Parashar A, Kumbhani D, Agarwal S, Garg J, Kitzman D, Levine B, Drazner M & Berry J. (2015). Exercise training in patients with heart failure and preserved ejection fraction: meta-analysis of randomized control trials. *Circulation Heart failure* **8,** 33-40.

Paturi S, Gutta AK, Kakarla SK, Katta A, Arnold EC, Wu M, Rice KM & Blough ER. (2010). Impaired overload-induced hypertrophy in obese Zucker rat slow-twitch skeletal muscle. *J Appl Physiol (1985)* **108,** 7-13.

Paudyal A, Slevin M, Maas H & Degens H. (2018). Time course of denervation-induced changes in gastrocnemius muscles of adult and old rats. *Exp Gerontol* **106,** 165-172.

Paulus WJ & Tschöpe C. (2013). A novel paradigm for heart failure with preserved ejection fraction: comorbidities drive myocardial dysfunction and remodeling through coronary microvascular endothelial inflammation. *J Am Coll Cardiol* **62,** 263-271.

Paulussen KJM, McKenna CF, Beals JW, Wilund KR, Salvador AF & Burd NA. (2021). Anabolic Resistance of Muscle Protein Turnover Comes in Various Shapes and Sizes. *Front Nutr* **8,** 615849.

Pereira MG, Dyar KA, Nogara L, Solagna F, Marabita M, Baraldo M, Chemello F, Germinario E, Romanello V, Nolte H & Blaauw B. (2017). Comparative Analysis of Muscle Hypertrophy Models Reveals Divergent Gene Transcription Profiles and Points to Translational Regulation of Muscle Growth through Increased mTOR Signaling. *Front Physiol* **8,** 968.

Petrella JK, Kim JS, Cross JM, Kosek DJ & Bamman MM. (2006). Efficacy of myonuclear addition may explain differential myofiber growth among resistance-trained young and older men and women. *Am J Physiol Endocrinol Metab* **291,** E937-946.

Petrella JK, Kim JS, Mayhew DL, Cross JM & Bamman MM. (2008). Potent myofiber hypertrophy during resistance training in humans is associated with satellite cell-mediated myonuclear addition: a cluster analysis. *J Appl Physiol (1985)* **104,** 1736-1742.

Phillips SM. (2014). A brief review of critical processes in exercise-induced muscular hypertrophy. *Sports Med* **44 Suppl 1,** S71-77.

Pitt B, Pfeffer MA, Assmann SF, Boineau R, Anand IS, Claggett B, Clausell N, Desai AS, Diaz R, Fleg JL, Gordeev I, Harty B, Heitner JF, Kenwood CT, Lewis EF, O'Meara E, Probstfield JL, Shaburishvili T, Shah SJ, Solomon SD, Sweitzer NK, Yang S & McKinlay SM. (2014). Spironolactone for heart failure with preserved ejection fraction. *N Engl J Med* **370,** 1383-1392.

Pitt B, Zannad F, Remme WJ, Cody R, Castaigne A, Perez A, Palensky J & Wittes J. (1999). The effect of spironolactone on morbidity and mortality in patients with severe heart failure. Randomized Aldactone Evaluation Study Investigators. *N Engl J Med* **341,** 709-717.

Ponikowski P, Voors AA, Anker SD, Bueno H, Cleland JG, Coats AJ, Falk V, Gonzalez-Juanatey JR, Harjola VP, Jankowska EA, Jessup M, Linde C, Nihoyannopoulos P, Parissis JT, Pieske B, Riley JP, Rosano GM, Ruilope LM, Ruschitzka F, Rutten FH, van der Meer P, Authors/Task Force M & Document R. (2016). 2016 ESC Guidelines for the diagnosis and treatment of acute and chronic heart failure: The Task Force for the diagnosis and treatment of acute and chronic heart failure of the European Society of Cardiology (ESC). Developed with the special contribution of

the Heart Failure Association (HFA) of the ESC. *Eur J Heart Fail* **18,** 891-975.

Poole DC, Hirai DM, Copp SW & Musch TI. (2012). Muscle oxygen transport and utilization in heart failure: implications for exercise (in)tolerance. *Am J Physiol Heart Circ Physiol* **302,** H1050-1063.

Poole DC, Richardson RS, Haykowsky MJ, Hirai DM & Musch TI. (2018). Exercise limitations in heart failure with reduced and preserved ejection fraction. *J Appl Physiol (1985)* **124,** 208-224.

Powers SK, Farkas GA, Demirel H, Coombes J, Fletcher L, Hughes MG, Hodge K, Dodd SL & Schlenker EH. (1996). Effects of aging and obesity on respiratory muscle phenotype in Zucker rats. *Journal of applied physiology (Bethesda, Md : 1985)* **81,** 1347-1354.

Ramamurthy B, Höök P & Larsson L. (1999). An overview of carbohydrate-protein interactions with specific reference to myosin and ageing. *Acta Physiol Scand* **167,** 327-329.

Ratchford SM, Lee JF, Bunsawat K, Alpenglow JK, Zhao J, Ma CL, Ryan JJ, Khor LL & Wray DW. (2022). The impact of obesity on the regulation of muscle blood flow during exercise in patients with heart failure with a preserved ejection fraction. *J Appl Physiol (1985)* **132,** 1240-1249.

Rider OJ, Francis JM, Tyler D, Byrne J, Clarke K & Neubauer S. (2013). Effects of weight loss on myocardial energetics and diastolic function in obesity. *Int J Cardiovasc Imaging* **29,** 1043-1050.

Romanello V, Guadagnin E, Gomes L, Roder I, Sandri C, Petersen Y, Milan G, Masiero E, Del Piccolo P, Foretz M, Scorrano L, Rudolf R & Sandri M. (2010). Mitochondrial fission and remodelling contributes to muscle atrophy. *Embo j* **29,** 1774-1785.

Rosca MG & Hoppel CL. (2013). Mitochondrial dysfunction in heart failure. *Heart Fail Rev* **18,** 607-622.

Rosenblatt JD & Parry DJ. (1992). Gamma irradiation prevents compensatory hypertrophy of overloaded mouse extensor digitorum longus muscle. *J Appl Physiol (1985)* **73,** 2538-2543.

Rosenblatt JD & Parry DJ. (1993). Adaptation of rat extensor digitorum longus muscle to gamma irradiation and overload. *Pflugers Arch* **423,** 255-264.

Rosenblatt JD, Yong D & Parry DJ. (1994). Satellite cell activity is required for hypertrophy of overloaded adult rat muscle. *Muscle Nerve* **17,** 608-613.

Ruiz JR, Sui X, Lobelo F, Morrow JR, Jr., Jackson AW, Sjöström M & Blair SN. (2008). Association between muscular strength and mortality in men: prospective cohort study. *Bmj* **337,** a439.

Sandri M. (2013). Protein breakdown in muscle wasting: role of autophagy-lysosome and ubiquitin-proteasome. *Int J Biochem Cell Biol* **45,** 2121-2129.

Sandri M, Lin J, Handschin C, Yang W, Arany ZP, Lecker SH, Goldberg AL & Spiegelman BM. (2006). PGC-1alpha protects skeletal muscle from atrophy by suppressing FoxO3 action and atrophy-specific gene transcription. *Proc Natl Acad Sci U S A* **103,** 16260-16265.

Santos M, Opotowsky AR, Shah AM, Tracy J, Waxman AB & Systrom DM. (2015). Central cardiac limit to aerobic capacity in patients with exertional pulmonary venous hypertension: implications for heart failure with preserved ejection fraction. *Circ Heart Fail* **8,** 278-285.

Schauer A, Adams V, Augstein A, Jannasch A, Draskowski R, Kirchhoff V, Goto K, Mittag J, Galli R, Männel A, Barthel P, Linke A & Winzer EB. (2021). Sacubitril/Valsartan Improves Diastolic Function But Not Skeletal Muscle Function in a Rat Model of HFpEF. *Int J Mol Sci* **22**.

Schauer A, Draskowski R, Jannasch A, Kirchhoff V, Goto K, Männel A, Barthel P, Augstein A, Winzer E, Tugtekin M, Labeit S, Linke A & Adams V. (2020). ZSF1 rat as animal model for HFpEF: Development of reduced diastolic function and skeletal muscle dysfunction. *ESC Heart Fail*.

Schiaffino S, Dyar KA, Ciciliot S, Blaauw B & Sandri M. (2013). Mechanisms regulating skeletal muscle growth and atrophy. *Febs j* **280,** 4294-4314.

Schiaffino S & Reggiani C. (2011). Fiber types in mammalian skeletal muscles. *Physiol Rev* **91,** 1447-1531.

Schiattarella GG, Altamirano F, Tong D, French KM, Villalobos E, Kim SY, Luo X, Jiang N, May HI, Wang ZV, Hill TM, Mammen PPA, Huang J, Lee DI, Hahn VS, Sharma K, Kass DA, Lavandero S, Gillette TG & Hill JA. (2019). Nitrosative stress drives heart failure with preserved ejection fraction. *Nature* **568,** 351-356.

Schmalbruch H. (1984). Regenerated muscle fibers in Duchenne muscular dystrophy: a serial section study. *Neurology* **34,** 60-65.

Schmederer Z, Rolim N, Bowen TS, Linke A, Wisloff U & Adams V. (2018). Endothelial function is disturbed in a hypertensive diabetic animal model of HFpEF: Moderate continuous vs. high intensity interval training. *Int J Cardiol* **273,** 147-154.

Scrutinio D, Lagioia R, Ricci A, Clemente M, Boni L & Rizzon P. (1994). Prediction of mortality in mild to moderately symptomatic patients with left ventricular dysfunction. The role of the New York Heart Association classification, cardiopulmonary exercise testing, two-dimensional echocardiography and Holter monitoring. *Eur Heart J* **15,** 1089-1095.

Seiler M, Bowen TS, Rolim N, Dieterlen MT, Werner S, Hoshi T, Fischer T, Mangner N, Linke A, Schuler G, Halle M, Wisloff U & Adams V. (2016). Skeletal Muscle Alterations Are Exacerbated in Heart Failure With Reduced Compared With Preserved Ejection Fraction: Mediated by Circulating Cytokines? *Circ Heart Fail* **9**.

Sente T, Van Berendoncks AM, Jonckheere AI, Rodenburg RJ, Lauwers P, Van Hoof V, Wouters A, Lardon F, Hoymans VY & Vrints CJ. (2016). Primary skeletal muscle myoblasts from chronic heart failure patients exhibit loss of anti-inflammatory and proliferative activity. *BMC Cardiovasc Disord* **16,** 107.

Shah SJ, Kitzman DW, Borlaug BA, van Heerebeek L, Zile MR, Kass DA & Paulus WJ. (2016). Phenotype-Specific Treatment of Heart Failure With Preserved Ejection Fraction: A Multiorgan Roadmap. *Circulation* **134,** 73-90.

Sharma K & Kass DA. (2014). Heart failure with preserved ejection fraction: mechanisms, clinical features, and therapies. *Circ Res* **115,** 79-96.

Silverman DN & Shah SJ. (2019). Treatment of Heart Failure With Preserved Ejection Fraction (HFpEF): the Phenotype-Guided Approach. *Curr Treat Options Cardiovasc Med* **21,** 20.

Simonini A, Long CS, Dudley GA, Yue P, McElhinny J & Massie BM. (1996). Heart failure in rats causes changes in skeletal muscle morphology and gene expression that are not explained by reduced activity. *Circ Res* **79,** 128-136.

Smart NA, Haluska B, Jeffriess L & Leung D. (2012). Exercise training in heart failure with preserved systolic function: a randomized controlled trial of the effects on cardiac function and functional capacity. *Congest Heart Fail* **18,** 295-301.

Snijders T, Nederveen JP, Joanisse S, Leenders M, Verdijk LB, van Loon LJ & Parise G. (2017). Muscle fibre capillarization is a critical factor in muscle fibre hypertrophy during resistance exercise training in older men. *J Cachexia Sarcopenia Muscle* **8,** 267-276.

Snijders T, Nederveen JP, McKay BR, Joanisse S, Verdijk LB, van Loon LJ & Parise G. (2015). Satellite cells in human skeletal muscle plasticity. *Front Physiol* **6,** 283.

Soare A, Weiss EP & Pozzilli P. (2014). Benefits of caloric restriction for cardiometabolic health, including type 2 diabetes mellitus risk. *Diabetes Metab Res Rev* **30 Suppl 1,** 41-47.

Solomon SD, McMurray JJV, Anand IS, Ge J, Lam CSP, Maggioni AP, Martinez F, Packer M, Pfeffer MA, Pieske B, Redfield MM, Rouleau JL, van Veldhuisen DJ, Zannad F, Zile MR, Desai AS, Claggett B, Jhund PS, Boytsov SA, Comin-Colet J, Cleland J, Düngen HD, Goncalvesova E, Katova T, Kerr Saraiva JF, Lelonek M, Merkely B, Senni M, Shah SJ, Zhou J, Rizkala AR, Gong J, Shi VC & Lefkowitz MP. (2019). Angiotensin-Neprilysin Inhibition in Heart Failure with Preserved Ejection Fraction. *N Engl J Med* **381,** 1609-1620.

Steinberg BA, Zhao X, Heidenreich PA, Peterson ED, Bhatt DL, Cannon CP, Hernandez AF & Fonarow GC. (2012). Trends in patients hospitalized with heart failure and preserved left ventricular ejection fraction: prevalence, therapies, and outcomes. *Circulation* **126,** 65-75.

Stevenson LW, Sietsema K, Tillisch JH, Lem V, Walden J, Kobashigawa JA & Moriguchi J. (1990). Exercise capacity for survivors of cardiac transplantation or sustained medical therapy for stable heart failure. *Circulation* **81,** 78-85.

Suzuki T, Palus S & Springer J. (2018). Skeletal muscle wasting in chronic heart failure. *ESC heart failure* **5,** 1099-1107.

Takatsu M, Nakashima C, Takahashi K, Murase T, Hattori T, Ito H, Murohara T & Nagata K. (2013). Calorie restriction attenuates cardiac remodeling and diastolic dysfunction in a rat model of metabolic syndrome. *Hypertension* **62,** 957-965.

Talbot J & Maves L. (2016). Skeletal muscle fiber type: using insights from muscle developmental biology to dissect targets for susceptibility and resistance to muscle disease. *Wiley Interdiscip Rev Dev Biol* **5,** 518-534.

Teh I, McClymont D, Burton RA, Maguire ML, Whittington HJ, Lygate CA, Kohl P & Schneider JE. (2016). Resolving Fine Cardiac Structures in Rats with High-Resolution Diffusion Tensor Imaging. *Sci Rep* **6,** 30573.

Terena SM, Fernandes KP, Bussadori SK, Deana AM & Mesquita-Ferrari RA. (2017). Systematic review of the synergist muscle ablation model for compensatory hypertrophy. *Rev Assoc Med Bras (1992)* **63,** 164-172.

Thomson DM. (2018). The Role of AMPK in the Regulation of Skeletal Muscle Size, Hypertrophy, and Regeneration. *Int J Mol Sci* **19**.

Thomson DM & Gordon SE. (2006). Impaired overload-induced muscle growth is associated with diminished translational signalling in aged rat fast-twitch skeletal muscle. *J Physiol* **574,** 291-305.

Tickle PG, Hendrickse PW, Degens H & Egginton S. (2020). Impaired skeletal muscle performance as a consequence of random functional capillary rarefaction can be restored with overload-dependent angiogenesis. *The Journal of physiology* **598,** 1187-1203.

Timmerman KL, Lee JL, Dreyer HC, Dhanani S, Glynn EL, Fry CS, Drummond MJ, Sheffield-Moore M, Rasmussen BB & Volpi E. (2010). Insulin stimulates human skeletal muscle protein synthesis via an indirect mechanism involving endothelial-dependent vasodilation and mammalian target of rapamycin complex 1 signaling. *J Clin Endocrinol Metab* **95,** 3848-3857.

Timson BF, Bowlin BK, Dudenhoeffer GA & George JB. (1985). Fiber number, area, and composition of mouse soleus muscle following enlargement. *J Appl Physiol (1985)* **58,** 619-624.

Toma M, McAlister FA, Coglianese EE, Vidi V, Vasaiwala S, Bakal JA, Armstrong PW & Ezekowitz JA. (2012). Testosterone supplementation in heart failure: a meta-analysis. *Circulation Heart failure* **5,** 315-321.

Toth MJ, Ward K, van der Velden J, Miller MS, Vanburen P, Lewinter MM & Ades PA. (2011). Chronic heart failure reduces Akt phosphorylation in human skeletal muscle: relationship to muscle size and function. *J Appl Physiol (1985)* **110,** 892-900.

Tryfonos A, Tzanis G, Pitsolis T, Karatzanos E, Koutsilieris M, Nanas S & Philippou A. (2021). Exercise Training Enhances Angiogenesis-Related Gene Responses in Skeletal Muscle of Patients with Chronic Heart Failure. *Cells* **10**.

Tucker WJ, Haykowsky MJ, Seo Y, Stehling E & Forman DE. (2018). Impaired Exercise Tolerance in Heart Failure: Role of Skeletal Muscle Morphology and Function. *Curr Heart Fail Rep* **15,** 323-331.

Tucker WJ, Nelson MD, Beaudry RI, Halle M, Sarma S, Kitzman DW, Gerche A & Haykowksy MJ. (2016). Impact of Exercise Training on Peak Oxygen Uptake and its Determinants in Heart Failure with Preserved Ejection Fraction. *Card Fail Rev* **2,** 95-101.

Vaduganathan M, Claggett BL, Jhund PS, Cunningham JW, Pedro Ferreira J, Zannad F, Packer M, Fonarow GC, McMurray JJV & Solomon SD. (2020). Estimating lifetime benefits of comprehensive disease-modifying pharmacological therapies in patients with heart failure with reduced ejection fraction: a comparative analysis of three randomised controlled trials. *Lancet* **396,** 121-128.

van Dijk CG, Oosterhuis NR, Xu YJ, Brandt M, Paulus WJ, van Heerebeek L, Duncker DJ, Verhaar MC, Fontoura D, Lourenço AP, Leite-Moreira AF, Falcão-Pires I, Joles JA & Cheng C. (2016). Distinct Endothelial Cell Responses in the Heart and Kidney Microvasculature Characterize the Progression of Heart Failure With Preserved Ejection Fraction in the Obese ZSF1 Rat With Cardiorenal Metabolic Syndrome. *Circ Heart Fail* **9,** e002760.

Vavvas D, Apazidis A, Saha AK, Gamble J, Patel A, Kemp BE, Witters LA & Ruderman NB. (1997). Contraction-induced changes in acetyl-CoA carboxylase and 5'-AMP-activated kinase in skeletal muscle. *J Biol Chem* **272,** 13255-13261.

Velingkaar N, Mezhnina V, Poe A, Makwana K, Tulsian R & Kondratov RV. (2020). Reduced caloric intake and periodic fasting independently contribute to metabolic effects of caloric restriction. *Aging Cell* **19,** e13138.

Vella CA, Ontiveros D & Zubia RY. (2011). Cardiac function and arteriovenous oxygen difference during exercise in obese adults. *Eur J Appl Physiol* **111,** 915-923.

Vescovo G, Dalla Libera L, Serafini F, Leprotti C, Facchin L, Volterrani M, Ceconi C & Ambrosio GB. (1998). Improved exercise tolerance after losartan and enalapril in heart failure: correlation with changes in skeletal muscle myosin heavy chain composition. *Circulation* **98,** 1742-1749.

von Haehling S, Ebner N, Dos Santos MR, Springer J & Anker SD. (2017). Muscle wasting and cachexia in heart failure: mechanisms and therapies. *Nat Rev Cardiol* **14,** 323-341.

Vos T, Flaxman AD, Naghavi M, Lozano R, Michaud C, Ezzati M, Shibuya K, Salomon JA, Abdalla S, Aboyans V, Abraham J, Ackerman I, Aggarwal R, Ahn SY, Ali MK, Alvarado M, Anderson HR, Anderson LM, Andrews KG, Atkinson C, Baddour LM, Bahalim AN, Barker-Collo S, Barrero LH, Bartels DH, Basanez MG, Baxter A, Bell ML, Benjamin EJ, Bennett D, Bernabe E, Bhalla K, Bhandari B, Bikbov B, Bin Abdulhak A, Birbeck G, Black JA, Blencowe H, Blore JD, Blyth F, Bolliger I, Bonaventure A, Boufous S, Bourne R, Boussinesq M, Braithwaite T, Brayne C, Bridgett L, Brooker S, Brooks P, Brugha TS, Bryan-Hancock C, Bucello C, Buchbinder R, Buckle G, Budke CM, Burch M, Burney P, Burstein R, Calabria B, Campbell B, Canter CE, Carabin H, Carapetis J, Carmona L, Cella C, Charlson F, Chen H, Cheng AT, Chou D, Chugh SS, Coffeng LE, Colan SD, Colquhoun S,

Colson KE, Condon J, Connor MD, Cooper LT, Corriere M, Cortinovis M, de Vaccaro KC, Couser W, Cowie BC, Criqui MH, Cross M, Dabhadkar KC, Dahiya M, Dahodwala N, Damsere-Derry J, Danaei G, Davis A, De Leo D, Degenhardt L, Dellavalle R, Delossantos A, Denenberg J, Derrett S, Des Jarlais DC, Dharmaratne SD, Dherani M, Diaz-Torne C, Dolk H, Dorsey ER, Driscoll T, Duber H, Ebel B, Edmond K, Elbaz A, Ali SE, Erskine H, Erwin PJ, Espindola P, Ewoigbokhan SE, Farzadfar F, Feigin V, Felson DT, Ferrari A, Ferri CP, Fevre EM, Finucane MM, Flaxman S, Flood L, Foreman K, Forouzanfar MH, Fowkes FG, Franklin R, Fransen M, Freeman MK, Gabbe BJ, Gabriel SE, Gakidou E, Ganatra HA, Garcia B, Gaspari F, Gillum RF, Gmel G, Gosselin R, Grainger R, Groeger J, Guillemin F, Gunnell D, Gupta R, Haagsma J, Hagan H, Halasa YA, Hall W, Haring D, Haro JM, Harrison JE, Havmoeller R, Hay RJ, Higashi H, Hill C, Hoen B, Hoffman H, Hotez PJ, Hoy D, Huang JJ, Ibeanusi SE, Jacobsen KH, James SL, Jarvis D, Jasrasaria R, Jayaraman S, Johns N, Jonas JB, Karthikeyan G, Kassebaum N, Kawakami N, Keren A, Khoo JP, King CH, Knowlton LM, Kobusingye O, Koranteng A, Krishnamurthi R, Lalloo R, Laslett LL, Lathlean T, Leasher JL, Lee YY, Leigh J, Lim SS, Limb E, Lin JK, Lipnick M, Lipshultz SE, Liu W, Loane M, Ohno SL, Lyons R, Ma J, Mabweijano J, MacIntyre MF, Malekzadeh R, Mallinger L, Manivannan S, Marcenes W, March L, Margolis DJ, Marks GB, Marks R, Matsumori A, Matzopoulos R, Mayosi BM, McAnulty JH, McDermott MM, McGill N, McGrath J, Medina-Mora ME, Meltzer M, Mensah GA, Merriman TR, Meyer AC, Miglioli V, Miller M, Miller TR, Mitchell PB, Mocumbi AO, Moffitt TE, Mokdad AA, Monasta L, Montico M, Moradi-Lakeh M, Moran A, Morawska L, Mori R, Murdoch ME, Mwaniki MK, Naidoo K, Nair MN, Naldi L, Narayan KM, Nelson PK, Nelson RG, Nevitt MC, Newton CR, Nolte S, Norman P, Norman R, O'Donnell M, O'Hanlon S, Olives C, Omer SB, Ortblad K, Osborne R, Ozgediz D, Page A, Pahari B, Pandian JD, Rivero AP, Patten SB, Pearce N, Padilla RP, Perez-Ruiz F, Perico N, Pesudovs K, Phillips D, Phillips MR, Pierce K, Pion S, Polanczyk GV, Polinder S, Pope CA, 3rd, Popova S, Porrini E, Pourmalek F, Prince M, Pullan RL, Ramaiah KD, Ranganathan D, Razavi H, Regan M, Rehm JT, Rein DB, Remuzzi G, Richardson K, Rivara FP, Roberts T, Robinson C, De Leon FR, Ronfani L, Room R, Rosenfeld LC, Rushton L, Sacco RL, Saha S, Sampson U, Sanchez-Riera L, Sanman E, Schwebel DC, Scott JG, Segui-Gomez M, Shahraz S, Shepard DS, Shin H, Shivakoti R, Singh D, Singh GM, Singh JA, Singleton J, Sleet DA, Sliwa K, Smith E, Smith JL, Stapelberg NJ, Steer A, Steiner T, Stolk WA, Stovner LJ, Sudfeld C, Syed S, Tamburlini G, Tavakkoli M, Taylor HR, Taylor JA, Taylor WJ, Thomas B, Thomson WM, Thurston GD, Tleyjeh IM, Tonelli M, Towbin JA, Truelsen T, Tsilimbaris MK, Ubeda C, Undurraga EA, van der Werf MJ, van Os J, Vavilala MS, Venketasubramanian N, Wang M, Wang W, Watt K, Weatherall DJ, Weinstock MA, Weintraub R, Weisskopf MG, Weissman MM, White RA, Whiteford H, Wiersma ST, Wilkinson JD, Williams HC, Williams SR, Witt E, Wolfe F, Woolf AD, Wulf S, Yeh PH, Zaidi AK, Zheng ZJ, Zonies D, Lopez AD, Murray CJ, AlMazroa MA & Memish ZA. (2012). Years lived with disability (YLDs) for 1160 sequelae of 289 diseases and injuries 1990-2010: a systematic analysis for the Global Burden of Disease Study 2010. *Lancet* **380,** 2163-2196.

Wang X, Pickrell AM, Rossi SG, Pinto M, Dillon LM, Hida A, Rotundo RL & Moraes CT. (2013). Transient systemic mtDNA damage leads to muscle wasting by reducing the satellite cell pool. *Hum Mol Genet* **22,** 3976-3986.

Wang Y & Pessin JE. (2013). Mechanisms for fiber-type specificity of skeletal muscle atrophy. *Curr Opin Clin Nutr Metab Care* **16,** 243-250.

Weavil JC, Thurston TS, Hureau TJ, Gifford JR, Kithas PA, Broxterman RM, Bledsoe AD, Nativi JN, Richardson RS & Amann M. (2021). Heart failure with preserved ejection fraction diminishes peripheral hemodynamics and accelerates exercise-induced neuromuscular fatigue. *Am J Physiol Heart Circ Physiol* **320,** H338-h351.

Weber JJ, Pereira Sena P, Singer E & Nguyen HP. (2019). Killing Two Angry Birds with One Stone: Autophagy Activation by Inhibiting Calpains in Neurodegenerative Diseases and Beyond. *BioMed research international* **2019,** 4741252.

Weiss K, Schär M, Panjrath GS, Zhang Y, Sharma K, Bottomley PA, Golozar A, Steinberg A, Gerstenblith G, Russell SD & Weiss RG. (2017). Fatigability, Exercise Intolerance, and Abnormal Skeletal Muscle Energetics in Heart Failure. *Circ Heart Fail* **10**.

White JP, Reecy JM, Washington TA, Sato S, Le ME, Davis JM, Wilson LB & Carson JA. (2009). Overload-induced skeletal muscle extracellular matrix remodelling and myofibre growth in mice lacking IL-6. *Acta Physiol (Oxf)* **197,** 321-332.

Wolfe RR. (2006). The underappreciated role of muscle in health and disease. *Am J Clin Nutr* **84,** 475-482.

Wolsk E, Kaye D, Komtebedde J, Shah SJ, Borlaug BA, Burkhoff D, Kitzman DW, Lam CSP, van Veldhuisen DJ, Ponikowski P, Petrie MC, Hassager C, Møller JE & Gustafsson F. (2019). Central and Peripheral Determinants of Exercise Capacity in Heart Failure Patients With Preserved Ejection Fraction. *JACC Heart Fail* **7,** 321-332.

Yamada K, Kinugasa Y, Sota T, Miyagi M, Sugihara S, Kato M & Yamamoto K. (2016). Inspiratory Muscle Weakness is Associated With Exercise Intolerance in Patients With Heart Failure With Preserved Ejection Fraction: A Preliminary Study. *J Card Fail* **22,** 38-47.

Yan L, Gao S, Ho D, Park M, Ge H, Wang C, Tian Y, Lai L, De Lorenzo MS, Vatner DE & Vatner SF. (2013). Calorie restriction can reverse, as well as prevent, aging cardiomyopathy. *Age (Dordr)* **35,** 2177-2182.

Yoshida T & Delafontaine P. (2016). An Intronic Enhancer Element Regulates Angiotensin II Type 2 Receptor Expression during Satellite Cell Differentiation, and Its Activity Is Suppressed in Congestive Heart Failure. *J Biol Chem* **291,** 25578-25590.

Yusuf S, Pfeffer MA, Swedberg K, Granger CB, Held P, McMurray JJ, Michelson EL, Olofsson B & Ostergren J. (2003). Effects of candesartan in patients with chronic heart failure and preserved left-ventricular ejection fraction: the CHARM-Preserved Trial. *Lancet* **362,** 777-781.

Zamani P, Proto EA, Mazurek JA, Prenner SB, Margulies KB, Townsend RR, Kelly DP, Arany Z, Poole DC, Wagner PD & Chirinos JA. (2020). Peripheral Determinants of Oxygen Utilization in Heart Failure With Preserved Ejection Fraction: Central Role of Adiposity. *JACC Basic to translational science* **5,** 211-225.

Zannad F, McMurray JJ, Krum H, van Veldhuisen DJ, Swedberg K, Shi H, Vincent J, Pocock SJ & Pitt B. (2011). Eplerenone in patients with systolic heart failure and mild symptoms. *N Engl J Med* **364,** 11-21.

Zhang H, Ryu D, Wu Y, Gariani K, Wang X, Luan P, D'Amico D, Ropelle ER, Lutolf MP, Aebersold R, Schoonjans K, Menzies KJ & Auwerx J. (2016). NAD^+ repletion improves mitochondrial and stem cell function and enhances life span in mice. *Science* **352,** 1436-1443.

Ziaeian B & Fonarow GC. (2016). Epidemiology and aetiology of heart failure. *Nat Rev Cardiol* **13,** 368-378.